IOWA STATE UNIVERSITY
Digital Repository

1966

The crystal structure determinations of CsCuCl3, C10H8Mo2(CO)6, and (NPCl2)5

Albert William Schlueter

Iowa State University

www.manaraa.com

THE CRYSTAL STRUCTURE DETERMINATIONS OF

$CsCuCl_3$, $C_{10}H_8Mo_2(CO)_6$, AND $(NPCl_2)_5$

by

Albert William Schlueter

A Dissertation Submitted to the

Graduate Faculty in Partial Fulfillment of

The Requirements for the Degree of

DOCTOR OF PHILOSOPHY

Major Subject: Physical Chemistry

Approved:

In Charge of Major Work

Head of Major Department

Dean of Graduate College

Iowa State University
Of Science and Technology
Ames, Iowa

1966

TABLE OF CONTENTS

INTRODUCTION

The crystal structures of $CsCuCl_3$, $C_{10}H_8Mo_2(CO)_6$, and $(NPCl_2)_5$ were determined by single crystal X-ray diffraction techniques. In addition, an unsuccessful attempt was made to solve the structure of $C_{64}H_{48}O_6Cl_4$. The methods used in these structure investigations represent essentially the entire spectrum of methods used by crystallographers. Thus, this thesis has two purposes: first, to illustrate the various methods available to crystallographers to solve structures, and second, to discuss the nature of the bonding in the compounds successfully completed.

The crystal structure of $CsCuCl_3$ was determined primarily by symmetry considerations and chemical reasoning. The high symmetry and simple atomic arrangement was sufficient to allow the correct model to be discovered without using a Patterson map. In this problem, a set of approximate atomic coordinates were assumed initially, and refined to their final values. The refined model contains a short copper-copper distance, but direct copper-copper interaction is ruled out by overlap integral calculations. The implications of these calculations to metal-metal bonding in general are discussed.

The azulene dimolybdenum hexacarbonyl structure was solved by using the conventional heavy-atom technique. From a Patterson map, the molybdenum atom positions were found. These atoms were then used to determine the signs of the observed structure factors and an electron density map generated. From this map and succeeding ones, the remaining atoms were found. The structure was found to contain a molybdenum-molybdenum bond, but because of disorder in the azulene ring, it was not possible to dis-

cover unambiguously the nature of the metal-azulene bonding.

The structure of decachloropentaphosphonitrile was determined by Patterson superposition techniques used in conjunction with a pseudo-electron density symmetry map. Some new techniques were employed in an attempt to solve this structure. Their merits will be discussed. The structure was found to consist of a nearly planar ten-membered ring of alternating phosphorus and nitrogen atoms. The implications of the structure to bonding in the cyclic phosphonitrilics will be discussed.

A direct method was used in an attempt to solve the structure of p-chlorophenoxybenztropone dimer. Because of the complexity of the problem, and lack of success with the structure using more conventional methods, the method of symbolic addion was used. With this method, over one-hundred signs of the most intense reflections were determined, each with greater than 80% probability. The signs determined were extremely consistent, but none of the electron density maps generated were completely consistent with a sharpened Patterson map generated from the data. Because a set of chlorine positions could not be found which were consistent with both the Patterson map and the electron density map, no further work was done on the structure. The method used in the attempt will be described.

THE STRUCTURE OF $CsCuCl_3$

Introduction

The structure determination of $CsCuCl_3$ was first attempted by Klug and Sears in 1946 (1). They observed no systematic extinctions and tried to find a model in the space group P6/mmm. They assumed the structure to be based on a close-packed arrangement of cesium ions and chlorine atoms as was found in $Cs_3Tl_2Cl_9$ (2), but they could find no reasonable model consistent with their space group. They thus suspected an unknown and perfect twinning of their crystals.

Wells (3) next investigated the problem, but observed $P6_122$ to be the space group. He also assumed the structure to be close-packed and assumed the copper atoms to occupy octahedral holes. Wells then considered all possible arrangements of the copper atoms in octahedral holes consistent with restrictions such that: (1) no cesium atoms touched and, (2) the octahedral holes the copper atoms occupied were surrounded by chlorine atoms. These considerations reduced the number of models to five, and one of these was found to give good agreement with the hk0 and 001 intensities. The atomic parameters for this model were shifted to produce good agreement for sixty-seven reflections judged as strong, medium, weak, etc.

Because of their interesting structural, optical and magnetic features several related copper compounds have recently been investigated, namely, $LiCuCl_3 \cdot 2H_2O$ (4, 5), $KCuCl_3$, NH_4CuCl_3 (6), and $(CH_3)_2NH_2CuCl_3$ (7). These structures all consist of $Cu_2Cl_6^{2-}$ dimers associated into chains by long unsymmetric Cu-Cl bridges and are quite different from the $CuCl_3^-$ infinite

chain found in $CsCuCl_3$. Thus, $CsCuCl_3$ appeared to represent a *different* and particularly simple system to study magnetically because *of its essen-* tially one-dimensional character. Preliminary to such a study it was de- cided to carry out an accurate determination of its structure.

Experimental

Dark red-brown crystals of $CsCuCl_3$ were obtained by evaporating to dryness a solution containing copper and cesium chlorides. A molar excess of copper chloride was used to prevent formation of Cs_2CuCl_4. The crystals appeared as hexagonal prisms often capped by hexagonal pyramids.

Weissenberg photographs exhibited 6/mmm Laue symmetry. The only sys- tematic extinction observed was for $l \neq 6n$ for 00l reflections, indicating the space group $P6_122$ and confirming Wells' observation. The lattice con- stants were determined by a least squares extrapolation treatment of twelve reflections in the back reflection region (8) observed using a sin- gle crystal orienter and CrK_α radiation. The orienter was previously a- ligned with an aluminum single crystal. All twelve reflections observed had nearly complete α_1, α_2 splitting. The observed two-theta was taken as the average of the low two-theta α_1, half-peak position and the high two- theta α_2 half-peak position. Each reflection was individually left-right and up-down centered before its two-theta value was taken. These reflec- tions with observed and calculated two-theta values can be seen in Table 1. The lattice constants calculated from these data were: $a = b = 7.2157 \pm 0.0005$ and $c = 18.1777 \pm 0.0010\text{Å}$.

Table 1. Accurate lattice constant data for CsCuCl$_3$

H	K	L	Observed two-theta	Estimated error	Calculated two-theta
4	2	0	151.92	0.07	151.94
4	2	1	152.93	0.04	152.93
4	2	2	156.11	0.04	156.11
3	3	3	152.46	0.06	152.47
3	3	4	160.45	0.05	160.47
5	0	5	151.60	0.04	151.57
4	1	8	157.02	0.06	156.99
3	2	9	157.08	0.05	157.08
4	0	10	150.48	0.05	150.48
3	0	13	161.44	0.04	161.43
1	0	15	148.72	0.06	148.74

Complete three-dimensional data to $\sin\theta/\lambda = 0.904$ were taken with

zirconium-filtered molybdenum K_α radiation using a General Electric XRD-5

X-ray unit equipped with a single crystal orienter. A small receiving ap-

perture of 1.2^o, a low take-off angle of 1° and a short 1.67^o two-theta

scan (at one degree per minute) were used to eliminate overlap of peaks

along the densely spaced lattice rows. For each of the 1092 reflections,

a total count was obtained from a one-hundred second, moving crystal-moving

counter scan. A correction for background and streak was made from the

recorder trace for each reflection. Beta-corrections were made with a

planimeter for a few intense, low-order reflections. An absorption cor-

rection was made using Busing's polyhedral absorption correction program

(9) rewritten for the IBM 7074 computor. Since the intensities measured

were considered to be a function of peak count, background and absorption,

the error in intensity was expressed as:

$$(\Delta I)^2 = (\frac{\partial I}{\partial TC})^2 \Delta TC^2 + (\frac{\partial I}{\partial BK})^2 \Delta BK^2 + (\frac{\partial I}{\partial A})^2 \Delta A^2.$$

The partials were calculated from:

$$I = (TC - BK)A.$$

Thus, by assigning errors to the total count, background and absorption, the error in the intensity could be calculated. The errors estimated for these quantities were calculated from the following formulae:

$$\Delta TC^2 = TC + [\overline{TC}(K_T)]^2$$
$$\Delta BK^2 = BK + [\overline{BK}(K_B)]^2$$
$$\Delta A^2 = K_A{}^2.$$

In the first two expressions, the first term represents the statistical error and the second term represents random instrument fluctuation errors. The quantities K_T, K_B and K_A are the estimated relative errors in the total count, background and absorption. In this structure, K_T was taken to be 0.03, K_B was felt to be best expressed as $0.03 + 0.04\log(BK/790)$, and K_A was set equal to 0.05.

The finite difference method was used to calculate the values of ΔF for each reflection. The formula used was:

$$\Delta F = \frac{(I + \Delta I)^{\frac{1}{2}} - I^{\frac{1}{2}}}{(LP)^{\frac{1}{2}}},$$

where I is not corrected for the Lorentz-polarization (LP) factor.

Structural Refinement

The parameters of Wells were tested and an agreement factor of R = 45% was obtained. Then, two cycles of refinement reduced the R-factor

to 35%, using a full-matrix least squares program.[1] A model constructed at this point indicated that the cesium atom, on the basis of a hexagonal close-packed arrangement, was displaced by $0.2\overset{\circ}{A}$ too close to two chlorine atoms. It was shifted to a more nearly close-packed position and further refined isotropically to an R-factor of 11%. At this point, seven of the strongest low-order reflections, suspected of being strongly affected by extinction, were removed. Anisotropic refinement lowered the R-factor for the 1062 non-zero reflections to a final agreement factor, $R = \Sigma \left\| F_o \right| - \left| F_c \right\| / \Sigma \left| F_o \right| = 5.05$, and a weighted agreement factor, $R_w = \Sigma w^{\frac{1}{2}} \left\| F_o \right| - \left| F_c \right\| / \Sigma w^{\frac{1}{2}} \left| F_o \right| = 4.82$. Before the final cycle, the weighting scheme was checked by a plot of $\Delta^2 w (\Delta^2 = (\left| F_o \right| - \left| F_c \right|)^2$ and $w = \dfrac{(\text{scale factor})^2}{(\text{sigma})^2})$,

versus $\sin \theta / \lambda$ for groups of one-hundred reflections. The plot was horizontal with an intercept of 0.92 implying a good weighting scheme. Because several atoms occupied special positions, the anisotropic least squares refinement was carried out using linear dependence relationships between the anisotropic parameters. According to Levy (10), the anisotropic thermal parameters transform as the quadratic positional parameters. Using this rule, the linear dependency relationships for the special positions of the space group $P6_1 22$ were determined.

The final parameters and their standard deviations are listed in Table 2. Wells' final parameters are also listed there for comparison. In Figure 1, the values of the observed and calculated structure factors

---

[1]Fitzwater, D. R., Benson, J. E., both of Ames Laboratory, Atomic Energy Commission, Ames, Iowa. Jackobs, J. J., (present address) Arizona State University, Tempe, Arizona. Least Squares Package. Private Communication. 1964.

Table 2. Final parameters and their standard errors from least squares refinement of $CsCuCl_3$

| Atom | Final atom positional parameters with standard deviations | | | | | |
	x/a	y/b	z/c	Δ_x	Δ_y	Δ_z
Cs[a]	0.35458 (0.345)[b]	0.70916	0.25000	0.0001	0.0002	...
Cu	0.0616 (0.07)	0.0000	0.0000	0.0003	...	...
Cl(1)[a]	0.8877 (0.90)	0.7754	0.2500	0.0003	0.0006	...
Cl(2)	0.3540 (0.35)	0.2095 (0.22)	0.2418 (0.25)	0.0005	0.0005	0.0002

| Atom | Final thermal parameters with deviations[c] | | | | | |
	β_{11}	β_{22}	β_{33}	β_{12}	β_{13}	β_{23}
Cs	0.01311 (14)	0.01113 (7)	0.00222 (2)	0.00570 (3)	-0.00094 (3)	0
Cu	0.01026 (22)	0.01123 (11)	0.00101 (2)	0.00562 (6)	0.00020 (2)	0.00040 (4)
Cl(1)	0.0125 (4)	0.0094 (2)	0.0012 (1)	0.0047 (1)	0.0001 (1)	0
Cl(2)	0.0097 (2)	0.0128 (3)	0.0014 (1)	0.0051 (2)	-0.0006 (1)	-0.0002 (1)

[a]Special positions: $y = 2x$, $z = \frac{1}{4}$.

[b]Wells' parameters in parentheses.

[c]The temperature factor is of the form: $\exp(-\beta_{11}h^2 - \beta_{22}k^2 - \beta_{33}l^2 - 2\beta_{12}hk - 2\beta_{13}hl - 2\beta_{23}kl)$.

8

Figure 1. Comparison of observed and calculated structure factors for
           CsCuCl$_3$

H	K	L	FOBS	FCAL	ACAL	BCAL
0	0	0	----	810.0	----	----
0	0	6	289.4	----	----	----
0	0	12	321.7	----	----	----
0	0	18	87.6	89.7	-89.7	0.5
0	0	24	105.1	107.6	107.6	-0.8
1	0	0	72.2	72.8	72.8	0.0
1	0	1	31.6	31.2	-15.4	27.1
1	0	2	21.2	21.6	10.6	18.8
1	0	3	165.3	182.0	182.0	0.0
1	0	4	48.0	46.3	-23.0	40.1
1	0	5	59.1	55.9	28.2	48.3
1	0	6	184.4	195.2	195.2	-0.5
1	0	7	20.3	17.2	-8.7	14.8
1	0	8	17.7	7.3	-3.6	-6.3
1	0	9	131.2	133.6	-133.6	-0.0
1	0	10	36.4	35.9	17.8	-31.2
1	0	11	12.5	10.9	-5.6	-9.4
1	0	12	49.5	40.4	40.4	-0.4
1	0	13	33.3	30.1	-14.9	26.2
1	0	14	9.7	8.5	-4.4	-7.3
1	0	15	19.9	80.2	80.2	-0.0
1	0	16	29.4	29.0	-14.5	25.1
1	0	17	44.2	43.3	21.6	37.5
1	0	18	81.0	77.7	77.7	-0.2
1	0	19	5.9	3.5	-1.8	3.0
1	0	20	8.9	9.6	4.8	8.3
1	0	21	42.0	41.4	-41.4	-0.0
1	0	22	17.8	16.2	8.0	-14.0
1	0	23	15.1	15.2	-7.6	-13.2
1	0	24	27.6	27.1	27.1	-0.2
1	0	25	13.6	12.4	-6.1	10.7
1	0	26	10.3	10.0	-5.0	-8.6
1	0	27	17.7	19.5	19.5	-0.0
1	0	28	8.2	9.2	-4.6	8.0
1	0	29	17.8	20.3	10.1	17.6
1	0	30	24.1	22.9	22.9	-0.0
1	0	31	4.4	3.5	-1.7	3.0
1	0	32	5.4	5.1	2.5	4.4
1	1	0	227.3	----	----	----
1	1	1	75.7	74.0	-63.9	37.2
1	1	2	14.4	13.1	6.6	-11.4
1	1	3	12.2	8.6	-0.0	8.6
1	1	4	32.1	29.0	14.6	25.1
1	1	5	27.2	21.3	18.2	11.1
1	1	6	74.1	72.5	-72.5	0.6
1	1	7	30.9	25.1	-21.8	12.4
1	1	8	16.7	15.8	-7.8	13.7
1	1	9	12.9	9.7	6.0	-9.7
1	1	10	19.8	17.5	-8.7	-15.1
1	1	11	54.3	50.4	43.6	25.2
1	1	12	196.0	190.4	190.4	-0.4
1	1	13	41.2	38.0	-32.7	19.3
1	1	14	36.5	35.1	17.5	-30.5
1	1	15	14.4	13.3	-0.0	13.3
1	1	16	24.9	24.2	12.5	21.0
1	1	17	12.4	12.0	10.3	6.1
1	1	18	20.3	16.6	-16.6	0.2
1	1	19	19.9	19.0	-16.4	9.6
1	1	20	24.9	23.9	-11.9	20.7
1	1	21	9.6	8.9	0.0	-8.9
1	1	22	10.5	9.9	-5.0	-8.6
1	1	23	17.0	16.9	14.6	8.6
1	1	24	65.0	62.8	62.8	-0.1
1	1	25	10.8	10.1	-8.7	5.0
1	1	26	22.3	22.5	11.2	-19.5
1	1	27	4.9	6.8	0.0	6.8
1	1	28	6.5	7.4	3.7	6.4
1	1	29	5.9	7.3	6.4	3.7
1	1	30	3.8	3.8	3.8	0.0
1	1	31	11.9	9.7	-8.3	4.9
1	1	32	9.4	10.4	-5.2	9.0
2	0	0	87.2	98.2	-98.2	0.0
2	0	1	44.3	44.2	22.0	-38.4
2	0	2	116.8	123.7	-62.8	-107.2
2	0	3	282.0	----	----	----
2	0	4	95.7	94.7	47.2	-82.1
2	0	5	134.3	133.7	66.6	116.0
2	0	6	249.0	----	----	----
2	0	7	126.8	122.0	0.7	105.9
2	0	8	68.0	66.2	33.0	57.4
2	0	9	287.6	----	----	----
2	0	10	83.4	74.0	-40.7	70.5
2	0	11	18.3	18.4	-9.2	-16.0
2	0	12	39.4	37.1	-37.1	-0.4
2	0	13	15.4	15.6	7.7	-13.5
2	0	14	53.5	52.0	-26.1	-45.0
2	0	15	140.9	144.3	-144.3	0.0
2	0	16	38.4	38.5	19.3	-33.4
2	0	17	55.5	55.0	27.5	47.7
2	0	18	102.3	102.1	102.1	-0.2
2	0	19	49.5	49.3	-24.6	42.8
2	0	20	18.3	18.8	9.4	16.3
2	0	21	74.0	73.3	73.3	0.0
2	0	22	26.2	26.9	-13.4	23.3
2	0	24	5.9	2.6	0.0	-0.1
2	0	25	3.8	0.2	0.0	-0.1
2	0	26	14.1	13.8	30.4	-12.0
2	0	27	30.0	30.4	-30.4	0.0
2	0	28	7.1	8.3	4.1	-7.2
2	0	29	16.9	16.1	8.0	14.0
2	0	30	26.2	26.4	26.4	-0.1
2	0	31	16.4	14.1	-7.0	12.3
2	0	32	5.4	2.4	1.2	2.1
2	1	0	6.5	11.4	-11.4	0.0
2	1	1	24.9	21.1	6.3	20.1
2	1	2	34.3	34.6	34.5	3.5
2	1	3	122.4	126.8	126.5	7.8
2	1	4	43.0	43.9	-27.0	34.6
2	1	5	92.1	85.7	67.5	52.8
2	1	6	155.4	154.1	153.9	-7.8
2	1	7	113.9	108.1	-95.4	50.9
2	1	8	45.1	44.8	-27.3	-35.6
2	1	9	95.2	94.5	-94.5	2.9
2	1	10	24.5	23.4	23.1	3.3
2	1	11	33.5	30.5	26.1	15.9
2	1	12	13.2	11.3	-4.6	10.4
2	1	13	22.7	22.5	18.5	12.8
2	1	14	23.4	23.2	23.2	1.6

H	K	L	FOBS	FCAL	ACAL	BCAL
2	1	15	61.0	56.2	55.9	5.7
2	1	16	18.0	16.4	-12.7	10.4
2	1	17	29.0	27.7	12.8	24.6
2	1	18	73.5	72.0	71.3	-9.7
2	1	19	57.0	56.6	-51.3	23.9
2	1	20	19.1	19.6	-14.2	-13.5
2	1	21	27.1	27.0	-27.0	0.5
2	1	22	13.6	11.7	8.8	7.8
2	1	23	24.7	24.7	23.4	7.9
2	1	24	8.5	7.5	2.6	7.1
2	1	25	7.8	9.5	6.6	6.8
2	1	26	10.9	10.6	10.2	-2.8
2	1	27	12.6	11.6	11.3	2.7
2	1	28	5.1	4.5	-4.5	0.5
2	1	29	7.4	8.6	0.0	8.6
2	1	30	25.1	24.5	24.2	-4.0
2	1	31	18.7	18.0	-16.0	8.2
2	2	0	243.5	----	----	----
2	2	1	186.1	213.5	-184.5	107.4
2	2	2	81.2	78.6	39.4	-68.0
2	2	3	14.8	13.7	0.0	13.7
2	2	4	29.4	28.2	-14.2	-24.3
2	2	5	80.7	81.4	-70.4	-40.9
2	2	6	162.6	164.9	-164.9	0.4
2	2	7	78.7	79.7	69.0	-39.9
2	2	8	26.4	25.0	-12.6	21.6
2	2	9	13.6	10.0	0.0	10.0
2	2	10	54.9	53.4	26.7	46.3
2	2	11	133.9	133.1	115.1	66.9
2	2	12	176.7	173.4	173.4	-0.3
2	2	13	131.4	127.6	-110.3	64.2
2	2	14	48.7	46.7	23.4	-40.5
2	2	15	11.7	8.7	0.0	8.7
2	2	16	11.5	11.1	-5.6	-9.5
2	2	17	22.9	24.3	-21.1	-12.1
2	2	18	55.0	53.6	-53.6	0.2
2	2	19	24.9	24.9	21.5	-12.5
2	2	20	9.4	8.4	-4.3	7.3
2	2	21	8.3	4.7	0.0	4.7
2	2	22	18.9	20.3	10.2	17.6
2	2	23	43.0	43.8	37.9	22.1
2	2	24	48.8	49.0	49.0	-0.1
2	2	25	40.6	41.4	-35.7	20.8
2	2	26	18.0	16.5	8.3	-14.3
2	2	29	5.2	0.7	0.6	0.4
2	2	30	4.3	2.5	-2.5	0.0
2	2	31	4.4	0.7	-0.6	0.4
3	0	0	172.6	201.7	201.7	0.0
3	0	1	111.1	118.1	-51.8	102.5
3	0	2	58.9	57.8	-28.9	-50.0
3	0	3	29.0	19.2	-19.2	0.0
3	0	4	29.3	27.8	14.2	-24.0
3	0	5	18.9	12.7	6.3	11.0
3	0	6	57.8	56.8	-56.8	-0.4
3	0	7	10.2	6.8	3.3	-6.0
3	0	8	7.3	5.6	-2.6	-5.0
3	0	9	19.0	17.8	17.8	0.0
3	0	10	62.9	61.5	-30.8	53.2
3	0	11	66.5	64.2	31.9	55.7
3	0	12	125.6	122.8	122.8	-0.3
3	0	13	85.8	84.3	-41.9	73.2
3	0	14	13.4	12.0	-6.1	-10.3
3	0	15	15.8	15.7	-15.7	0.0
3	0	16	24.1	24.3	12.2	-21.0
3	0	17	19.6	19.5	9.8	16.9
3	0	18	15.2	12.2	-12.2	-0.2
3	0	19	4.6	4.2	2.1	-3.6
3	0	20	17.0	17.7	-8.7	-15.4
3	0	21	14.5	14.3	14.3	0.0
3	0	22	27.0	29.6	-14.8	25.6
3	0	23	18.7	20.0	9.9	17.3
3	0	24	40.0	39.0	39.0	-0.1
3	0	25	33.1	34.1	-17.0	29.6
3	0	26	4.0	2.2	1.1	2.0
3	0	27	10.0	9.9	-9.9	0.0
3	0	28	14.7	7.5	3.8	-6.5
3	0	29	14.1	10.5	5.2	9.1
3	0	30	4.3	3.8	3.8	-0.1
3	0	31	6.2	1.3	-0.7	1.1
3	1	0	25.1	28.6	-28.6	0.0
3	1	1	36.8	28.9	-16.6	23.6
3	1	2	81.2	79.2	-32.4	-72.3
3	1	3	122.8	124.4	-124.3	4.8
3	1	4	32.7	32.8	20.0	-25.9
3	1	5	89.7	85.4	55.6	64.9
3	1	6	106.9	104.5	103.9	-10.3
3	1	7	74.2	69.5	-54.7	42.9
3	1	8	28.3	28.5	27.0	9.1
3	1	9	100.4	99.7	96.0	18.3
3	1	10	62.3	62.4	-13.2	60.5
3	1	11	22.4	18.0	18.0	1.4
3	1	12	19.4	20.0	-13.7	14.6
3	1	13	34.6	32.1	-24.4	28.7
3	1	14	39.4	39.9	-22.9	-32.7
3	1	15	63.8	63.5	-63.2	-6.3
3	1	16	13.0	14.5	0.5	-14.5
3	1	17	46.6	48.3	22.1	42.9
3	1	18	48.8	48.9	46.9	-13.9
3	1	19	25.2	27.0	-22.8	14.4
3	1	20	13.5	13.6	12.3	-5.7
3	1	21	39.4	39.5	37.2	13.3
3	1	22	22.5	24.4	1.4	24.3
3	1	23	14.8	14.4	14.1	-2.9
3	1	24	9.1	10.0	0.4	10.0
3	1	25	18.4	19.2	-11.1	15.6
3	1	26	9.5	11.3	-7.5	-8.5
3	1	27	19.0	19.1	-18.8	-3.7
3	1	28	3.0	4.1	-3.3	-2.4
3	1	29	18.3	18.0	5.1	17.3
3	1	30	16.0	15.3	14.2	-5.7
3	1	31	9.9	8.5	-6.2	5.8
3	2	0	27.4	29.0	-29.0	0.0
3	2	1	63.6	58.1	-35.4	46.1
3	2	2	60.9	60.1	58.8	12.6
3	2	3	73.7	74.0	71.0	21.1
3	2	4	89.8	90.2	-51.6	74.0
3	2	5	50.9	48.0	46.0	13.7
3	2	6	63.7	62.1	62.0	-1.7
3	2	7	39.0	36.9	-34.9	12.1

H	K	L	FOBS	FCAL	ACAL	BCAL
3	2	8	54.9	54.5	-31.3	-44.6
3	2	9	56.8	56.5	-55.7	9.1
3	2	10	60.1	60.2	54.1	-26.5
3	2	11	40.9	37.1	21.1	30.5
3	2	12	12.1	12.1	-11.9	2.4
3	2	13	47.8	46.0	-33.8	31.2
3	2	14	28.3	27.5	25.1	-11.3
3	2	15	42.1	41.3	36.7	18.9
3	2	16	58.3	59.0	-32.3	49.4
3	2	17	28.5	29.0	26.7	11.4
3	2	18	22.6	22.7	22.6	-2.3
3	2	19	15.6	14.2	-11.8	7.9
3	2	20	14.7	13.0	-6.5	-11.1
3	2	21	20.6	20.1	-20.3	1.6
3	2	22	27.2	27.6	23.8	-13.9
3	2	23	14.7	14.7	10.2	10.7
3	2	24	9.2	4.3	3.8	1.8
3	2	25	23.2	22.5	-18.7	12.5
3	2	26	11.3	12.3	5.9	-10.8
3	2	27	17.0	13.9	10.8	8.7
3	2	28	21.1	20.9	-10.3	18.0
3	2	29	9.2	12.1	10.1	6.8
3	3	0	91.6	91.3	91.3	-0.0
3	3	1	112.3	111.7	-96.8	55.6
3	3	2	33.0	31.6	15.8	-27.4
3	3	3	32.5	31.7	0.0	31.7
3	3	4	28.0	24.7	12.3	21.4
3	3	5	33.0	34.5	-29.8	-17.3
3	3	6	79.5	78.3	-78.3	0.3
3	3	7	21.9	23.9	20.6	-12.1
3	3	8	15.6	12.1	6.1	-10.5
3	3	10	14.1	14.6	7.3	12.6
3	3	11	85.9	84.3	73.1	42.1
3	3	12	63.8	62.0	62.0	-0.2
3	3	13	65.8	65.0	-56.4	32.4
3	3	14	30.8	30.7	15.3	-26.6
3	3	15	34.9	36.3	0.0	36.3
3	3	16	19.9	19.2	9.6	16.6
3	3	17	14.6	14.6	-12.6	-7.4
3	3	18	37.7	38.2	-38.2	0.1
3	3	19	5.1	4.2	0.2	-0.2
3	3	20	5.8	2.2	1.1	-1.9
3	3	21	7.5	6.0	0.0	-6.0
3	3	22	9.0	5.7	2.8	4.9
3	3	23	32.6	33.6	29.2	16.8
3	3	24	21.6	23.8	23.8	-0.2
3	3	25	21.3	21.3	-18.5	10.6
3	3	26	17.2	16.6	8.3	-14.4
3	3	27	19.0	17.7	0.0	17.7
3	3	28	6.8	7.0	3.5	6.1
3	3	29	3.1	0.5	-0.4	-0.3
4	0	0	92.3	94.6	-94.6	0.0
4	0	1	28.7	23.5	-11.8	20.3
4	0	2	115.6	120.9	60.2	104.8
4	0	3	139.0	143.0	143.0	0.0
4	0	4	167.6	174.6	-87.1	151.4
4	0	5	76.0	72.2	36.0	62.6
4	0	6	139.0	138.7	-40.3	-0.3
4	0	7	80.0	75.8	-37.8	65.7
4	0	9	142.4	144.0	-71.7	-134.8
4	0	10	108.1	107.2	-107.2	0.0
4	0	11	87.7	88.8	44.3	-77.0
4	0	12	28.5	25.8	12.9	22.3
4	0	13	55.2	54.2	-54.2	-0.3
4	0	14	18.0	15.4	-7.7	13.3
4	0	15	56.8	57.0	28.4	49.4
4	0	16	67.0	65.1	65.1	-0.0
4	0	17	85.8	85.5	-42.6	74.0
4	0	18	32.3	31.9	15.9	27.6
4	0	19	61.2	59.4	59.4	-0.2
4	0	20	36.6	37.0	-18.4	32.0
4	0	21	53.3	54.0	-27.0	-46.9
4	0	22	29.5	29.5	-29.5	-0.3
4	0	23	27.2	26.4	13.2	-22.9
4	0	24	17.5	16.4	8.2	14.2
4	0	25	10.9	10.9	-10.9	-0.1
4	0	26	14.4	14.0	-5.6	9.6
4	0	27	8.4	11.1	4.8	8.4
4	0	28	13.0	11.1	11.1	-0.0
4	0	29	20.2	22.2	-11.0	19.2
4	0	30	8.6	10.3	5.1	8.9
4	0	31	14.1	14.2	14.2	-0.1
4	1	0	102.4	103.1	103.1	0.0
4	1	1	118.5	119.8	-82.8	86.6
4	1	2	42.8	40.1	14.5	-37.4
4	1	3	11.8	11.1	-8.8	6.8
4	1	4	16.2	14.3	-36.0	25.8
4	1	5	19.1	22.3	-13.9	-17.5
4	1	6	63.6	63.4	-63.2	4.7
4	1	7	22.9	24.5	22.7	-9.3
4	1	8	25.5	23.0	-15.4	-17.1
4	1	9	22.0	22.1	6.8	21.0
4	1	10	31.4	31.0	24.2	19.4
4	1	11	83.3	81.6	50.8	63.9
4	1	12	68.1	66.1	65.7	-7.1
4	1	13	79.8	78.4	-61.1	49.1
4	1	14	28.1	27.5	-3.8	-27.3
4	1	15	5.5	6.3	-1.4	-6.2
4	1	16	35.3	36.1	-28.0	22.8
4	1	17	10.3	5.9	0.2	-5.9
4	1	18	25.5	25.4	-24.6	6.5
4	1	19	12.9	13.2	12.0	5.5
4	1	20	9.5	10.1	0.6	-10.1
4	1	21	16.2	15.9	0.4	15.9
4	1	22	14.8	13.8	13.7	-1.6
4	1	23	29.6	31.3	18.9	24.9
4	1	24	21.8	22.4	22.0	-4.5
4	1	25	29.3	30.3	-26.0	15.5
4	1	26	12.7	12.5	-6.0	-10.9
4	1	27	4.7	2.3	-4.1	
4	1	28	14.4	15.2	-10.2	11.3
4	2	0	27.3	27.2	-27.2	0.0
4	2	1	65.5	66.5	-0.7	-66.4
4	2	2	101.4	100.5	-78.6	-62.7
4	2	3	97.8	98.4	-96.1	20.9
4	2	4	80.4	79.5	78.8	-10.3
4	2	5	117.8	117.6	50.2	106.4
4	2	6	26.2	24.7	24.6	-1.1

Figure 1 (Continued)

H	K	L	FOBS	FCAL	ACAL	BCAL
4	2	7	110.6	110.0	-50.5	97.8
4	2	8	64.8	63.2	63.2	-0.6
4	2	9	79.5	7815	76.2	19.0
4	2	10	79.6	80.8	-62.0	51.9
4	2	11	46.3	46.4	6.7	-45.9
4	2	12	13.7	14.6	-14.5	1.6
4	2	13	36.0	36.0	-3.3	-35.9
4	2	14	50.8	50.9	-39.0	-32.7
4	2	15	48.2	48.4	-46.7	12.8
4	2	16	39.2	39.0	38.9	-3.8
4	2	17	55.8	56.8	22.6	52.1
4	2	18	7.5	7.0	6.9	-2.2
4	2	19	47.1	48.4	-23.6	42.2
4	2	20	21.6	22.9	21.0	-9.1
4	2	21	27.1	26.4	24.4	10.0
4	2	22	27.9	28.6	-20.3	20.2
4	2	23	14.0	14.3	8.4	-11.7
4	2	24	6.4	1.2	-0.9	0.7
4	2	25	10.9	8.8	-6.1	-6.4
4	2	26	11.5	13.0	-7.9	-10.3
4	2	27	7.4	10.4	-8.6	5.8
4	2	28	9.6	8.4	7.9	2.7
4	2	29	14.5	15.2	6.4	13.7
4	3	0	14.9	4.0	-4.0	0.0
4	3	1	19.5	19.5	19.1	3.8
4	3	2	32.1	31.9	23.9	21.1
4	3	3	49.0	49.3	42.1	25.7
4	3	4	59.6	59.9	-15.7	57.8
4	3	5	56.7	55.8	52.0	20.3
4	3	6	15.8	15.6	-14.5	-5.8
4	3	7	68.5	67.7	-62.6	25.7
4	3	8	59.9	59.7	-6.9	-59.3
4	3	9	44.1	42.9	-32.9	27.6
4	3	10	23.3	24.1	22.7	-8.2
4	3	11	5.1	7.0	-1.4	6.9
4	3	12	9.9	9.8	-3.4	9.2
4	3	13	20.1	20.3	20.2	-2.4
4	3	14	16.9	16.9	10.7	13.2
4	3	15	25.3	25.4	-21.4	13.7
4	3	16	26.7	27.7	-10.8	25.6
4	3	17	23.5	23.4	20.9	10.5
4	3	18	11.1	11.8	-7.5	-9.0
4	3	19	41.1	41.5	-37.4	17.9
4	3	20	30.5	29.9	0.7	-29.9
4	3	21	18.0	19.2	-10.4	16.1
4	3	22	9.8	10.7	10.3	2.9
4	3	23	7.6	6.8	5.7	3.8
4	3	24	2.9	7.2	-3.0	6.6
4	3	25	8.4	8.1	7.8	-1.9
4	3	26	6.7	3.8	3.4	1.7
4	3	27	9.1	7.8	4.7	6.2
4	4	0	22.0	24.2	24.2	0.0
4	4	1	83.5	84.4	-73.0	42.3
4	4	2	76.6	75.6	37.7	-65.5
4	4	3	30.6	30.5	0.0	30.5
4	4	4	38.8	39.1	-19.5	-33.9
4	4	5	44.5	45.0	-38.9	-22.5
4	4	6	48.9	49.5	-49.5	0.2
4	4	7	46.2	46.8	40.5	-23.5
4	4	8	36.2	37.1	-18.5	32.2
4	4	9	19.2	22.5	0.0	22.5
4	4	10	53.8	53.1	26.5	46.1
4	4	11	53.4	54.0	46.7	27.0
4	4	12	13.7	13.8	13.8	-0.1
4	4	13	53.8	55.1	-47.7	27.6
4	4	14	50.3	50.5	25.2	-43.8
4	4	15	22.5	23.0	0.0	23.0
4	4	16	18.1	16.2	-8.1	-14.0
4	4	17	14.6	12.4	-10.7	-6.3
4	4	18	23.7	23.5	-23.5	0.1
4	4	19	16.3	15.4	13.3	-7.8
4	4	20	14.9	12.9	-6.1	11.2
4	4	21	13.1	12.0	0.0	12.0
4	4	22	19.7	18.9	9.4	16.3
4	4	23	16.1	15.1	13.1	7.6
4	4	24	4.2	1.0	1.0	0.0
4	4	25	16.5	15.9	-13.8	8.0
4	4	26	17.3	17.4	8.7	-15.1
5	0	0	17.2	19.1	-19.1	0.0
5	0	1	17.7	22.1	11.0	-19.1
5	0	2	13.4	14.2	-21.1	-36.6
5	0	3	67.7	69.0	-69.0	0.0
5	0	4	18.9	18.2	-8.1	14.0
5	0	5	83.8	83.6	41.7	72.0
5	0	6	29.2	29.6	29.6	-0.3
5	0	7	100.6	100.4	-50.1	87.1
5	0	8	29.7	28.1	-14.0	-24.4
5	0	9	54.3	54.3	54.3	0.0
5	0	10	41.1	40.7	-20.3	35.2
5	0	11	6.2	5.1	2.5	4.5
5	0	12	13.6	14.5	-14.5	-0.2
5	0	13	23.0	24.7	12.3	-21.4
5	0	14	16.7	17.2	-8.7	-14.9
5	0	15	30.7	31.1	-31.1	0.0
5	0	16	7.7	7.8	-3.9	6.8
5	0	17	28.8	30.8	15.3	26.8
5	0	18	17.1	17.7	17.7	-0.2
5	0	19	55.4	57.6	-28.7	49.9
5	0	20	20.9	22.3	-11.1	-19.4
5	0	21	16.0	16.7	16.7	0.0
5	0	22	15.9	18.8	-9.4	16.3
5	0	23	11.0	12.7	6.3	11.0
5	0	24	7.4	7.5	-7.5	-0.1
5	0	25	8.6	8.6	4.3	-7.5
5	0	26	9.2	5.6	-2.8	-4.9
5	0	27	6.4	4.8	-4.8	0.0
5	0	28	6.0	4.4	-2.2	3.8
5	0	29	9.6	8.0	4.0	7.0
5	1	0	31.2	31.8	-31.8	0.0
5	1	1	18.2	14.2	-13.8	-3.1
5	1	2	43.5	42.7	34.3	25.4
5	1	3	58.0	57.6	56.7	10.4
5	1	4	93.0	92.5	-48.6	79.7
5	1	5	52.3	50.9	27.3	43.3
5	1	6	26.2	25.9	23.7	11.1
5	1	7	57.4	56.3	-23.1	51.4
5	1	8	88.7	90.1	-47.7	-76.5
5	1	9	47.0	46.9	-44.8	1.2

H	K	L	FOBS	FCAL	ACAL	BCAL
5	1	10	22.3	22.2	18.0	-13.0
5	1	11	11.9	11.0	8.7	6.8
5	1	12	29.7	28.1	-22.3	-17.2
5	1	13	15.3	15.2	-13.3	-7.3
5	1	14	27.3	26.4	21.0	16.0
5	1	15	39.9	32.7	32.6	3.4
5	1	16	43.0	44.5	-19.4	40.0
5	1	17	24.7	24.8	16.9	18.2
5	1	18	20.8	20.5	11.9	16.7
5	1	19	32.4	32.1	-10.9	30.2
5	1	20	42.4	44.3	-20.8	-39.1
5	1	21	23.5	19.7	-17.4	9.2
5	1	22	6.1	0.9	-0.5	-0.7
5	1	23	8.9	8.7	4.2	7.6
5	1	24	14.3	15.3	-9.5	-11.9
5	1	25	8.7	7.6	-7.4	-1.7
5	1	26	7.2	5.9	4.6	3.7
5	1	27	13.4	10.9	10.8	0.9
5	1	28	14.9	14.0	-3.5	13.5
5	2	0	34.2	34.3	34.3	0.0
5	2	1	63.6	62.6	-54.7	30.4
5	2	2	56.5	56.8	-15.1	-54.7
5	2	3	35.9	34.7	27.6	21.0
5	2	4	11.3	11.2	10.2	-4.6
5	2	5	16.4	15.9	-14.0	7.5
5	2	6	50.5	50.5	-50.4	-3.4
5	2	7	22.3	21.1	19.7	-7.5
5	2	8	3.8	2.7	2.5	-0.9
5	2	9	27.3	28.5	-20.3	20.0
5	2	10	49.9	49.7	-20.2	45.4
5	2	11	34.9	35.0	34.0	8.4
5	2	12	27.5	22.2	21.6	5.4
5	2	13	49.5	51.0	-40.9	30.5
5	2	14	32.9	33.6	-5.4	-33.1
5	2	15	17.6	18.5	13.6	12.6
5	2	16	12.6	11.8	11.5	-2.7
5	2	17	17.4	15.6	-0.7	15.6
5	2	18	24.0	24.6	-24.1	-4.9
5	2	19	9.2	11.0	9.0	-6.3
5	2	20	8.1	6.3	-0.7	-6.3
5	2	21	11.7	12.4	-4.4	11.6
5	2	22	22.0	25.1	-13.2	21.3
5	2	23	12.5	11.9	11.9	-1.4
5	2	24	5.8	6.5	5.5	3.5
5	2	25	20.7	21.7	-16.6	14.1
5	2	26	11.9	12.4	-4.5	-12.3
5	2	27	3.0	5.9	2.1	5.5
5	3	0	24.5	23.8	-23.8	0.0
5	3	1	29.0	29.5	13.4	-26.2
5	3	2	60.5	60.3	-41.2	-44.0
5	3	3	30.7	31.2	-20.8	23.3
5	3	4	38.1	37.6	36.9	-6.8
5	3	5	55.5	55.5	37.3	41.2
5	3	6	13.5	10.2	-6.1	-8.1
5	3	7	45.7	47.3	-32.1	34.7
5	3	8	37.9	36.5	36.2	4.4
5	3	9	36.3	36.4	14.5	31.3
5	3	10	44.5	44.9	-29.3	34.1
5	3	11	23.7	25.4	-10.6	-23.0
5	3	12	21.8	21.8	-17.8	12.7
5	3	13	13.2	14.4	4.3	-13.8
5	3	14	38.2	39.7	-26.5	-29.5
5	3	15	17.3	15.6	-13.0	8.6
5	3	16	18.6	16.9	16.8	-1.8
5	3	17	31.5	33.1	21.2	25.5
5	3	18	12.5	12.9	-4.5	-12.1
5	3	19	20.7	21.1	-13.5	16.2
5	3	20	16.4	17.1	17.1	-1.1
5	3	21	23.1	23.1	10.0	20.8
5	3	22	17.3	17.7	-10.4	14.4
5	3	23	9.7	10.6	-2.3	-10.4
5	3	24	7.1	12.3	-8.3	9.1
5	3	25	3.0	4.3	-1.7	-3.9
5	4	0	45.6	45.0	-45.0	0.0
5	4	1	22.8	23.0	17.3	15.1
5	4	2	23.7	24.8	24.8	0.3
5	4	3	27.2	29.6	-5.2	29.4
5	4	4	33.6	35.0	31.1	-11.0
5	4	5	31.5	33.0	33.0	2.3
5	4	6	12.5	11.4	11.1	2.3
5	4	7	25.4	25.1	-24.6	-5.0
5	4	8	21.7	21.7	-15.2	-15.6
5	4	9	17.8	18.6	2.9	18.3
5	4	10	24.5	25.9	25.1	-6.2
5	4	11	22.5	21.9	-15.1	15.9
5	4	12	32.6	32.2	-32.0	-3.3
5	4	13	10.9	9.1	6.5	6.4
5	4	14	15.1	14.7	12.2	-8.2
5	4	15	23.9	25.8	-1.5	25.8
5	4	16	23.0	25.5	-18.5	17.5
5	4	17	17.4	20.4	18.7	-8.1
5	4	18	7.6	8.8	-8.8	0.3
5	4	19	5.8	6.2	-4.2	-4.6
5	4	20	6.5	8.1	1.3	8.0
5	4	21	11.1	13.1	12.7	-3.5
5	4	22	8.4	9.5	-5.3	7.8
5	5	0	21.9	24.2	-24.2	0.0
5	5	1	36.9	38.6	-33.4	19.3
5	5	2	26.0	24.1	12.0	-20.9
5	5	3	26.9	27.9	0.0	27.9
5	5	4	17.1	16.2	-8.1	-14.0
5	5	5	31.2	33.9	-29.3	-17.0
5	5	6	7.8	4.8	4.8	0.1
5	5	7	28.5	29.2	25.3	-24.7
5	5	8	10.8	12.3	-6.2	10.6
5	5	9	12.2	12.3	0.0	12.3
5	5	10	19.5	20.5	20.5	17.8
5	5	11	29.5	31.4	27.2	15.7
5	5	12	15.9	17.6	-17.6	-0.1
5	5	13	24.7	22.9	-19.8	11.4
5	5	14	16.0	16.6	8.3	-14.4
5	5	15	28.2	28.2	0.0	28.2
5	5	16	13.4	11.9	-5.9	-10.3
5	5	17	18.6	18.5	-16.0	-9.3
5	5	18	5.0	5.2	-5.2	0.0
5	5	19	8.3	12.2	10.5	-6.1
6	0	0	55.1	55.0	55.0	0.0
6	0	1	123.0	125.1	-62.3	108.5

H	K	L	FOBS	FCAL	ACAL	BCAL
6	0	2	76.4	76.9	-38.2	-66.7
6	0	3	50.8	48.9	48.9	0.0
6	0	4	7.6	8.5	4.2	-7.4
6	0	5	65.3	65.7	-32.7	-57.0
6	0	6	63.7	62.8	-62.8	-0.2
6	0	7	66.3	66.2	33.1	-57.5
6	0	8	12.4	10.6	5.2	9.2
6	0	9	38.9	39.2	-39.2	0.0
6	0	10	52.5	54.1	-26.9	47.0
6	0	11	81.3	81.6	40.6	70.8
6	0	12	34.1	32.3	32.3	-0.2
6	0	13	80.3	81.9	-40.8	71.0
6	0	14	49.8	50.8	-25.2	-44.1
6	0	15	31.7	29.9	29.9	0.0
6	0	16	5.5	3.5	-1.8	3.0
6	0	17	22.6	21.2	-10.5	-18.4
6	0	18	25.7	24.9	-24.9	-0.1
6	0	19	22.9	22.9	11.4	-19.9
6	0	20	3.8	0.4	-0.2	-0.3
6	0	21	17.2	15.6	-15.6	0.0
6	0	22	19.2	20.5	-10.2	17.8
6	0	23	25.0	24.9	21.4	21.6
6	0	25	24.5	25.4	-12.7	22.1
6	0	26	18.1	17.9	-8.9	-15.5
6	0	27	5.2	10.1	10.1	0.0
6	1	0	38.3	36.2	-36.2	0.0
6	1	1	32.1	31.7	-5.6	-3122
6	1	2	69.5	70.9	-43.5	-56.0
6	1	3	18.7	18.7	-10.4	15.5
6	1	4	26.4	24.4	24.3	-2.5
6	1	5	60.8	61.8	18.5	59.0
6	1	6	13.6	10.8	10.4	3.0
6	1	8	48.0	47.4	-14.4	45.1
6	1	8	15.3	14.1	14.1	0.1
6	1	9	11.5	9.6	9.6	-0.4
6	1	10	59.6	61.0	-41.8	44.4
6	1	11	28.2	29.7	1.8	-29.6
6	1	12	26.2	25.1	-24.7	-4.5
6	1	13	10.2	11.5	-7.2	-9.1
6	1	14	42.0	43.2	-23.1	-36.5
6	1	15	20.9	20.2	-4.0	19.8
6	1	16	17.4	17.4	17.3	1.3
6	1	17	36.4	37.3	12.8	35.0
6	1	18	8.3	5.4	5.4	4.8
6	1	19	18.4	17.0	-6.8	15.6
6	1	20	2.7	4.8	3.0	-3.8
6	1	21	8.8	6.5	4.6	-4.6
6	1	22	27.9	29.1	-21.4	19.7
6	1	23	12.2	11.4	0.2	-11.4
6	1	24	9.2	9.5	-8.8	-3.5
6	1	25	5.9	4.8	-4.1	2.5
6	1	26	16.7	16.8	-8.1	-14.7
6	2	0	59.6	58.2	-58.2	0.0
6	2	1	27.1	26.3	20.7	16.3
6	2	2	50.0	50.6	23.0	45.1
6	2	3	21.3	20.3	7.0	19.0
6	2	4	91.5	93.3	-38.1	85.1
6	2	5	36.4	36.7	34.9	-7.5
6	2	6	26.8	25.9	25.8	1.4
6	2	7	36.4	35.2	-35.2	0.2
6	2	8	79.5	80.1	-29.3	-74.5
6	2	9	18.0	18.5	-3.9	18.1
6	2	10	37.3	37.1	17.4	-32.7
6	2	11	19.9	20.7	-11.6	17.2
6	2	12	41.7	40.7	-40.7	-1.9
6	2	13	13.3	14.5	13.1	6.3
6	2	14	24.4	22.1	8.4	20.5
6	2	15	11.6	12.8	3.5	12.3
6	2	16	46.8	48.7	-19.8	44.5
6	2	17	18.6	17.5	16.1	-5.9
6	2	18	10.9	9.8	9.6	1.8
6	2	19	17.5	17.1	-16.7	4.0
6	2	20	31.7	32.2	-8.6	-32.0
6	2	21	10.7	10.2	0.8	10.2
6	2	22	7.7	7.2	2.7	-6.7
6	2	23	11.4	7.8	-1.4	7.7
6	2	24	16.8	15.0	-14.9	-0.9
6	2	25	6.0	2.8	2.3	1.7
6	3	0	16.4	15.8	-15.8	0.0
6	3	1	36.2	37.7	-23.8	29.2
6	3	2	39.8	40.3	0.3	-40.3
6	3	3	28.4	28.8	-18.5	22.1
6	3	4	14.7	13.3	-11.0	-7.4
6	3	5	27.7	28.2	-9.2	-26.6
6	3	6	14.7	14.2	-13.2	5.5
6	3	7	25.6	25.8	13.6	-21.9
6	3	8	14.1	14.8	-6.2	13.1
6	3	9	26.3	28.2	16.2	23.1
6	3	10	23.3	23.9	2.5	23.8
6	3	11	28.1	27.9	14.1	24.1
6	3	12	15.4	15.3	-13.3	-8.0
6	3	13	25.8	25.8	-19.5	17.0
6	3	14	31.7	31.9	-2.0	-31.9
6	3	15	14.8	16.1	-9.7	12.9
6	3	16	12.9	10.0	-9.5	3.1
6	3	17	15.7	15.5	-1.4	-15.5
6	3	18	10.2	10.8	-7.2	8.0
6	3	19	11.8	11.6	8.0	-8.4
6	3	20	9.1	6.0	-1.6	5.7
6	3	21	14.3	16.0	6.8	14.5
6	3	22	9.3	7.2	1.5	7.0
6	3	23	11.1	9.5	8.7	5.7
6	4	0	44.3	44.5	-3.5	-44.4
6	4	1	33.9	34.9	-33.3	-10.5
6	4	2	24.5	26.1	-14.2	21.9
6	4	3	28.4	27.7	27.7	0.6
6	4	4	40.7	40.7	-0.2	40.7
6	4	5	17.6	17.4	-17.3	-2.0
6	4	7	35.6	35.4	-1.4	-5.3
6	4	8	23.8	22.9	22.2	-5.3
6	4	9	24.1	25.2	12.6	21.8
6	4	10	28.0	29.5	-27.3	11.2
6	4	11	34.0	33.6	5.4	-33.1
6	4	12	8.2	8.7	-8.0	3.2
6	4	13	26.3	24.4	-1.5	-25.4
6	4	14	17.8	17.6	-16.8	-5.1
6	4	15	16.1	16.7	-8.5	14.3
6	4	16	13.6	13.1	13.0	-1.1

Figure 1 (Continued)

H	K	L	FOBS	FCAL	ACAL	BCAL
6	4	17	20.3	19.7	-1.4	19.6
6	4	18	10.0	9.9	-9.5	-2.5
6	4	19	14.9	12.7	-0.7	12.7
6	4	20	10.6	8.5	6.5	-5.4
6	4	21	15.7	14.4	6.1	13.0
6	5	1	11.1	9.6	4.1	8.6
6	5	2	21.4	21.8	6.4	20.8
6	5	3	16.7	17.1	0.3	17.1
6	5	4	23.5	22.7	-11.5	19.6
6	5	5	15.4	13.5	1.9	-13.4
6	5	6	21.0	20.9	-20.9	-1.5
6	5	7	10.3	9.4	-3.9	-8.5
6	5	8	22.6	22.8	-7.4	-21.6
6	5	9	22.0	22.5	0.1	22.5
6	5	10	15.3	15.2	6.6	-13.7
6	5	11	8.0	9.4	-0.3	9.5
6	5	12	7.6	5.	5.0	1.8
6	5	13	16.8	15.2	2.3	15.1
6	5	14	9.6	7.	-0.3	7.7
6	5	15	14.3	1?.5	-8.4	8.3
6	5	16	5.1	0.7	-0.2	-8.7
6	5	17	9.8	8.1	-8.1	0.0
6	6	0	16.0	16.4	-14.1	8.3
6	6	1	24.8	23.9	11.9	-20.7
6	6	2	17.7	15.7	0.0	15.7
6	6	3	27.8	28.6	-14.3	-24.8
6	6	4	19.5	18.1	-15.7	-9.1
6	6	5	9.9	8.1	-8.1	0.1
6	6	6	19.0	19.4	16.8	-9.7
6	6	7	26.1	27.0	-13.4	23.4
6	6	8	12.2	9.8	0.0	9.8
6	6	9	15.6	15.2	7.6	13.2
6	6	10	9.6	10.4	9.0	5.3
6	6	11	5.0	5.4	-5.4	0.0
6	6	12	13.1	10.7	-9.3	5.4
7	0	0	61.4	60.5	-60.5	0.0
7	0	1	22.7	21.6	-10.8	18.7
7	0	2	4.4	4.0	2.0	3.4
7	0	3	22.9	22.4	22.4	0.0
7	0	4	66.2	67.8	-33.8	58.8
7	0	5	3.2	2.7	-1.4	-2.3
7	0	6	31.4	30.0	30.0	-0.2
7	0	7	8.9	3.3	-1.6	2.8
7	0	8	14.7	15.0	-22.5	-39.0
7	0	9	19.0	17.8	-17.8	0.0
7	0	10	19.0	14.5	7.3	-12.6
7	0	11	23.1	21.9	11.0	19.0
7	0	12	11.5	11.3	-11.3	-0.1
7	0	13	15.4	13.2	-6.6	11.4
7	0	14	14.2	13.6	-6.8	-11.8
7	0	15	16.6	16.2	16.2	0.0
7	0	16	45.6	47.8	-23.8	41.4
7	0	17	3.7	4.8	-2.4	-4.1
7	0	18	11.7	10.8	10.8	-0.1
7	0	19	.6?7	3.5	-.47	3.0
7	0	20	15.2	15.1	-7.5	-13.0
7	0	21	7.5	8.2	-8.2	0.0
7	0	22	8.1	6.7	3.4	-5.8
7	0	23	14.8	11.8	5.9	10.2
7	0	24	15.3	14.0	-14.0	-0.1
7	0	25	7.3	6.4	-3.2	5.5
7	1	0	13.5	9.3	-9.3	0.0
7	1	1	53.0	54.4	-35.2	41.5
7	1	2	47.8	49.8	-31.4	-38.6
7	1	3	14.1	14.1	3.7	13.6
7	1	4	12.1	9.9	6.3	7.7
7	1	5	41.8	42.5	-26.1	-33.6
7	1	6	17.9	17.3	-17.0	-3.0
7	1	7	35.1	35.4	20.2	-29.1
7	1	8	12.5	10.1	9.7	-2.8
7	1	9	5.4	2.4	-2.0	-1.4
7	1	10	31.6	34.2	-21.4	26.6
7	1	11	42.1	43.6	28.7	32.8
7	1	12	10.4	9.0	-7.6	4.8
7	1	13	31.8	33.0	-19.4	26.7
7	1	14	35.7	38.1	-23.2	-30.1
7	1	15	17.8	18.9	4.5	18.4
7	1	16	9.6	4.4	-4.1	9.5
7	1	17	24.3	23.9	-14.1	-19.3
7	1	18	11.0	11.1	-10.2	-4.3
7	1	19	14.3	13.8	5.5	-12.6
7	1	20	4.9	4.9	4.5	-1.9
7	1	21	4.1	5.0	-4.1	-4.9
7	1	22	13.6	14.2	-8.1	11.6
7	1	23	16.1	18.2	11.4	14.1
7	1	24	8.4	5.1	-4.0	3.2
7	2	0	4.2	1.3	-1.3	0.0
7	2	1	21.9	22.7	9.2	-20.8
7	2	2	33.3	32.6	-28.8	-15.4
7	2	3	34.8	35.2?	-32.1	14.5
7	2	4	16.7	17.1	13.1	10.9
7	2	5	19.5	19.5	11.8	15.5
7	2	6	22.4	23.1	-23.0	0.9
7	2	7	25.2	25.0	-16.6	18.7
7	2	8	22.0	22.2	8.5	-20.5
7	2	9	31.7	33.1	28.1	17.5
7	2	10	31.8	33.4	-26.3	20.6
7	2	11	11.6	11.9	-2.4	-11.6
7	2	12	4.6	3.7	-3.5	-1.2
7	2	13	18.6	19.2	10.4	-16.1
7	2	14	15.7	16.2	-15.8	-3.9
7	2	15	19.3	19.3	-17.9	7.3
7	2	16	8.7	8.0	7.3	3.1
7	2	17	8.4	4.3	4.3	4.6
7	2	18	9.4	11.3	-11.2	1.6
7	2	19	16.5	15.5	-11.5	10.5
7	2	20	16.6	16.6	1.4	-16.5
7	2	21	16.6	16.8	12.5	11.2
7	2	22	13.9	17.5	-12.6	12.2
7	3	0	17.2	15.3	-15.3	0.0
7	3	1	14.3	8.6	8.0	3.3
7	3	2	25.1	24.9	17.6	17.6
7	3	3	22.6	23.1	-15.7	17.0
7	3	4	41.6	43.5	-27.7	33.5
7	3	5	14.9	9.7	9.3	-9.3
7	3	6	11.4	9.7	-7.8	5.8
7	3	7	12.3	14.2	-10.5	-9.5
7	3	8	41.3	42.9	-27.2	-33.1
7	3	9	21.7	23.4	14.0	18.7
7	3	10	15.9	15.2	9.4	-11.9
7	3	12	15.9	15.4	-12.8	-8.5
7	3	13	8.7	7.5	7.0	2.9
7	3	14	17.7	17.3	12.3	12.0
7	3	15	11.3	13.1	-8.8	9.7

H	K	L	FOBS	FCAL	ACAL	BCAL
7	3	16	23.3	23.4	-13.9	18.9
7	3	17	8.1	7.0	4.4	-5.5
7	3	18	9.6	9.7	-4.2	8.8
7	3	19	10.5	8.5	-6.2	-5.8
7	3	20	22.0	22.6	-13.2	-18.3
7	4	0	9.0	8.6	-8.6	0.0
7	4	1	17.3	18.8	-18.6	2.1
7	4	2	15.8	15.2	7.5	-13.2
7	4	3	22.0	22.4	13.9	17.5
7	4	4	18.2	16.3	-15.3	-5.7
7	4	5	17.9	17.2	-15.9	-6.6
7	4	6	10.6	11.0	-10.5	-3.1
7	4	7	20.8	21.8	18.4	-11.6
7	4	8	17.5	17.4	-16.1	-6.7
7	4	9	16.0	17.2	-10.9	13.3
7	4	10	7.4	8.6	2.2	8.3
7	4	11	14.4	12.8	12.2	-3.8
7	4	12	8.5	8.6	-6.7	5.3
7	4	13	16.4	15.3	-11.6	4.5
7	4	14	11.1	12.2	6.4	-10.4
7	4	15	15.9	16.2	7.9	14.0
7	4	16	8.2	7.7	-7.4	-2.0
7	4	17	8.8	7.0	-7.0	-0.4
7	5	0	10.2	5.9	5.9	0.0
7	5	1	17.4	18.8	1.2	-18.8
7	5	2	17.6	15.4	-15.3	2.4
7	5	3	17.0	16.9	11.4	12.4
7	5	4	4.9	7.4	7.3	0.8
7	5	5	12.0	11.1	0.6	11.1
7	5	6	18.7	19.6	-19.4	-2.9
7	5	7	12.8	11.4	2.2	11.2
7	5	8	8.6	6.4	6.4	0.7
7	5	9	18.6	17.4	-9.2	14.8
7	5	10	15.3	13.8	-13.1	-4.3
7	5	11	12.0	14.2	-1.9	-14.0
7	5	12	6.5	6.0	3.6	4.8
7	6	0	2.9	3.3	-3.3	0.0
7	6	1	14.5	14.1	14.0	1.5
7	6	2	10.9	9.9	-3.7	9.2
7	6	3	12.7	11.7	-5.8	10.2
8	0	0	18.2	17.7	17.7	0.0
8	0	1	46.2	48.8	24.3	-42.3
8	0	2	57.0	57.6	-28.7	-50.0
8	0	3	26.1	25.6	-25.6	0.0
8	0	4	16.7	14.8	7.3	-12.8
8	0	5	47.7	48.3	24.1	41.9
8	0	6	39.7	39.5	-39.5	-0.1
8	0	7	42.4	42.3	-21.1	36.7
8	0	8	7.9	5.2	2.6	4.5
8	0	9	23.0	22.4	22.4	0.0
8	0	10	49.7	51.6	-25.7	44.7
8	0	11	35.4	35.5	-17.7	-30.7
8	0	12	12.4	11.0	11.0	-0.1
8	0	13	25.8	25.9	12.9	-22.5
8	0	14	31.1	32.3	-16.1	-28.0
8	0	15	12.3	12.6	-12.6	0.0
8	0	16	9.8	7.2	3.5	-6.2
8	0	17	20.5	21.5	10.7	18.6
8	0	18	19.6	20.5	-20.5	-0.1
8	0	19	13.0	14.6	-7.3	12.6
8	0	20	8.6	4.8	-2.4	-4.1
8	0	21	8.2	9.2	9.1	0.0
8	0	22	22.8	23.3	-11.6	20.2
8	0	23	9.4	9.5	-4.7	-8.3
8	1	0	7.5	5.2	-5.2	0.0
8	1	1	12.0	9.4	5.2	7.8
8	1	2	21.0	20.6	-6.0	20.6
8	1	3	11.2	8.9	-8.9	6.6
8	1	4	18.1	51.0	-17.7	47.8
8	1	5	14.9	8.4	-4.3	-15.6
8	1	6	16.5	16.5	-15.8	-4.9
8	1	7	13.1	11.4	-5.9	-9.8
8	1	8	50.9	51.9	-16.5	49.2
8	1	9	13.5	11.2	6.8	8.9
8	1	10	6.9	9.3	-2.1	-9.1
8	1	11	10.6	9.4	-2.8	9.0
8	1	12	12.5	9.2	-5.0	7.8
8	1	13	8.5	5.3	5.1	1.5
8	1	14	16.6	15.0	-0.6	15.0
8	1	15	25.0	26.5	-11.2	23.9
8	1	16	13.3	12.1	1.9	-11.2
8	1	17	11.8	11.4	-8.8	-7.3
8	1	18	8.7	4.2	4.2	-2.5
8	1	19	28.5	28.2	-9.3	-26.6
8	1	20	7.8	7.5	4.8	5.8
8	2	0	12.5	11.2	-11.2	0.0
8	2	1	32.1	32.1	-18.3	26.6
8	2	2	34.5	36.1	-4.2	-35.8
8	2	3	26.1	27.8	24.8	12.6
8	2	4	16.8	16.8	-12.4	-11.3
8	2	5	36.9	37.4	-16.2	-33.7
8	2	6	7.0	7.2	-7.2	0.1
8	2	7	36.4	37.7	17.7	-33.6
8	2	8	16.3	16.3	-19.1	8.7
8	2	9	20.4	21.0	-9.4	18.7
8	2	10	23.3	23.9	-3.0	23.7
8	2	11	22.1	19.6	16.3	16.3
8	2	12	10.3	8.2	-8.2	0.3
8	2	13	20.7	21.2	-11.9	17.6
8	2	14	23.7	24.9	-3.7	-24.6
8	2	15	17.3	17.6	-16.2	10.4
8	2	16	10.7	9.4	-9.4	-0.1
8	2	17	17.3	17.2	-5.7	-16.2
8	2	18	5.1	5.6	-5.6	0.2
8	2	19	18.8	17.4	7.2	-15.9
8	3	0	5.4	4.5	4.5	0.0
8	3	1	26.8	29.0	4.1	-28.7
8	3	2	12.5	8.6	-8.1	-2.8
8	3	3	15.2	16.6	8.1	14.5
8	3	4	9.1	7.4	-4.6	6.3
8	3	5	18.4	18.7	3.4	18.4
8	3	6	12.0	11.8	-0.9	-1.2
8	3	7	12.7	11.8	-2.0	11.6
8	3	8	10.8	8.3	-4.6	-7.0
8	3	9	10.1	9.2	-6.1	6.8
8	3	10	6.9	8.8	-8.8	3.4
8	3	11	27.0	26.8	-3.4	-26.7
8	3	12	6.4	4.7	-3.3	2.4
8	3	13	14.6	15.2	2.1	-15.1
8	3	14	6.4	5.0	-5.0	-1.9
8	3	15	15.4	15.5	5.4	14.5
8	4	0	15.7	13.7	-13.7	0.0
8	4	1	16.0	13.0	12.1	4.7

H	K	L	FOBS	FCAL	ACAL	BCAL
8	4	2	22.8	23.8	-0.1	23.8
8	4	3	13.6	14.1	-9.2	10.7
8	4	4	25.0	25.9	-10.8	23.5
8	4	5	18.0	18.7	9.8	-16.0
8	4	6	5.7	2.7	1.9	1.9
8	4	7	14.6	15.5	-9.8	-12.1
8	4	8	24.0	23.0	-8.3	-21.5
8	4	9	13.2	13.5	7.4	11.3
8	4	10	18.9	17.9	-0.3	-17.9
8	4	11	7.7	8.9	-7.5	4.7
9	0	0	11.8	10.8	10.8	0.0
9	0	1	16.5	16.8	-8.4	14.6
9	0	2	26.6	29.4	-14.7	-25.5
9	0	3	25.1	24.0	24.0	0.0
9	0	4	6.9	5.2	-2.6	4.5
9	0	5	22.1	20.5	-10.2	-17.7
9	0	6	27.4	26.4	-26.4	-0.1
9	0	7	30.2	29.3	14.6	-25.4
9	0	8	9.2	3.3	-1.7	-2.8
9	0	9	18.3	18.3	-18.3	0.0
9	0	10	23.0	23.6	-11.7	20.4
9	0	11	9.8	2.7	1.3	2.3
9	0	12	8.7	8.0	8.0	-0.1
9	0	13	18.1	18.1	-9.0	15.7
9	0	14	20.7	21.7	-10.8	-18.8
9	0	15	15.5	14.1	14.1	0.0
9	0	16	5.7	5.4	-2.7	4.7
9	0	17	7.0	5.4	-2.7	-0.1
9	0	18	16.4	15.9	-15.9	-4.6
9	0	19	17.8	18.6	9.3	-16.1
9	1	0	10.7	11.1	11.1	0.0
9	1	1	30.5	31.6	20.5	-24.1
9	1	2	20.7	19.9	-14.2	-13.9
9	1	3	5.4	7.0	6.1	3.4
9	1	5	19.6	21.1	17.5	11.8
9	1	6	24.1	22.6	-23.5	-2.0
9	1	7	15.4	14.5	-11.9	8.2
9	1	8	9.5	6.4	-1.5	-6.2
9	1	9	12.6	10.2	-3.9	9.4
9	1	10	15.2	16.7	-12.8	10.7
9	1	11	28.6	28.7	-19.0	-21.5
9	1	12	6.9	8.9	8.2	3.5
9	1	13	16.8	17.5	10.1	-14.3
9	1	14	14.0	14.2	-8.5	-11.3
9	1	16	11.2	7.0	-1.4	6.8
9	1	17	14.9	13.0	11.0	7.0
9	2	0	21.7	21.4	-21.4	0.0
9	2	1	15.9	12.8	12.1	-4.1
9	2	2	9.6	8.0	3.1	7.3
9	2	3	4.8	9.0	-3.4	8.3
9	2	4	25.4	27.6	-17.8	21.0
9	2	5	15.3	14.9	7.7	-12.8
9	2	6	13.4	11.0	10.9	1.8
9	2	7	11.6	11.1	-8.6	-7.0
9	2	8	21.1	20.0	-12.7	-15.5
9	2	10	9.9	9.6	4.6	-8.4
9	2	11	9.0	7.9	-7.9	0.6
9	2	12	14.4	15.6	-15.5	-2.2
9	2	13	11.9	11.5	9.4	-6.7
9	3	0	11.0	18.3	-18.3	0.0
9	3	1	5.7	7.8	-7.1	-3.2
9	3	2	12.4	13.9	-6.7	-12.2
9	3	3	16.1	15.5	12.3	9.4
9	3	4	13.7	13.9	-6.1	-8.3
9	3	5	13.7	13.9	-8.5	-11.1
9	3	6	12.8	10.6	10.6	-0.3
9	3	7	11.9	11.5	7.8	-8.4
9	3	9	10.8	10.9	-10.3	3.7
10	0	0	18.0	18.5	-18.5	0.0
10	0	1	10.2	9.2	4.6	-7.9
10	0	2	21.6	20.1	10.0	17.4
10	0	3	19.8	20.2	-20.2	0.0
10	0	4	38.2	41.1	-20.4	35.6
10	0	5	9.6	8.9	-4.4	-7.8
10	0	6	10.4	9.3	9.3	-0.1
10	0	7	4.8	3.2	1.6	-2.8
10	0	8	35.7	36.5	-18.2	-31.7
10	0	9	19.1	17.2	17.2	0.0
10	0	10	13.6	13.3	6.6	-11.5
10	0	11	5.7	4.4	-2.2	-3.8
10	0	12	12.1	12.5	-12.5	-0.1
10	0	13	9.1	10.9	5.5	-9.5
10	0	14	15.0	10.0	5.0	8.7
10	0	15	13.0	9.7	-9.7	0.0
10	1	0	14.6	11.3	-11.4	0.0
10	1	1	7.4	4.8	4.8	-0.1
10	1	2	22.2	23.8	-7.6	-22.6
10	1	3	8.9	8.7	8.3	2.7
10	1	4	8.0	7.8	-3.3	-7.1
10	1	5	17.5	15.5	-1.9	-15.4
10	1	6	7.0	7.1	6.7	2.2
10	1	7	12.8	12.3	0.0	-12.3
10	1	8	10.7	10.7	-2.7	10.3
10	1	9	9.1	8.2	-6.7	4.7
10	1	10	16.3	16.0	-6.4	14.7
10	1	11	5.0	2.4	-2.3	0.6
10	1	12	10.5	9.0	-8.4	-3.1
10	2	0	17.5	18.5	13.5	0.0
10	2	1	24.7	26.5	5.2	-26.0
10	2	2	14.7	12.9	-10.0	-8.1
10	2	3	8.1	4.8	2.8	4.4
10	2	4	4.1	3.4	0.9	4.7
10	2	5	10.4	12.1	2.1	11.9
10	2	6	18.1	18.0	-18.0	-0.7
11	0	0	12.8	12.9	12.9	0.0
11	0	1	21.6	21.2	10.6	-18.4
11	0	2	13.7	13.8	-6.9	-12.0
11	0	3	12.8	8.4	-8.4	0.0
11	0	4	8.6	3.5	1.7	-3.0
11	0	6	11.5	11.5	-11.5	-0.1
11	0	7	7.7	5.0	-2.5	4.4
11	0	8	5.0	2.5	-1.3	-2.1

are listed.

Discussion

The $CsCuCl_3$ structure consists of distorted hexagonally close-packed layers of cesium ions and chlorine atoms, with the copper atoms, located on the two-fold axes, occupying all the octahedral holes which have six chlorine nearest neighbors. Two chlorines are at a distance of $2.35Å$, two at $2.28Å$ and two at $2.78Å$ from the coppers (Figure 2). The distortion from perfect close-packing is slight with $Cl(2')$ $0.149Å$ above the plane and $Cl(2)$ the same distance below (Figure 3). The copper atoms are $0.42Å$ from the 6_1 c-axis and are oriented to form spiraling chains by sharing faces of the chlorine octahedra about them. One of the bridging chlorines, $Cl(1)$ is bound symmetrically to two coppers - a feature that has been found in all the garnet-colored copper compounds (5, 6). The three-dimensional character of the compound can be considered to be an infinite parallel chain held together by cesium ions. The more important bond distances and angles along with their standard deviations can be seen in Figures 1 and 2.

A very interesting feature of the structure is the very short copper-copper distance. As can be seen in Table 3, this distance is much shorter than that found in any other halogen-bridged copper compound. Two possible explanations for this short distance can be proposed: (1) the copper atoms form copper-copper bonds along the chain axis, thus bonding each copper strongly to four chlorines, weakly to two others and to two neighboring copper atoms, or (2) in this compound, the copper octahedra are connected together by sharing faces while in the other compounds listed in Table 3,
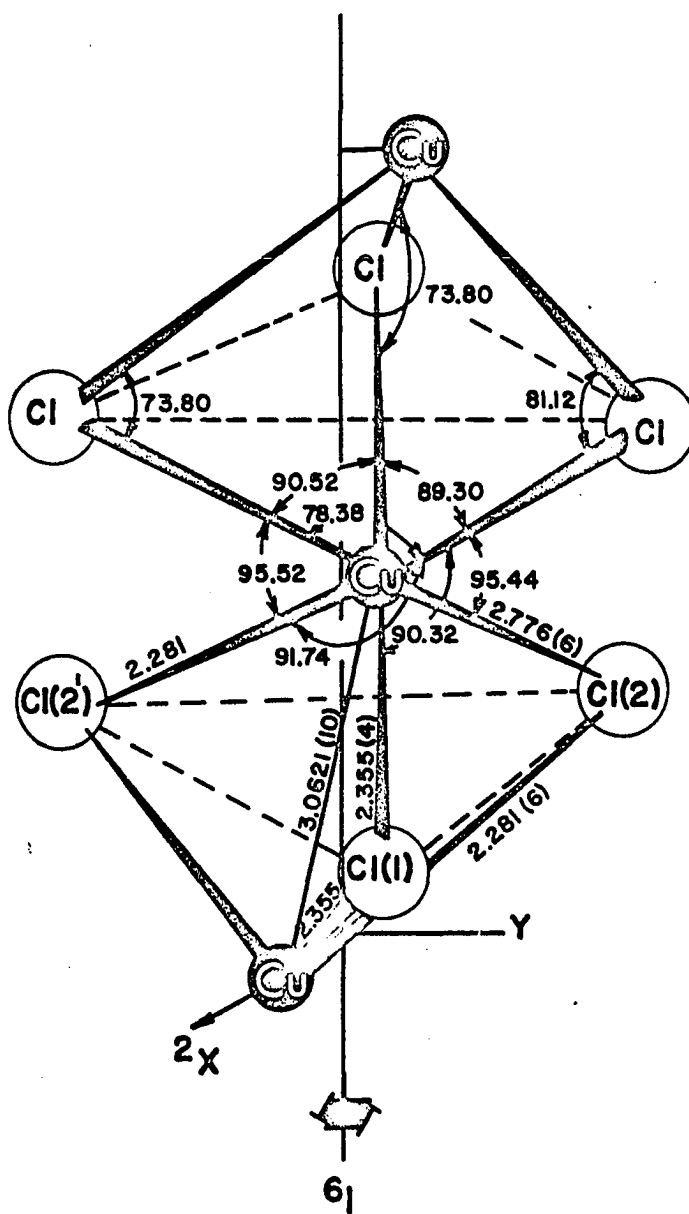
Figure 2. The molecular configuration of $CuCl_3^-$ in $CsCuCl_3$
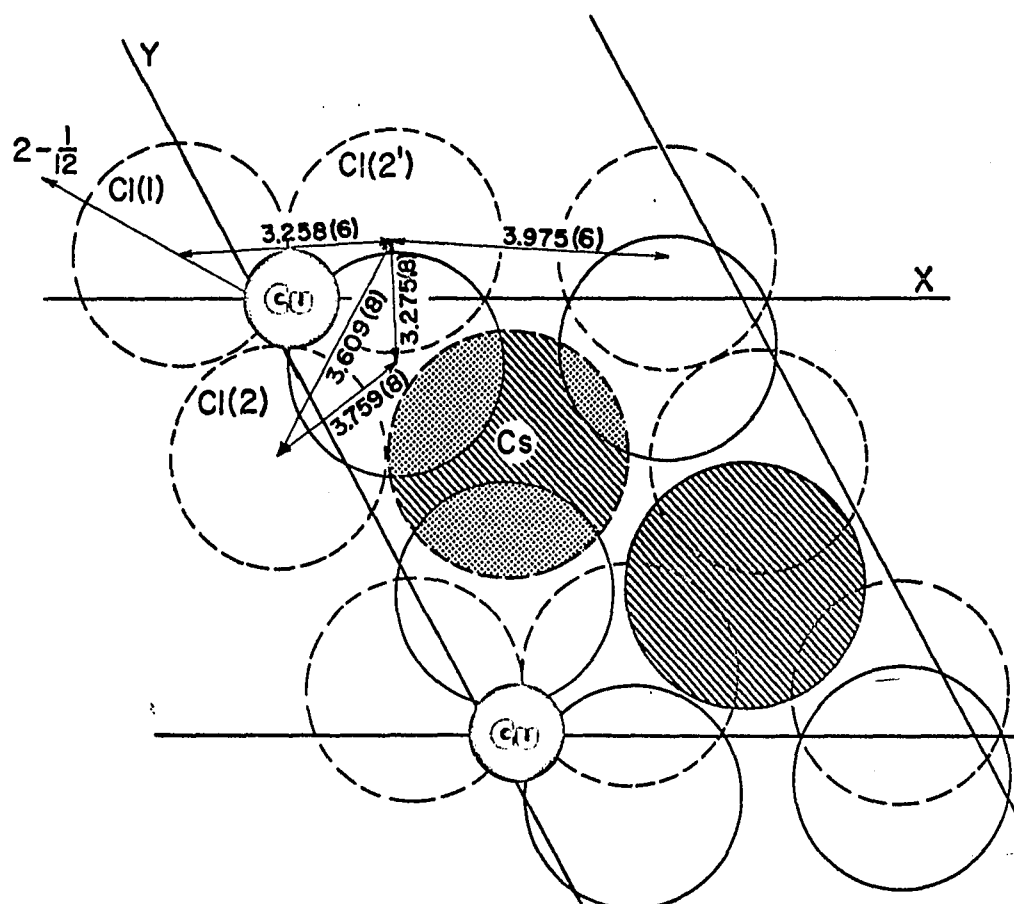
AVERAGE Cs-Cl DISTANCE 3.629 (2)

Figure 3. The hexagonal close packing in CsCuCl$_3$

the octahedra are connected together by sharing edges. The sharing of faces would force the copper-copper distance to be shorter than in the other compounds previously investigated. In this description, no direct copper-copper bonding is suggested.

Evidence seems to support the latter explanation. As can be seen from Table 3, the angles in $CsCuCl_3$ are distorted from the angles observed in the other copper compounds in such a way as to suggest the sharing of faces. Further evidence for the latter explanation is found in overlap integral calculations. In order to consider the likelihood of the formation of a metal-metal bond, D_{3d} symmetry was assumed at a copper atom. Under this symmetry, the representation for sigma bonding by copper breaks down into the irreducible representations: $2A_{1g} + E_g + 2A_{2u} + E_u$. Considering only

Table 3. Distances and angles in copper chloride compounds

Formula	Cu-Cu	Average Cl-Cu-Cl	Average Cu-Cl-Cu
$KCuCl_3$	$3.443Å$	$84.1°$	$95.9°$
$LiCuCl_3 \cdot 2H_2O$	3.47	85.	95.
NH_4CuCl_3	3.42	84.9	
$Cu_2Cl_4(CH_3CN)_2$	3.39	86.	94.
$Cu_3Cl_6(CH_3CN)_2$	3.346	88.	94.2
$Cu_5Cl_{10}(C_3H_7OH)_2$	3.310	87.	92.8
$CuCl_2 \cdot 2H_2O$	3.73		92.9
$CuCl_2$	3.30	87.	
$CsCuCl_3$	3.0621	90.2	76.2

the chlorine atoms, the sigma bonds transform as $A_{1g} + E_g + A_{2u} + E_u$. This leaves A_{1g} and A_{2u} for metal-metal bonding in this simple treatment. The A_{1g} transforms as d_z2 which is directed right at the copper atoms along the chain, while A_{2u} is a non-bonding orbital. Thus, metal-metal bonds could possibly be formed by sigma overlap of $3d_z2$ orbital along the chain axis.

In order to calculate the extent of the overlap in the above case, it is necessary to discuss the manner in which overlap integrals are computed. Overlap integrals are most conveniently calculated by utilizing ellipsoidal coordinates ξ, η and φ (11) given by $\xi = (r_a + r_b)/R$, $\eta = (r_a - r_b)/R$ and $\varphi = \varphi_a = \varphi_b$ where R is the distance between atoms a and b, r_a is the distance from an electron at point P to atom a, and r_b is the distance of that electron from atom b. Since the overlap values differ for different pairs of atoms and for various interatomic distances, the overlap integrals are usually expressed in terms of suitable parameters and the overlap values calculated and listed as a function of the chosen parameters (see Table 4 for $3d_z2$-$3d_z2$ overlap values). For this purpose, the parameters p and t have been defined as:

$$p = \tfrac{1}{2}(\mu_a + \mu_b)R/A_H$$
$$t = (\mu_a - \mu_b)/(\mu_a + \mu_b)$$

where μ is the orbital exponent, ($\mu = (Z - \sigma)/n^*$, where Z = atomic number, σ = shielding constant and n^* = effective quantum number), and A_H is the Bohr radius. Using these parameters, the overlap integral for two $3d_z2$ orbitals can be expressed as a rather complex integral which can be evaluated (11, 12).

It can now be noticed that in evaluating overlap integrals between

Table 4. Overlap integrals for sigma $3d_{z^2} - 3d_{z^2}$ bonding; t = 0.0

p	Overlap	p	Overlap	p	Overlap
0.000	1.000000	6.500	0.138303	13.000	0.027932
0.500	0.936482	7.000	0.154959	14.000	0.016465
1.000	0.767291	7.500	0.160719	15.000	0.009362
1.500	0.543780	8.000	0.157532	16.000	0.005163
2.000	0.321797	8.500	0.147793	17.000	0.002772
2.500	0.142244	9.000	0.133840	18.000	0.001455
3.000	0.024182	9.500	0.117733	19.000	0.000748
3.500	-0.032410	10.000	0.101028	20.000	0.000378
4.000	-0.039597	10.500	0.084868	22.000	0.000092
4.500	-0.014288	11.000	0.069983	24.000	0.000021
5.000	0.027059	11.500	0.056771	26.000	0.000005
5.500	0.071378	12.000	0.045388	28.000	0.000001
6.000	0.109986	12.500	0.035817		

identical atoms in identical environments the orbital exponents of atoms a

and b will be the same and thus, t = 0. This simplifies the problem be-

cause in this case, the overlap values need only be calculated as a func-

tion of p, where now, $p = \mu R/A_H$. It can be seen from this case that the

value of the orbital exponent is of crucial importance in determining the

overlap value at a given value of R. If for example, μ is taken at only

half its proper value, the maximum overlap will be associated with an

interatomic distance twice as great as it should be. The values which fol-

low were determined using the orbital exponents calculated by Clementi

(13): these values are listed in Table 5 for the 3d orbitals of the first

transition metal series, and for comparison, the values calculated using

Slater's rules (14) are also listed. Clementi's values were calculated

using sets of self-consistent atomic orbitals and appear to be the most

accurate reported to date. It still must be realized that even if accurate

Table 5. Comparison of Slater and Clementi 3d orbital exponents

Atom	Slater orbital exp.	Clementi orbital exp.
Sc	1.00	2.3733
Ti	1.22	2.7138
V	1.43	2.9943
Cr	1.65	3.2522
Mn	1.87	3.5094
Fe	2.08	3.7266
Co	2.30	3.9518
Ni	2.52	4.1765
Cu	2.73	4.4002
Zn	2.95	4.6261

orbital exponents are used, these calculations give only an approximate value of the overlap because the overlap values are calculated based on orbital exponents of isolated atoms and the orbital exponents are certainly affected when that atom is chemically bonded. To investigate this effect, the iron-iron bond in diamagnetic $Fe_2(CO)_9$ was considered. In this compound, the electron density on the iron atoms would be increased by the three bridging and three terminal carbonyls, thus shielding the d electrons more effectively, causing these orbitals to increase in size. Calculating the overlap for the iron atoms, 2.46Å apart (15), using Clementi's value of the orbital exponent, a value of only 0.003 is obtained. If, however, the orbital exponent is decreased by only 1/3 (equivalent to additional shielding of one electron), an overlap of 0.05 results, which is appreciable considering that the maximum $3d_{z^2}$ - $3d_{z^2}$ overlap is less than 0.17. This calculation illustrates the importance of the orbital exponent, but also shows that the maximum likely change in the overlap is approximately one order of magnitude. Therefore, if an extremely small value of overlap is calculated, it can be concluded that essentially no interaction

occurs.

In considering, now, the overlap between two copper atoms in $CsCuCl_3$ the calculated value would be expected to be more nearly correct than in the $Fe_2(CO)_9$ example above because the chlorine atoms would not effect the copper electron density as much as the carbonyls effect the iron's electron density. Thus, the overlap associated with a sigma $3d_z2$ bond between two copper atoms $3.062Å$ apart is less than 10^{-5} and this value is so small that the metal-metal bond order must be considered as essentially zero. This result is confirmed by the magnitude of the magnetic moment for $CsCuCl_3$ which is normal for one unpaired electron down to $80°K$ (16).

Similar calculations for other metal-halogen systems lend credence to this type of approach. Thus, for $CsNiCl_3$, which crystallizes in a close-packed structure isomorphous with $CsCuCl_3$ with a nickel-nickel distance of $2.96Å$ (17), the overlap integral for $3d_z2$ orbitals between nickel atoms is less than 10^{-4}, and $CsNiCl_3$ also has a normal moment for two unpaired electrons (18). Overlap calculations have also been performed for $TiCl_3$ and $ZrCl_3$, the structures of which have recently been deduced from powder diffraction studies (19). These compounds have D_{3d} symmetry at the metal and form chains similar to $CsCuCl_3$ by sharing faces of chlorine octahedra. The metal-metal distance in both of these imomorphous compounds is $3.07Å$ (19). The calculation of the overlap integrals for sigma d_z2 overlap gave a value of approximately 0.01 for the titanium-titanium bonds and 0.10, almost the maximum possible overlap for $4d_z2$ orbitals, for the zirconium-zirconium bonds. Subnormal magnetic moments have been

observed for these substances. $TiCl_3$ has a moment of 1.38 B. M. (compared to the normal moment for one unpaired electron of 1.75 B. M.) indicating some interaction between the metals, and $ZrCl_3$ is almost diamagnetic with a moment of only 0.4 B. M. (20). In the latter case, the fourteen sigma bonding electrons (1 from Zr^{+3}, 12 from six chlorines and $\frac{1}{2} \times 2$ from two neighboring zirconium atoms) enter the A_{1g}, E_g, E_u and A_{1g}' bonding orbitals, the last being the metal-metal d_z2-d_z2 bonding orbital.

This treatment thus consistently explains the magnetic properties of the above materials and also gives evidence that no direct metal-metal bonding occurs in $CsCuCl_3$. In fact, from these overlap calculations, it was found that for the metals at the right of the first transition series, the single bond length for d_z2-d_z2 sigma bonding is so extremely short that such metal-metal bonding cannot possibly occur unless there are gross changes in the orbital exponent of the combined metal.

The choice of orbital exponents also has a strong bearing on any discussion of the bonding in copper acetate monohydrate where many approaches have been used to attempt to explain the short copper-copper distance (21 - 27). All, until recently, have invoked some sort of direct 3d-3d bonding, the delta bond being very popular; however, none has been completely successful in explaining all the observed data. Our calculations of overlap rule out any direct 3d-3d bonding. Since our calculations were made, Kokoszka (28, 29), and Hansen and Ballhausen (30) have given consistent interpretations of the available data assuming no direct copper-copper interaction.

Further Applications of

Accurate Overlap Calculations

The above calculations show that overlap integrals represent a reliable method of evaluating the existence of direct metal-metal interactions. However, the above examples do not illustrate the cases where overlap calculations can be most valuable. In the cases considered, the cation-anion-cation angles were all near 90° and in these cases, super-exchange through the bridges is very weak (31). Thus, the pairing of electrons, where observed, can generally only be attributed to direct cation-cation interactions. The case of metal oxides, however, represents a more ambiguous situation because the generally larger cation-anion-cation angle can allow a strong super-exchange mechanism to pair electrons. Cation-anion-cation and cation-cation interactions have been considered by many people (31 - 36). The radial extension of the d-orbital functions has been mentioned as a contributing factor in cation-cation interactions by several, but very little use has been made of this factor to explain the magnetic features of these compounds. By using other information such as the magnitude of the ligand-field splitting and the degree of covalency in the anion-cation bond, Goodenough (35) has been able to deduce results concerning cation-cation bonding which could have been readily deduced from orbital overlap calculations using reliable orbital exponents. For example, he considers the NaCl type compounds (35), which can be considered as cubic close-packed anions with cations occupying all octahedral holes. These compounds are of particular interest because each anion octahedron shares both corners and edges with neighboring octahedra and thus, both

direct cation-cation and cation-anion-cation interactions are possible.
Goodenough concludes for the metal oxides, MO, if $m \geq 5$ (where m = the
number of 3d electrons), cation-anion-cation interactions predominate over
direct interactions whereas, if $m \leq 3$, the cation-cation interactions may
be stronger than the bridged path (35, 37). This is exactly the conclusion
which a consideration of overlap integrals would lead to, because the ra-
dial extension of the d-orbitals for elements with $m \geq 5$ is so small, sig-
nificant overlap occurs only at prohibitatively small distances. Thus,
overlap integral values represent a good way of determining the extent of
metal-metal bonding and would be particularly powerful if a greater under-
standing of the effect of ligands on the cation orbitals could be achieved.

THE STRUCTURE OF $C_{10}H_8Mo_2(CO)_6$

Introduction

Three independent three-dimensional X-ray analyses of the structure of of dibenzenechromium have produced conflicting results concerning the nature of metal-aromatic π-bonding. The discussion involves the question as to whether the double bonds in the π-bonded benzene are localized or not. Jellinek (38, 39) found a significant difference in adjacent bond lengths which he interpreted to be the result of a partial localization of electrons resulting from the bonding of the chromium. Cotton, Dollase and Wood (40), however, found all the C-C bonds equivalent within the estimated error and thus, no localization. Ibers (41) considered the comparison of adjacent C-C bonds to be less reliable than a comparison of parallel refinements of the structure of both models. Using the data of Cotton, et al., he independently refined both models and found the data to be consistent with D_{6h} symmetry for the dibenzenechromium molecule. Theoretical treatments have been produced for both models (42 - 46). More recently, Bailey and Dahl have determined the structure of hexamethylbenzenechromium tricarbonyl (47), thiophenechromium tricarbonyl (48), and benzenechromium tricarbonyl (49). These structures further support delocalization in π-bonded arene systems. In addition, recent spectral data have given additional evidence for the D_{6h} model (50).

Because of the interest in the question of localization of double bonds in π-bonded systems, it was decided to determine the structure of azulenedi-iron pentacarbonyl. Some analogues of this compound prepared

by Wilkinson existed as two isomers identical in all physical properties, but separable by an ion exchange column (51). This fact seemed to indicate the possibility of the existence of two isomers differing only in the position of the localized double bonds, and this evidence as well as NMR evidence for two non-equivalent hydrogens led Wilkinson to suggest localized double bonds in these compounds (51). While localization in the benzene-chromium case must be considered disproven, there is reason to believe that localization in a π-bonded azulene system would be more likely. This is true because the resonance energy of azulene has been reported as 35 (52) and 46 kcal./mole (53) as compared to 61 (52, 53) for naphthalene. It would seem, then, that since less energy would be lost in localizing double bonds in azulene, it would be more likely that the gain in energy from the strengthened metal-ring bonds in the localized system would be more likely to offset the loss in a π-bonded azulene than in a π-bonded naphthalene system. Thus, it seemed likely that an X-ray structure determination might reveal the existence of alternating double-single bonds in azulene-iron pentacarbonyl. If the data were not good enough to reveal this, at least the correct structure of the three proposed by Wilkinson (see Figure 4) could be determined.

Before attempting this structure, it was noted that the structure of molecular azulene was disordered (54). While the likelihood of this was considered for the complexed azulene, it was felt that the structures "b" and "c" of Figure 4, which were most likely correct, were asymmetric enough to prohibit azulene disorder in the lattice. Thus, attempts were made to grow single crystals of the iron-azulene complex. Unfortunately, all attempts to grow crystals from a multitude of solvents as well as by subli-

(a)

(b)

(c)
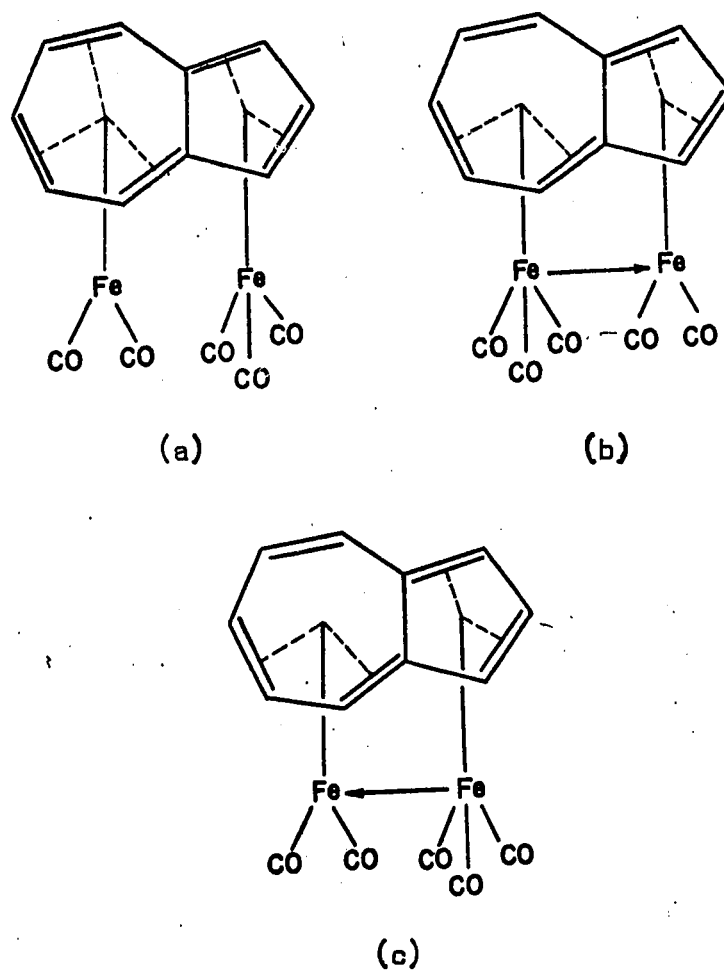
Figure 4. Suggested structures for $C_{10}H_8Fe_2(CO)_5$

mation, failed. As a result, efforts were directed toward azulene dimolyb-
denum hexacarbonyl, and crystals of it were successfully grown. This com-
pound was also prepared by Wilkinson, but because of quite limited solu-
bility, very little structural data could be obtained. It was felt, how-
ever, that the nature of the metal-azulene bonding would be revealed as
well by this compound as the iron complex.

Samples of both the molybdenum and iron compounds were kindly sup-
plied by R. B. King.

Experimental

Dark red crystals of the molybdenum compound were grown from a chlo-
roform solution. Small prismatic crystals formed which had very sharply
defined faces. A crystal was mounted in a capillary, and Weissenberg and
precession pictures taken. All pictures showed an absence of mirroring,
implying a triclinic space group. A cell was found with the following
parameters:

$$a = 9.567\text{Å} \qquad \alpha = 103.06°$$

$$b = 7.023 \qquad \beta = 130.68$$

$$c = 16.323 \qquad \gamma = 70.59,$$

which contained two molecules.

Complete three-dimensional data to $\sin \theta/\lambda = 0.704$, were taken with
zirconium filtered molybdenum K_α radiation using a General Electric XRD-5
X-ray unit equipped with a single crystal orienter. Using a take-off angle
of $8°$, a receiving aperature of $2.4°$ and a forty second stationary crystal-
stationary counter counting technique, intensities for 4932 reflections

were obtained and indexed for the above cell. A number of backgrounds
were compiled for differing values of chi and phi and were plotted as a
function of two-theta. A slight phi dependence was observed and three
background curves made up. Background, streak, absorption, polarization
and Lorentz corrections were made on the intensities. The streak correc-
tions were made using two modifications of the method of Williams (55),
where the streak is calculated as:

$$I_s^n = \frac{I_m Lp(\theta_n)\cos\theta_n}{\sin\theta_n} K(\frac{n}{m})$$

where m stands for an mth order reflection occurring at a lower two-theta
than the nth order, and K is an experimentally obtained constant which is
a function of λ. It is obtained from an average of the streak constants
determined from the streaks of several prime reflections. They are calcu-
lated from the formula:

$$K = \frac{I_s Lp(\theta_p)\tan\theta_s}{Lp(\theta_s)I_p},$$

where p stands for peak and s for streak. A correction was also applied to
convert peak height data to integrated intensity data. The corrections
were calculated using the two-theta separation of $K\alpha_1$ and $K\alpha_2$ for Mo radia-
tion given by Furnas (56), and the formulae given by Alexander and Smith
(57). The standard deviations in the observed structure factors were cal-
culated in the manner described in the $CsCuCl_3$ experimental section. The
conventional reduced cell was calculated (58) and the reflections trans-
formed to this cell. Accurate reduced cell lattice constants were deter-
mined by a least squares treatment (8) of sixteen reflections observed us-
ing a single crystal orienter, and CrK_α radiation. These reflections with

their observed and calculated two-theta values are listed in Table 6.

Table 6. The accurate lattice constant data for $C_{10}H_8Mo_2(CO)_6$

H	K	L	Observed two-theta	Estimated error	Calculated two-theta
7	5	0	153.70^o	0.05^o	153.66^o
-2	10	0	157.92	0.04	157.81
-8	1	1	154.61	0.02	154.60
-5	8	1	155.85	0.02	155.88
-4	9	1	158.23	0.02	158.21
8	3	-3	154.08	0.02	154.07
6	7	-3	151.51	0.02	151.49
5	8	-3	155.13	0.03	155.19
6	6	-4	157.03	0.02	157.03
5	7	-4	162.20	0.03	162.20
7	0	-5	158.07	0.02	158.04
7	1	-5	160.21	0.02	160.24
-7	0	-1	155.93	0.02	155.93
-1	10	-1	159.35	0.02	159.38
-1	9	-2	150.33	0.02	150.31
-2	7	-3	155.67	0.02	155.66

The orienter was previously aligned with an aluminum single crystal before the data were taken. The final lattice constants obtained along with their standard deviations are:

$$a = 9.791 \pm 0.001 Å \qquad \alpha = 87.68 \pm 0.01^o$$

$$b = 12.402 \pm 0.001 \qquad \beta = 113.11 \pm 0.01$$

$$c = 6.995 \pm 0.001 \qquad \gamma = 86.75 \pm 0.01.$$

Structural Refinement

A Patterson map was generated using all the collected intensities. The resulting map contained five large peaks considered to be molybdenum-

molybdenum vectors. All their peaks occurred on or near the W × 0 section. The largest, with coordinates ($\frac{1}{2}$, $\frac{1}{2}$, 0), had a multiplicity of four, and the others a multiplicity of two. These peaks could only be interpreted as resulting from a set of C-centered molybdenum atoms. A check of the intense reflections revealed that all but a very few corresponded to the h + k = 2n type. The positional parameters were then determined from the Patterson to be:

Mo1   0.09125, 0.21125, 0.0

Mo2   0.40875, 0.28875, 0.0,

assuming the space group to be P$\bar{1}$. Two cycles of positional refinement on the molybdenum atoms, using the 1500 most intense reflections, lowered the agreement factor for these data to 0.34. It was thought that difficulties might be encountered in finding the carbonyls and rings because of the presence of a false image arising from the pseudo-centering. However, the least squares refinement of the molybdenum positions succeeded in determining signs of enough h + k = 2n + 1 reflections that the centered image was essentially destroyed. Faint C-centered images of carbonyls could be seen in an electron density map calculated from the refined molybdenum positions but no difficulty was encountered in finding one set of carbonyls and the azulene ring in the map. Two cycles of positional refinement on all atoms reduced the R-factor to 0.181. Further isotropic refinement on all atoms gave an agreement factor of 0.0986 for the 1500 most intense reflections. An electron density map generated from these parameters showed several extra peaks occurring near the azulene ring. These peaks could be interpreted as resulting from disorder in the azulene ring. However, it was

also thought that they could be the result of refinement in the wrong

space group. That is, it was thought that the rings could be inconsistent

with a center of symmetry and thus, that refinement in the space group $P\bar{1}$

was producing the second image. To check this last possibility, the two

molecules in the unit cell were input with the rings, (but only the rings),

inconsistent with the center of symmetry and positioned such that they

would generate all the observed peaks if a center of symmetry was assumed.

Two cycles of least squares on these parameters were run assuming only P1

symmetry, and an electron density map generated. The disorder in the im-

ages still existed, and thus it was concluded that the ring disorder was

real. Judging from the heights of the disordered atoms, it appeared as if

the disorder was 50-50. The disorder was only visible in the four central

carbons, as can be seen in Figure 5. Refinement on the disordered model,

with molybdenums anisotropic, reduced the agreement factor to 0.0421 on the

1500 most intense reflections. At this point, approximately fifty reflec-

tions were removed for which the agreement between F_o and F_c was poor.

Since the structure was over-determined and since the data were taken by

stationary methods, where errors in setting are less likely to be caught,

it was felt that this was justified. Fritchie (59) further justifies this

action by pointing out the fact that a few bad reflections can severely

affect bond distances and thus, if at all questionable, should be rejected.

Refinement continued for two cycles, with the molybdenum atoms anisotropic,

using the remaining 3545 observed reflections, and a final agreement factor

of 0.0606 was obtained. Before the last cycle, a weighting scheme check

was run and the weights were found to be inadequate. They were changed
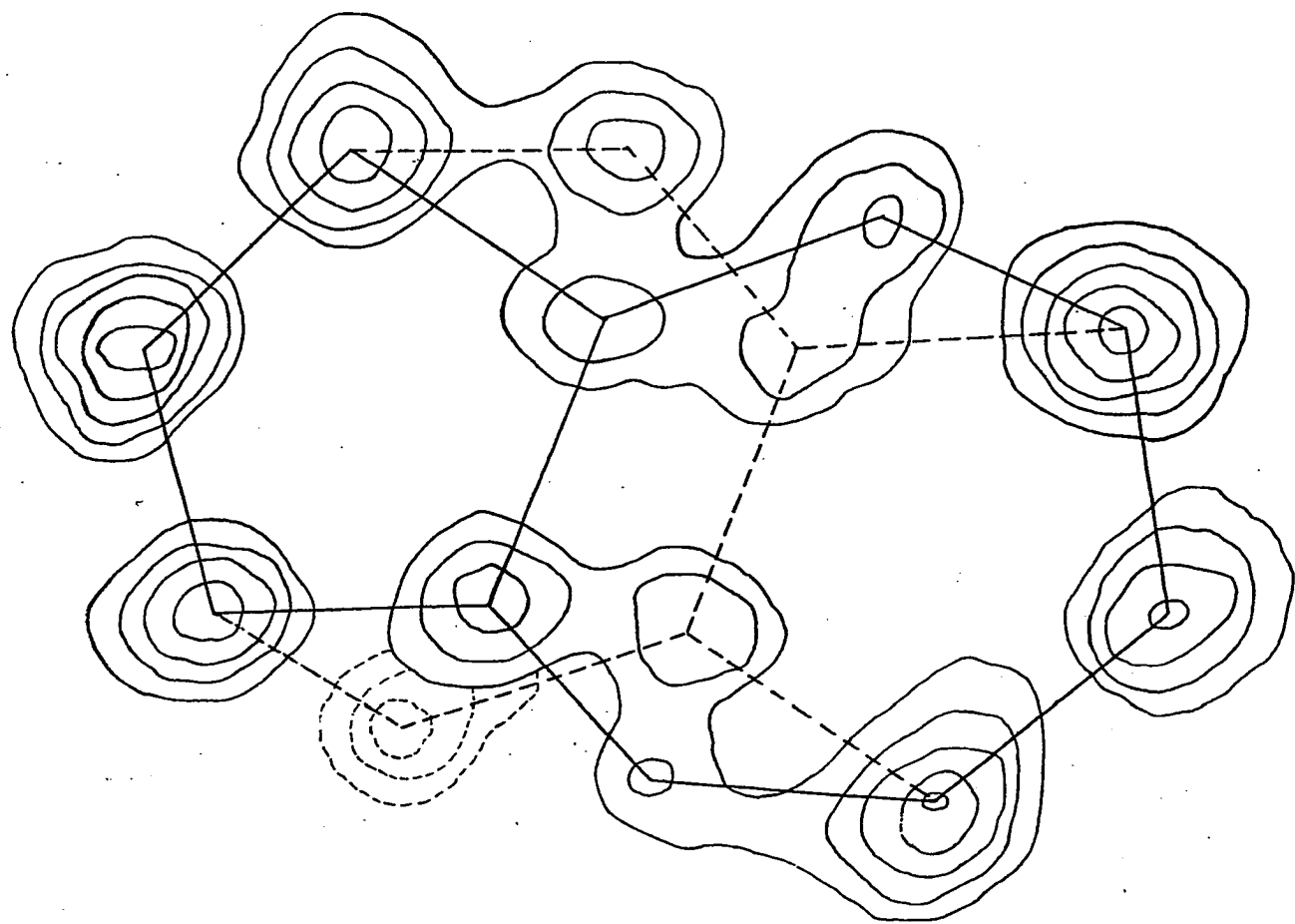
Figure 5. The disorder in the azulene ring in $C_{10}H_8Mo_2(CO)_6$

such that a plot of $\Delta^2 w$ (where $\Delta^2 = (|F_o| - |F_c|)^2$ and $w = $ (scale factor)$^2/$

sigma^2), versus average F_o for groups of one-hundred reflections, gave a

straight horizontal line. The final weighted R-factor with these weights

was 0.0576. The final parameters can be seen in Table 7. In Figure 5,

the molecular structure can be seen. The final distances and angles with

standard deviations were calculated using Busing's ORFFE program (60), and

are listed in Table 8. In Figure 7 are listed the observed and calculated

structure factors. A final electron density map clearly showed anisotropic

motion in the carbonyl oxygens, but no evidence could be seen for disorder

in any but the previously mentioned four atoms. No evidence of the azu-

lene hydrogens could be seen, possibly because of the disorder. Because

of the great length of time required per least squares cycle, anisotropic

refinement of the light atoms was not attempted.

Discussion

The structure of azulene dimolybdenum hexacarbonyl can be profitably

compared with π-cyclopentadienyl molybdenum tricarbonyl dimer (61). The

dimer is held together solely by a long molybdenum-molybdenum bond of

3.222 which compares very well with the 3.262 observed in the azulene

compound. The other distances compare very favorably also: 2.345Å molyb-

denum-ring carbon and 1.960Å molybdenum-carbonyl distances compared to

2.325 and 1.968 respectively observed in the azulene complex. Thus, the

moiety associated with the molybdenum bound to the five membered ring of

azulene can be considered as virtually identical with half of the dimer.

Table 7. Final parameters and standard deviations from least squares refinement of $C_{10}H_8Mo_2(CO)_6$

Atom	X	Sigma X	Y	Sigma Y	Z	Sigma Z	B^a	Sigma B
Mo1	0.07975	0.00006	0.21386	0.00004	-0.04246	0.00008	-----	-----
Mo2	0.40684	0.00006	0.28941	0.00004	-0.00520	0.00007	-----	-----
C1	-0.04728	0.00086	0.28845	0.00062	-0.36471	0.00114	4.628	0.292
C2	-0.07348	0.00089	0.17759	0.00063	-0.36489	0.00118	4.841	0.306
C3	0.04690	0.00084	0.09858	0.00059	-0.32328	0.00110	4.191	0.275
C4	0.17470	0.00146	0.16871	0.00106	-0.29576	0.00189	3.440	0.446
C5	0.32723	0.00156	0.12847	0.00114	-0.22973	0.00205	3.836	0.486
C6	0.43937	0.00081	0.17886	0.00059	-0.27264	0.00108	4.242	0.272
C7	0.46031	0.00082	0.28813	0.00058	-0.30411	0.00109	4.288	0.275
C8	0.34213	0.00079	0.36734	0.00055	-0.32662	0.00105	3.987	0.257
C9	0.20550	0.00143	0.37362	0.00108	-0.29841	0.00187	3.435	0.440
C10	0.11618	0.00147	0.28573	0.00109	-0.32126	0.00185	3.295	0.431
C4'	0.20155	0.00134	0.09878	0.00100	-0.25461	0.00176	2.942	0.399
C5'	0.28088	0.00142	0.18448	0.00103	-0.28429	0.00183	3.056	0.436
C9'	0.22078	0.00136	0.30034	0.00101	-0.31570	0.00175	3.016	0.400
C10'	0.07646	0.00170	0.34144	0.00126	-0.31190	0.00216	4.069	0.536
C11	0.06555	0.00070	0.34154	0.00051	0.13191	0.00094	3.412	0.221
O1	0.04846	0.00059	0.41706	0.00042	0.22810	0.00077	4.858	0.207
C12	-0.08578	0.00077	0.17178	0.00055	0.03597	0.00102	3.906	0.251
O2	-0.17795	0.00067	0.14280	0.00045	0.08647	0.00087	5.909	0.244
C13	0.19370	0.00070	0.11189	0.00050	0.17540	0.00093	3.284	0.217
O3	0.25150	0.00057	0.04685	0.00041	0.29236	0.00076	4.791	0.205
C14	0.49196	0.00071	0.18462	0.00050	0.21757	0.00094	3.319	0.220
O4	0.55065	0.00058	0.12248	0.00041	0.34244	0.00077	4.859	0.205
C15	0.60141	0.00079	0.34303	0.00055	0.11345	0.00101	3.939	0.246
O5	0.71913	0.00065	0.37416	0.00045	0.18922	0.00084	5.469	0.226
C16	0.35863	0.00070	0.41144	0.00052	0.15977	0.00094	3.322	0.218
O6	0.33737	0.00058	0.48768	0.00043	0.24875	0.00078	4.903	0.208

^{a}Anisotropic thermal parameters: β_{11}, β_{22}, β_{33}, β_{12}, β_{13}, β_{23},

Mo1: 0.01047(8), 0.00500(4), 0.01584(12), -0.00093(4), 0.00486(7), -0.00089(5),

Mo2: 0.00924(7), 0.00562(4), 0.01703(13), -0.00107(4), 0.00182(7), -0.00080(5).

36
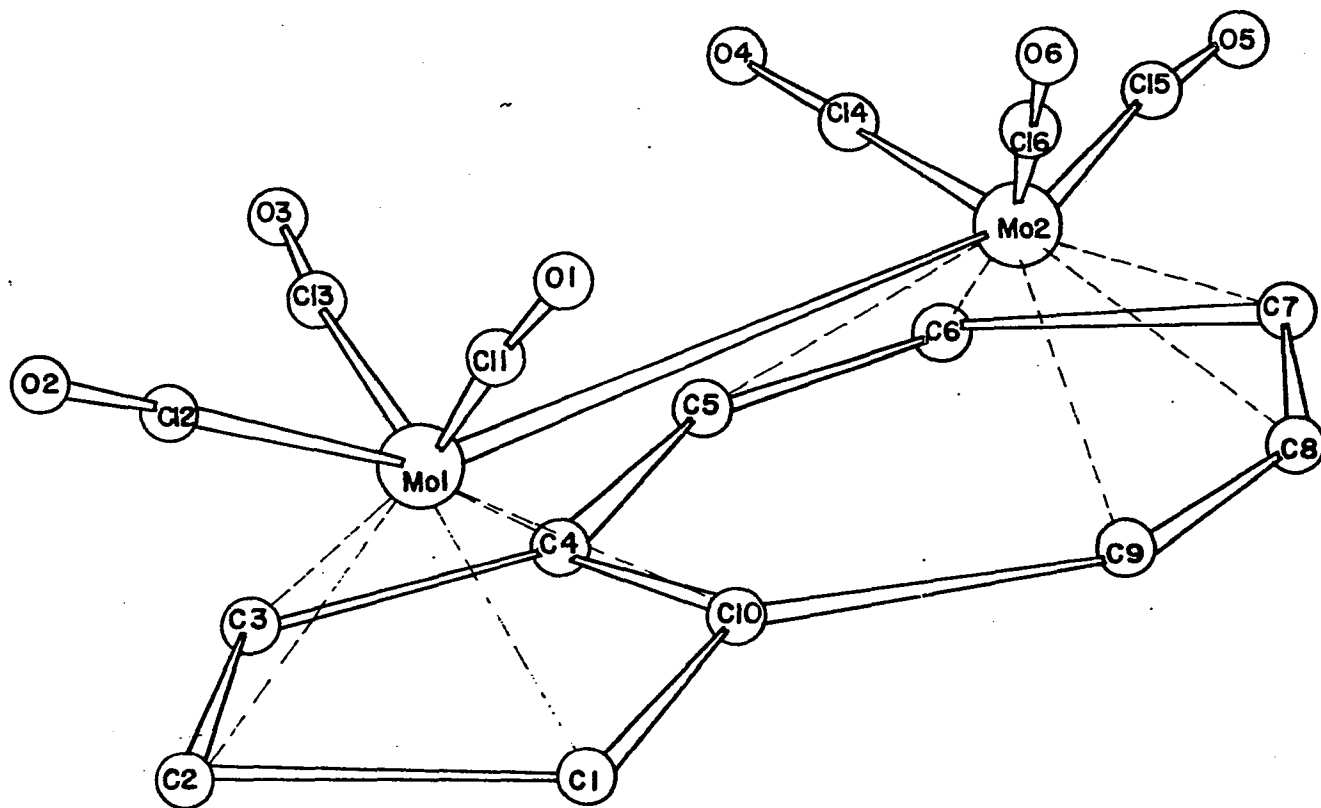
Figure 6. The molecular configuration of $C_{10}H_8Mo_2(CO)_6$

Table 8. Distances and angles in $C_{10}H_8Mo_2(CO)_6$ and their standard deviations

Atom 1	Atom 2	Distance	Error		Atom 1	Atom 2	Distance	Error
Mo1	Mo2	3.2620Å	0.0009Å		C11	O1	1.162Å	0.009Å
					C12	O2	1.140	0.010
Mo1	C11	1.982	0.008		C13	O3	1.141	0.008
Mo1	C12	1.951	0.008		C14	O4	1.152	0.009
Mo1	C13	1.981	0.007		C15	O5	1.165	0.010
Mo2	C14	1.980	0.007		C16	O6	1.151	0.009
Mo2	C15	1.932	0.009					
Mo2	C16	1.980	0.008		C1	C2	1.419	0.012
					C6	C7	1.423	0.012
Mo1	C1	2.361	0.009		C2	C3	1.403	0.012
Mo1	C2	2.298	0.009		C7	C8	1.401	0.011
Mo1	C3	2.334	0.009		C3	C4	1.516	0.017
Mo1	C4	2.273	0.015		C8	C9'	1.506	0.016
MO1	C10	2.316	0.015		C4	C5	1.424	0.022
Mo2	C5'	2.228	0.014		C9'	C10'	1.434	0.018
Mo2	C6	2.362	0.009		C5	C6	1.404	0.018
Mo2	C7	2.309	0.008					
Mo2	C8	2.350	0.008		C10'	C1	1.338	0.019
Mo2	C9'	2.307	0.014		C4	C10	1.504	0.021
					C5'	C9'	1.496	0.020
Mo1	C4'	2.503	0.014		C3	C4'	1.393	0.016
Mo1	C10'	2.500	0.017		C8	C9	1.277	0.017
Mo2	C5	2.500	0.016		C4'	C5'	1.417	0.020
Mo2	C9	2.491	0.015		C9	C10	1.414	0.022
					C5'	C6	1.483	0.017
Mo1	C5'	2.941	0.015		C10	C1	1.485	0.018
Mo1	C9'	2.955	0.014					
Mo2	C4	2.939	0.015					
Mo2	C10	2.923	0.015					

Table 8 (Continued)

Atoms			Angle	Error	Atoms			Angle	Error
Mo1	Mo2	C14	87.44°	0.22°	C1	C2	C3	119.60°	0.87°
Mo1	Mo2	C15	159.80	0.24	C2	C3	C4	100.68	0.88
Mo1	Mo2	C16	85.12	0.22	C3	C4	C10	109.53	1.17
Mo2	Mo1	C11	85.63	0.22	C4	C10	C1	106.75	
Mo2	Mo1	C12	160.28	0.23	C10	C1	C2	103.42	0.93
Mo2	Mo1	C13	84.33	0.22	C4	C5	C6	123.49	1.45
					C5	C6	C7	133.88	1.02
C11	Mo1	C12	82.65°	0.32°	C6	C7	C8	119.10	
C11	Mo1	C13	97.76	0.30	C7	C8	C9	136.28	0.98
C12	Mo1	C13	81.63	0.31	C8	C9	C10	124.74	1.40
C14	Mo2	C15	81.03	0.32	C9	C10	C4	124.71	1.42
C14	Mo2	C16	97.17	0.30	C10	C4	C5	126.34	
C15	Mo2	C16	779.96	0.32	C7	C8	C9'	101.46	
					C8	C9'	C5'	108.96	
Mo1	C11	O1	176.05	0.67	C9'	C5'	C6	107.60	
Mo1	C12	O2	176.54	0.74	C5'	C6	C7	102.81	
Mo1	C13	O3	174.28	0.68	C2	C3	C4'	135.76	0.98
Mo2	C14	O4	174.88	0.67	C3	C4'	C5'	124.50	1.28
Mo2	C15	O5	178.40	0.73	C4'	C5'	C9'	125.05	1.34
Mo2	C16	O6	174.13	0.67	C5'	C9'	C10'	124.81	1.41
					C9'	C10'	C1	127.12	
					C10'	C1	C2	133.40	

Plane 1	Plane 2	Dihedral angle	Error
C1-C2-C3	C6-C7-C8	166.27°	1.22°
C1-C3-C10	C6-C7-C8	167.87	1.03
C1-C2-C3	C5-C7-C9	161.07	0.98
C6-C7-C8	C2-C4'-C10'	162.26	0.91

Figure 7. Comparison of observed and calculated structure factors for $C_{10}H_8Mo_2(CO)_6$

Figure 7 (Continued)

Figure 7 (Continued)

Figure 7 (Continued)

46

Figure 7 (Continued)

48

Structure factor listing (H, K, L, FOBS, FCAL). The six column-groups read top-to-bottom, then continue in the next group.

Group 1

H	K	L	FOBS	FCAL
-1	-6	-1	24.3	-24.8
-1	-7	-1	71.2	-73.2
-1	-9	-1	71.0	71.4
-1	-10	-1	9.0	-6.1
-1	-11	-1	28.8	-30.1
-1	-13	-1	20.4	20.4
-1	-17	-1	8.4	-7.6
-1	15	-1	12.8	17.9
-1	13	-2	7.6	-7.2
-1	11	-2	8.3	-7.2
-1	10	-2	11.2	-11.7
-1	9	-2	23.8	22.4
-1	8	-2	17.4	17.2
-1	7	-2	72.2	-72.9
-1	6	-2	23.2	-20.1
-1	5	-2	79.7	85.4
-1	4	-2	46.7	48.6
-1	3	-2	115.4	-120.2
-1	2	-2	34.5	-34.9
-1	1	-2	71.4	67.2
-1	0	-2	27.4	25.7
-1	-2	-2	11.8	-0.1
-1	-3	-2	59.3	-57.5
-1	-4	-2	18.3	-17.2
-1	-5	-2	86.2	88.0
-1	-6	-2	55.0	54.8
-1	-7	-2	69.7	-69.8
-1	-8	-2	15.5	-15.8
-1	-9	-2	44.5	45.6
-1	-11	-2	30.7	-31.7
-1	-12	-2	7.9	-5.2
-1	-13	-2	15.3	14.2
-1	16	-3	8.5	-6.7
-1	15	-3	8.6	7.5
-1	14	-3	7.2	6.6
-1	13	-3	5.9	-5.3
-1	12	-3	7.1	5.6
-1	11	-3	11.6	-10.6
-1	10	-3	21.5	-22.1
-1	9	-3	27.9	30.0
-1	8	-3	17.0	17.6
-1	7	-3	43.3	-45.0
-1	6	-3	19.6	-19.5
-1	5	-3	62.3	60.3
-1	4	-3	57.0	59.0
-1	3	-3	64.8	-72.4
-1	2	-3	27.8	-26.5
-1	1	-3	41.6	42.1
-1	0	-3	19.2	20.5
-1	-1	-3	5.3	1.1
-1	-2	-3	29.0	24.8
-1	-3	-3	51.4	-50.5
-1	-4	-3	27.8	-28.3
-1	-5	-3	66.4	69.5
-1	-6	-3	22.7	22.9
-1	-7	-3	71.1	-71.2
-1	-8	-3	20.6	-24.7
-1	-9	-3	34.7	34.8
-1	-10	-3	22.3	21.4
-1	-11	-3	29.7	-28.5
-1	-13	-3	7.4	8.8
-1	12	-4	5.8	5.5
-1	11	-4	10.5	-9.5
-1	10	-4	17.4	-18.9
-1	9	-4	27.9	27.3
-1	8	-4	35.2	35.3
-1	7	-4	25.8	-23.0
-1	6	-4	34.7	-38.6
-1	5	-4	44.5	45.5
-1	4	-4	12.6	13.9
-1	3	-4	45.8	-46.5
-1	2	-4	19.1	-19.4
-1	1	-4	21.1	23.9
-1	0	-4	13.0	13.7
-1	-2	-4	13.4	11.3
-1	-3	-4	34.6	-37.0
-1	-4	-4	38.7	-38.7
-1	-5	-4	54.9	53.4
-1	-6	-4	25.1	25.1
-1	-7	-4	49.9	-50.1
-1	-8	-4	28.1	-28.2
-1	-9	-4	38.1	38.8
-1	-10	-4	22.1	22.0
-1	-11	-4	19.4	-19.3
-1	12	-5	6.2	6.2
-1	11	-5	7.7	-7.6
-1	10	-5	8.8	-9.8
-1	9	-5	16.2	14.7
-1	8	-5	26.0	26.9
-1	7	-5	27.6	-25.5
-1	6	-5	41.5	-44.0
-1	5	-5	28.5	30.9
-1	4	-5	22.2	21.3
-1	3	-5	25.3	-23.8
-1	2	-5	14.0	-14.5
-1	1	-5	13.5	14.4
-1	-1	-5	15.4	14.2
-1	-2	-5	9.7	8.9
-1	-3	-5	38.0	-36.7
-1	-4	-5	31.4	-29.7
-1	-5	-5	41.8	41.3
-1	-6	-5	40.6	41.2
-1	-7	-5	23.9	-24.9
-1	-8	-5	31.4	-30.7
-1	-9	-5	27.6	26.8
-1	-10	-5	8.0	9.7
-1	-11	-5	9.0	-10.3
-1	11	-6	8.5	-6.3
-1	10	-6	14.6	-13.1
-1	9	-6	12.4	11.8
-1	7	-6	22.2	-22.8
-1	8	-6	20.2	22.9
-1	6	-6	24.4	-26.2
-1	5	-6	16.3	15.4
-1	4	-6	28.9	28.0
-1	3	-6	5.9	-8.0
-1	2	-6	13.1	-12.7
-1	0	-6	7.2	-6.9

Group 2

H	K	L	FOBS	FCAL
-1	-1	-6	16.1	14.0
-1	-2	-6	30.3	27.1
-1	-3	-6	28.3	-26.0
-1	-4	-6	32.7	-30.3
-1	-5	-6	22.6	24.7
-1	-7	-6	22.9	-22.4
-1	-8	-6	21.7	-23.1
-1	-9	-6	16.2	14.8
-1	-10	-6	7.2	7.0
-1	-11	-6	8.2	-5.6
-1	10	-7	14.5	-15.7
-1	9	-7	9.4	5.8
-1	8	-7	21.0	20.9
-1	7	-7	9.9	-9.5
-1	6	-7	15.3	-15.6
-1	5	-7	9.1	8.0
-1	4	-7	14.2	16.3
-1	0	-7	8.2	-7.6
-1	-2	-7	19.8	19.2
-1	-3	-7	11.8	-11.9
-1	-4	-7	27.1	-26.9
-1	-5	-7	18.1	17.0
-1	-6	-7	27.8	27.3
-1	-7	-7	21.8	-19.2
-1	-8	-7	19.0	-17.4
-1	-9	-7	9.7	7.9
-1	-10	-7	9.9	8.6
-1	8	-8	11.8	11.6
-1	6	-8	14.2	-14.2
-1	4	-8	8.7	10.9
-1	0	-8	9.7	-10.4
-1	-2	-8	13.5	13.3
-1	-3	-8	8.1	-6.7
-1	-4	-8	19.1	-19.4
-1	-5	-8	13.3	11.5
-1	-6	-8	22.5	20.5
-1	-7	-8	9.3	-8.6
-1	-8	-8	14.6	-13.1
-1	0	-9	11.3	-10.4
-2	10	0	58.0	60.6
-2	9	0	16.7	15.7
-2	5	0	6.6	5.7
-2	4	0	16.3	-18.2
-2	14	-1	8.4	7.5
-2	13	-1	9.6	-9.9
-2	12	-1	16.8	-16.5
-2	11	-1	16.7	-18.8
-2	10	-1	47.1	48.1
-2	9	-1	10.8	10.6
-2	8	-1	75.2	-75.4
-2	7	-1	25.9	-26.6
-2	6	-1	66.2	65.6
-2	5	-1	6.0	6.1
-2	4	-1	16.9	-17.4
-2	3	-1	13.5	-13.4
-2	2	-1	22.1	-21.2
-2	1	-1	29.3	-26.9
-2	0	-1	45.4	46.6
-2	-1	-1	13.0	12.2
-2	-2	-1	62.8	-63.6
-2	-3	-1	20.9	-20.4
-2	-4	-1	154.4	146.7
-2	-5	-1	30.3	31.6
-2	-6	-1	89.5	-87.1
-2	-8	-1	19.6	-19.2
-2	-8	-1	48.7	47.7
-2	-10	-1	11.8	-12.4
-2	-12	-1	12.1	-10.6
-2	-14	-1	21.2	21.1
-2	-15	-1	6.1	2.3
-2	-16	-1	20.6	-20.6
-2	-17	-1	7.8	-3.3
-2	14	-2	6.0	5.9
-2	13	-2	12.9	13.2
-2	12	-2	27.0	-25.7
-2	11	-2	20.8	-20.6
-2	10	-2	34.7	34.6
-2	9	-2	10.4	9.9
-2	8	-2	44.4	-44.8
-2	7	-2	8.2	-8.9
-2	6	-2	50.1	51.5
-2	5	-2	36.0	34.9
-2	4	-2	12.6	-14.8
-2	3	-2	28.9	-28.4
-2	2	-2	25.5	-24.7
-2	1	-2	15.3	-14.2
-2	-1	-2	83.9	82.7
-2	-2	-2	45.7	45.8
-2	-3	-2	80.5	-77.0
-2	-4	-2	28.1	-27.6
-2	-5	-2	89.0	88.5
-2	-6	-2	19.4	19.4
-2	-7	-2	68.3	-70.8
-2	-8	-2	34.2	-32.2
-2	-12	-2	38.0	38.0
-2	-12	-2	18.2	-19.4
-2	-13	-2	6.6	-4.5
-2	-14	-2	23.9	22.6
-2	-16	-2	16.0	-16.2
-2	13	-3	8.5	6.9
-2	12	-3	11.1	11.8
-2	12	-3	23.4	-24.6
-2	11	-3	18.5	-17.9
-2	10	-3	37.0	36.9
-2	9	-3	26.3	26.9
-2	8	-3	29.8	-32.4
-2	7	-3	12.8	-12.7
-2	6	-3	19.3	19.0
-2	5	-3	19.4	21.7
-2	4	-3	8.9	-11.1
-2	2	-3	31.1	-34.1
-2	3	-3	24.8	-24.5
-2	0	-3	67.9	69.0
-2	-1	-3	58.2	64.6
-2	-2	-3	87.2	-86.3
-2	-3	-3	58.3	-58.6
-2	-4	-3	46.9	46.6

Group 3

H	K	L	FOBS	FCAL
-2	-5	-3	22.1	23.0
-2	-6	-3	55.2	-55.3
-2	-8	-3	26.1	27.1
-2	-12	-3	15.1	-15.1
-2	-13	-3	6.4	-7.9
-2	-14	-3	18.9	19.7
-2	-16	-3	16.3	-15.8
-2	14	-4	10.0	8.8
-2	13	-4	11.5	11.9
-2	12	-4	14.6	-14.8
-2	11	-4	14.0	-16.3
-2	10	-4	20.9	21.6
-2	9	-4	19.9	21.7
-2	8	-4	23.5	-22.7
-2	7	-4	25.9	-24.8
-2	6	-4	16.6	17.9
-2	5	-4	9.3	11.3
-2	4	-4	6.6	-7.0
-2	3	-4	6.6	7.0
-2	2	-4	32.6	-34.1
-2	1	-4	30.2	-30.4
-2	0	-4	45.2	46.3
-2	-1	-4	45.6	47.3
-2	-2	-4	51.6	-52.5
-2	-4	-4	55.3	52.8
-2	-5	-4	38.4	38.7
-2	-6	-4	37.8	-35.6
-2	-10	-4	5.8	6.6
-2	-11	-4	6.7	6.5
-2	-12	-4	12.3	-12.8
-2	-13	-4	6.9	-8.8
-2	-14	-4	11.7	12.9
-2	-15	-4	8.3	8.9
-2	13	-5	12.7	11.4
-2	12	-5	12.4	-4.3
-2	11	-5	14.1	-13.6
-2	10	-5	11.5	11.4
-2	9	-5	12.4	13.3
-2	8	-5	14.8	-13.6
-2	7	-5	20.0	-22.2
-2	6	-5	15.3	15.5
-2	5	-5	8.7	7.9
-2	3	-5	9.5	10.4
-2	2	-5	18.4	-18.0
-2	1	-5	27.0	-26.2
-2	0	-5	43.4	43.1
-2	-1	-5	42.6	42.9
-2	-2	-5	44.9	-42.5
-2	-3	-5	45.4	-46.3
-2	-4	-5	40.0	38.0
-2	-5	-5	27.7	26.3
-2	-6	-5	12.0	-12.5
-2	-7	-5	11.2	-10.6
-2	-10	-5	6.2	6.2
-2	-11	-5	8.2	9.0
-2	-12	-5	12.9	-14.0
-2	-13	-5	10.9	-12.0
-2	12	-6	10.9	-5.0
-2	11	-6	13.1	-12.6
-2	10	-6	9.2	7.4
-2	9	-6	17.7	16.9
-2	8	-6	8.0	-7.4
-2	7	-6	10.3	-11.5
-2	3	-6	14.5	14.3
-2	2	-6	7.3	-6.7
-2	1	-6	26.0	-24.9
-2	0	-6	20.7	22.2
-2	-1	-6	36.8	36.1
-2	-2	-6	34.5	-34.4
-2	-3	-6	33.7	-34.2
-2	-4	-6	20.3	21.3
-2	-5	-6	16.6	17.0
-2	-7	-6	11.7	-10.9
-2	-11	-6	9.5	10.1
-2	-12	-6	8.4	-8.5
-2	9	-7	13.8	13.4
-2	2	-7	11.9	14.2
-2	1	-7	13.5	-11.0
-2	0	-7	12.1	11.9
-2	-1	-7	24.7	26.4
-2	-2	-7	14.8	-16.3
-2	-3	-7	18.7	-19.4
-2	-4	-7	11.3	10.5
-2	-5	-7	18.5	17.9
-2	-7	-7	6.6	-4.2
-2	-9	-7	6.6	-6.1
-2	3	-8	10.7	13.4
-2	2	-8	9.0	-6.9
-2	1	-8	22.6	-22.3
-2	0	-8	12.4	9.8
-2	-1	-8	22.8	21.2
-2	-3	-8	17.9	-16.3
-2	-5	-8	13.7	13.0

Group 4

H	K	L	FOBS	FCAL
-3	-8	-1	12.9	-13.1
-3	-9	-1	38.6	40.1
-3	-10	-1	8.1	5.9
-3	-11	-1	40.2	-41.4
-3	-13	-1	28.7	29.5
-3	-15	-1	23.3	-22.7
-3	15	-2	11.4	10.9
-3	14	-2	7.4	7.1
-3	13	-2	20.6	-19.4
-3	12	-2	13.1	-14.0
-3	11	-2	30.1	29.4
-3	10	-2	17.4	16.8
-3	9	-2	13.0	-13.6
-3	8	-2	14.0	-17.3
-3	5	-2	39.8	41.7
-3	4	-2	46.5	46.5
-3	3	-2	63.7	-64.1
-3	2	-2	64.1	-64.1
-3	1	-2	96.3	97.2
-3	0	-2	23.3	21.6
-3	-1	-2	63.4	-60.8
-3	-2	-2	55.1	-52.0
-3	-3	-2	40.9	41.5
-3	-4	-2	12.4	12.4
-3	-5	-2	22.2	-20.7
-3	-7	-2	9.9	-10.1
-3	-8	-2	14.6	-15.1
-3	-9	-2	32.0	30.6
-3	-10	-2	10.2	11.8
-3	-11	-2	30.2	-31.5
-3	-12	-2	10.5	-10.4
-3	-13	-2	31.3	31.6
-3	-15	-2	18.6	-18.8
-3	15	-3	11.8	8.8
-3	14	-3	8.0	8.8
-3	13	-3	14.3	-14.8
-3	12	-3	9.8	-9.8
-3	11	-3	16.7	17.8
-3	10	-3	13.2	13.7
-3	9	-3	7.1	-5.6
-3	8	-3	6.9	-6.5
-3	7	-3	13.2	-15.4
-3	6	-3	12.3	-14.4
-3	5	-3	33.9	34.4
-3	4	-3	30.7	32.0
-3	3	-3	40.6	-39.4
-3	1	-3	51.0	51.7
-3	-1	-3	37.4	38.5
-3	-2	-3	44.3	-44.4
-3	-3	-3	32.5	-31.1
-3	-5	-3	38.7	40.4
-3	-7	-3	21.2	-22.4
-3	-9	-3	36.4	37.0
-3	-10	-3	15.1	16.3
-3	-11	-3	27.8	-28.1
-3	-12	-3	16.2	-16.3
-3	-13	-3	23.1	23.8
-3	-14	-3	7.6	7.7
-3	-15	-3	13.6	-14.3
-3	14	-4	10.7	10.8
-3	13	-4	12.4	-11.3
-3	12	-4	10.2	-10.2
-3	11	-4	8.5	8.6
-3	9	-4	5.7	-6.5
-3	7	-4	8.1	-5.2
-3	6	-4	21.4	-21.5
-3	5	-4	23.1	23.5
-3	4	-4	26.2	28.5
-3	2	-4	48.6	-51.5
-3	1	-4	30.2	-31.2
-3	0	-4	53.8	49.2
-3	-1	-4	51.0	53.1
-3	-2	-4	43.6	-42.3
-3	-3	-4	25.0	-24.2
-3	-4	-4	28.2	25.7
-3	-7	-4	10.5	8.1
-3	-8	-4	10.6	12.3
-3	-9	-4	23.4	-21.8
-3	-10	-4	16.3	-16.4
-3	-11	-4	27.4	29.1
-3	-12	-4	20.0	19.6
-3	-13	-4	29.5	-30.4
-3	-14	-4	15.0	-17.1
-3	-12	-5	16.5	17.5
-3	-14	-5	9.0	9.7
-3	12	-5	9.9	-8.8
-3	11	-5	6.8	5.5
-3	7	-5	6.4	-6.2
-3	6	-5	12.9	-12.4
-3	5	-5	22.4	23.9
-3	4	-5	34.6	33.5
-3	3	-5	20.1	-20.5
-3	2	-5	41.2	-42.2
-3	1	-5	27.1	26.5
-3	0	-5	36.7	37.7
-3	-1	-5	27.2	-25.7
-3	-2	-5	26.0	-24.3
-3	-3	-5	7.3	4.4
-3	-4	-5	6.9	4.8
-3	-5	-5	8.5	6.6
-3	-6	-5	11.6	11.9
-3	-7	-5	11.1	-10.6
-3	-8	-5	19.4	-19.9
-3	-9	-5	12.9	7.1
-3	-10	-5	17.0	18.7
-3	-11	-5	20.7	-20.9
-3	-12	-5	12.7	-14.2
-3	-13	-5	14.1	14.9
-3	7	-6	8.4	-9.3
-3	5	-6	12.5	-14.4
-3	5	-6	16.5	17.4
-3	4	-6	24.0	24.9
-3	3	-6	16.6	-15.8
-3	2	-6	33.5	-35.4
-3	1	-6	22.8	24.0
-3	-1	-6	8.8	-7.7

Group 5

H	K	L	FOBS	FCAL
-3	-2	-6	11.1	-11.5
-3	-4	-6	6.9	-5.4
-3	-5	-6	7.0	7.4
-3	-6	-6	10.0	10.5
-3	-7	-6	11.7	-11.2
-3	-8	-6	14.8	-16.3
-3	-9	-6	16.1	14.0
-3	-10	-6	16.1	17.2
-3	-11	-6	9.9	-10.6
-3	8	-7	8.2	7.9
-3	6	-7	16.3	-15.6
-3	3	-7	15.4	-14.2
-3	2	-7	24.5	-24.8
-3	1	-7	13.8	11.7
-3	0	-7	22.7	21.4
-3	-2	-7	6.5	-7.6
-3	-6	-7	13.0	13.6
-3	-7	-7	12.3	-9.0
-3	-8	-7	20.9	-19.5
-3	-9	-7	12.9	10.3
-3	4	-8	15.2	15.9
-3	2	-8	18.0	-16.9
-3	1	-8	6.8	4.8
-3	0	-8	15.7	14.3

Group 6

H	K	L	FOBS	FCAL
-4	10	0	18.9	19.3
-4	9	0	10.9	11.0
-4	8	0	40.3	-44.2
-4	7	0	16.7	-17.7
-4	6	0	49.8	52.5
-4	15	-1	7.5	4.8
-4	14	-1	13.6	-12.9
-4	10	-1	8.6	7.9
-4	9	-1	13.6	16.0
-4	8	-1	23.6	-21.2
-4	7	-1	22.3	-22.0
-4	6	-1	60.3	60.0
-4	5	-1	30.9	28.3
-4	4	-1	73.5	-76.5
-4	3	-1	19.6	-20.2
-4	2	-1	73.0	73.7
-4	1	-1	39.3	39.0
-4	0	-1	77.1	-80.1
-4	-1	-1	15.3	-13.2
-4	-2	-1	5.8	5.0
-4	-4	-1	36.0	36.6
-4	-5	-1	20.0	20.0
-4	-6	-1	76.9	-75.5
-4	-7	-1	31.8	-33.1
-4	-8	-1	60.6	60.8
-4	-9	-1	15.7	14.8
-4	-10	-1	44.3	-45.5
-4	-12	-1	18.9	20.6
-4	-13	-1	7.4	6.8
-4	-14	-1	8.7	-8.1
-4	10	-2	10.5	10.4
-4	9	-2	8.3	7.8
-4	8	-2	24.4	-25.0
-4	7	-2	18.4	-19.0
-4	6	-2	45.3	46.2
-4	5	-2	23.6	23.0
-4	4	-2	50.8	-49.0
-4	3	-2	47.6	-52.9
-4	2	-2	52.3	55.4
-4	1	-2	22.0	22.0
-4	0	-2	35.3	-34.9
-4	-1	-2	7.3	-8.7
-4	-2	-2	18.1	-17.1
-4	-3	-2	7.7	-6.6
-4	-4	-2	44.0	43.3
-4	-5	-2	17.9	15.5
-4	-6	-2	52.9	-53.9
-4	-7	-2	15.4	-15.5
-4	-8	-2	54.9	56.3
-4	-9	-2	18.4	18.4
-4	-10	-2	28.1	-27.9
-4	-11	-2	14.9	-14.8
-4	-12	-2	15.4	15.0
-4	-13	-2	9.0	-0.4
-4	-14	-2	9.7	-7.9
-4	-16	-2	6.7	-3.4
-4	14	-3	7.3	-4.2
-4	10	-3	15.8	15.8
-4	9	-3	15.6	15.5
-4	8	-3	34.5	-35.5
-4	7	-3	33.4	-33.3
-4	6	-3	28.3	27.6
-4	5	-3	30.6	32.1
-4	4	-3	33.8	-32.0
-4	3	-3	25.6	-28.0
-4	2	-3	49.3	49.3
-4	1	-3	10.9	8.9
-4	0	-3	11.9	-10.0
-4	-2	-3	12.2	-12.0
-4	-3	-3	21.8	-21.3
-4	-4	-3	39.3	40.6
-4	-5	-3	22.3	23.1
-4	-6	-3	46.5	-47.3
-4	-7	-3	13.8	-14.3
-4	-8	-3	45.9	46.1
-4	-9	-3	14.5	15.2
-4	-10	-3	24.6	-26.1
-4	-11	-3	20.1	-19.1
-4	-12	-3	14.6	14.6
-4	10	-4	7.9	9.7
-4	9	-4	14.9	16.4
-4	8	-4	20.4	-19.7
-4	7	-4	29.7	-29.9
-4	6	-4	27.0	24.1
-4	5	-4	44.4	46.6
-4	4	-4	26.6	-28.3
-4	3	-4	22.4	-22.6
-4	2	-4	20.0	18.8
-4	1	-4	7.9	4.7
-4	-1	-4	11.1	-10.4
-4	-3	-4	14.0	-14.0
-4	-4	-4	29.2	29.5

Figure 7 (Continued)

H	K	L	FOBS	FCAL
-4	-5	-4	25.5	26.2
-4	-6	-4	36.9	-36.2
-4	-7	-4	30.5	-30.8
-4	-8	-4	21.5	22.3
-4	-9	-4	21.2	21.2
-4	-10	-4	21.0	-22.1
-4	-11	-4	10.8	-11.2
-4	-12	-4	13.5	13.8
-4	10	-5	7.4	6.1
-4	9	-5	12.6	12.2
-4	8	-5	10.3	-9.6
-4	7	-5	18.8	-21.9
-4	6	-5	22.2	20.5
-4	5	-5	28.9	32.5
-4	4	-5	20.1	-19.8
-4	3	-5	22.8	-21.7
-4	-2	-5	17.5	-16.7
-4	-3	-5	18.4	-17.3
-4	-4	-5	24.0	22.3
-4	-5	-5	25.7	24.4
-4	-6	-5	19.4	-20.2
-4	-7	-5	24.4	-25.4
-4	-8	-5	13.6	15.2
-4	-9	-5	20.7	22.1
-4	-10	-5	16.7	-15.1
-4	-11	-5	7.4	-8.0
-4	9	-6	12.6	12.3
-4	8	-6	9.6	-8.3
-4	7	-6	20.1	-20.5
-4	6	-6	12.1	13.7
-4	5	-6	15.3	16.0
-4	4	-6	10.4	-10.1
-4	3	-6	13.7	-14.4
-4	1	-6	6.4	7.1
-4	-2	-6	9.4	-10.8
-4	-3	-6	19.9	-20.1
-4	-4	-6	15.0	14.4
-4	-5	-6	23.8	24.2
-4	-6	-6	15.2	-13.9
-4	-7	-6	23.1	-22.7
-4	-8	-6	16.9	15.1
-4	-9	-6	17.1	16.8
-4	-10	-6	7.2	-7.5
-4	7	-7	14.5	-15.0
-4	5	-7	13.6	12.7
-4	3	-7	9.3	-10.9
-4	0	-7	8.9	6.4
-4	-1	-7	9.0	10.5
-4	-3	-7	15.6	-16.8
-4	-4	-7	7.5	5.6
-4	-5	-7	19.3	19.4
-4	-6	-7	11.3	-9.1
-4	-7	-7	21.4	-20.3
-5	13	-1	12.6	-12.6
-5	12	-1	8.4	-7.7
-5	11	-1	21.8	20.9
-5	10	-1	22.3	23.6
-5	9	-1	27.2	-28.1
-5	8	-1	14.6	-13.7
-5	7	-1	38.5	39.5
-5	6	-1	8.2	10.1
-5	5	-1	46.1	-49.4
-5	4	-1	11.7	-10.7
-5	1	-1	27.3	26.6
-5	0	-1	18.7	18.9
-5	-1	-1	61.3	-62.1
-5	-2	-1	27.2	-25.9
-5	-3	-1	66.7	64.9
-5	-4	-1	19.6	18.6
-5	-5	-1	74.1	-74.3
-5	-6	-1	11.6	-0.2
-5	-7	-1	47.6	48.8
-5	-8	-1	18.0	16.5
-5	-9	-1	21.1	-21.2
-5	-13	-1	14.2	14.1
-5	-14	-1	7.5	5.8
-5	-15	-1	17.0	-16.5
-5	-16	-1	7.4	-4.1
-5	13	-2	11.2	-10.2
-5	12	-2	12.6	-13.7
-5	11	-2	21.7	20.5
-5	10	-2	20.0	19.4
-5	9	-2	29.9	-28.1
-5	8	-2	25.7	-25.3
-5	7	-2	22.4	21.8
-5	6	-2	10.7	13.7
-5	5	-2	18.7	-18.5
-5	3	-2	9.4	10.4
-5	1	-2	14.0	13.7
-5	0	-2	23.0	23.0
-5	-1	-2	54.0	-55.1
-5	-2	-2	31.7	-30.2
-5	-3	-2	61.2	61.1
-5	-4	-2	34.7	35.5
-5	-5	-2	40.5	-40.6
-5	-6	-2	13.8	-13.9
-5	-7	-2	39.6	40.7
-5	-8	-2	15.7	15.0
-5	-9	-2	27.7	-27.4
-5	-10	-2	7.4	-6.5
-5	-11	-2	6.6	-5.8
-5	-13	-2	14.4	14.4
-5	-14	-2	8.4	7.4
-5	-15	-2	15.8	-15.2
-5	13	-3	7.8	-5.1
-5	12	-3	12.6	-11.9
-5	11	-3	14.5	13.9
-5	10	-3	15.4	15.2
-5	9	-3	23.8	-22.3
-5	8	-3	20.4	-20.6
-5	7	-3	21.7	20.3
-5	6	-3	18.0	14.6
-5	4	-3	5.2	-7.5
-5	1	-3	26.1	27.9

H	K	L	FOBS	FCAL
-5	0	-3	18.6	17.3
-5	-1	-3	43.1	-44.1
-5	-2	-3	28.2	-29.1
-5	-3	-3	45.0	46.5
-5	-4	-3	29.0	30.2
-5	-5	-3	36.3	-36.0
-5	-6	-3	31.5	-31.8
-5	-7	-3	26.4	24.6
-5	-8	-3	12.5	11.3
-5	-11	-3	10.7	-9.7
-5	-12	-3	7.5	-6.4
-5	-13	-3	13.5	12.9
-5	-14	-3	9.5	7.6
-5	12	-4	10.2	-9.3
-5	11	-4	12.2	11.6
-5	10	-4	16.0	16.0
-5	9	-4	14.7	-13.6
-5	8	-4	14.0	-15.0
-5	7	-4	14.4	14.1
-5	6	-4	14.3	14.9
-5	5	-4	8.8	-7.7
-5	3	-4	9.4	-8.4
-5	2	-4	14.5	-16.2
-5	1	-4	28.6	27.6
-5	0	-4	23.1	23.2
-5	-1	-4	35.5	-34.6
-5	-2	-4	32.5	-32.3
-5	-3	-4	33.1	33.4
-5	-4	-4	33.8	33.5
-5	-5	-4	31.4	-31.0
-5	-6	-4	25.7	-26.0
-5	-7	-4	12.9	14.5
-5	-12	-4	8.0	-8.3
-5	-13	-4	13.1	12.5
-5	10	-5	13.6	14.0
-5	9	-5	9.1	-6.7
-5	8	-5	15.3	-14.3
-5	6	-5	9.6	12.0
-5	3	-5	6.1	-7.2
-5	2	-5	18.4	-17.8
-5	1	-5	7.3	8.0
-5	0	-5	22.5	21.8
-5	-1	-5	15.0	-16.4
-5	-2	-5	28.0	-27.6
-5	-3	-5	25.1	24.2
-5	-4	-5	32.1	32.6
-5	-5	-5	19.8	-19.4
-5	-6	-5	14.1	-16.0
-5	-7	-5	7.3	7.0
-5	8	-6	10.1	-10.9
-5	7	-6	6.6	4.3
-5	6	-6	6.6	-6.5
-5	2	-6	9.3	-10.7
-5	1	-6	9.9	8.3
-5	0	-6	20.1	20.7
-5	-1	-6	10.2	-9.0
-5	-2	-6	23.8	-23.6
-5	-3	-6	12.5	12.6
-5	-4	-6	17.9	18.1
-5	-5	-6	10.4	-9.9
-5	-6	-6	11.6	-10.7
-5	2	-7	10.9	-11.9
-5	1	-7	9.2	7.7
-5	0	-7	22.2	21.1
-5	-1	-7	9.8	-7.6
-5	-2	-7	21.4	-21.3
-5	-4	-7	10.7	11.5
-6	14	-1	13.7	-13.1
-6	13	-1	6.6	-4.5
-6	12	-1	18.1	16.9
-6	11	-1	10.4	11.7
-6	10	-1	21.5	-20.4
-6	9	-1	12.9	-12.5
-6	8	-1	12.2	13.7
-6	5	-1	7.7	6.4
-6	4	-1	33.9	-36.2
-6	3	-1	27.4	-27.9
-6	2	-1	56.9	57.2
-6	1	-1	39.1	38.8
-6	0	-1	75.2	-75.7
-6	-1	-1	22.4	-19.6
-6	-2	-1	60.2	60.3
-6	-3	-1	23.9	24.9
-6	-4	-1	21.4	-22.5
-6	-5	-1	17.5	-16.6
-6	-6	-1	11.3	10.5
-6	-8	-1	13.0	12.5
-6	-9	-1	15.5	15.5
-6	-10	-1	23.2	-23.6
-6	-11	-1	12.3	-11.0
-6	-12	-1	24.6	25.1
-6	-13	-1	6.3	6.4
-6	-14	-1	19.0	-19.7
-6	13	-2	10.5	-10.1
-6	12	-2	11.0	9.8
-6	11	-2	10.0	10.7
-6	10	-2	15.0	-15.6
-6	9	-2	8.6	-8.7
-6	8	-2	6.9	6.2
-6	6	-2	8.1	9.8
-6	5	-2	11.1	11.9
-6	4	-2	25.2	-25.7
-6	3	-2	24.5	-24.9
-6	2	-2	47.0	46.7
-6	1	-2	31.4	32.3
-6	0	-2	52.1	-53.0
-6	-1	-2	18.4	-18.8
-6	-2	-2	28.5	28.4
-6	-3	-2	31.9	32.4
-6	-4	-2	14.5	-14.4
-6	-5	-2	17.1	-15.9
-6	-8	-2	8.5	8.5
-6	-9	-2	9.7	8.5
-6	-10	-2	26.8	-25.3

H	K	L	FOBS	FCAL
-6	-11	-2	13.3	-13.5
-6	-12	-2	22.2	22.0
-6	-13	-2	11.4	11.1
-6	-14	-2	14.9	-15.4
-6	12	-3	8.9	7.1
-6	11	-3	10.0	9.2
-6	10	-3	6.7	-7.6
-6	6	-3	10.1	10.5
-6	5	-3	15.7	15.6
-6	4	-3	21.8	-22.0
-6	3	-3	16.2	-17.5
-6	2	-3	40.2	40.6
-6	1	-3	20.4	19.6
-6	0	-3	41.4	-39.3
-6	-1	-3	32.0	-32.2
-6	-2	-3	23.4	21.7
-6	-3	-3	20.9	20.1
-6	-4	-3	15.6	-15.4
-6	-8	-3	20.1	19.4
-6	-9	-3	10.6	10.1
-6	-10	-3	25.4	-25.8
-6	-11	-3	13.9	-13.7
-6	-12	-3	20.7	21.2
-6	-13	-3	11.9	12.7
-6	11	-4	8.3	7.4
-6	6	-4	14.1	14.3
-6	4	-4	19.8	-20.3
-6	3	-4	26.0	-25.2
-6	2	-4	18.9	22.5
-6	1	-4	26.1	24.1
-6	0	-4	17.7	-17.8
-6	-1	-4	27.0	-27.6
-6	-2	-4	21.4	21.9
-6	-3	-4	19.5	19.5
-6	-4	-4	12.1	-11.4
-6	-7	-4	10.1	-10.5
-6	-8	-4	17.2	17.4
-6	-9	-4	15.7	16.7
-6	-10	-4	15.7	-16.8
-6	-11	-4	12.8	-14.4
-6	-12	-4	15.3	16.0
-6	6	-5	8.5	7.5
-6	5	-5	10.8	11.7
-6	4	-5	13.5	-13.6
-6	3	-5	19.4	-21.2
-6	2	-5	13.2	12.4
-6	1	-5	25.7	27.2
-6	0	-5	10.3	-9.1
-6	-1	-5	18.2	-20.5
-6	-2	-5	9.7	9.6
-6	-3	-5	13.5	13.1
-6	-6	-5	10.9	-8.1
-6	-7	-5	8.6	-10.5
-6	-9	-5	13.0	14.6
-6	-10	-5	11.8	-10.8
-6	5	-6	12.7	12.9
-6	4	-6	6.8	-6.3
-6	3	-6	16.4	-16.3
-6	2	-6	10.6	8.0
-6	1	-6	22.3	21.9
-6	0	-6	11.2	-8.2
-6	-1	-6	18.5	-17.9
-6	-5	-6	9.0	-6.5
-6	-6	-6	7.1	-7.3
-6	-7	-6	9.7	-10.6
-7	13	-1	6.7	5.4
-7	9	-1	8.3	-8.6
-7	8	-1	9.5	-10.0
-7	7	-1	21.6	20.8
-7	6	-1	15.1	15.3
-7	5	-1	39.0	-40.1
-7	4	-1	15.3	-14.7
-7	3	-1	14.3	-15.1
-7	2	-1	43.2	44.5
-7	1	-1	23.4	-22.9
-7	-1	-1	19.0	20.6
-7	-2	-1	9.9	7.8
-7	-3	-1	8.9	9.5
-7	-5	-1	26.2	-27.1
-7	-6	-1	15.7	-13.4
-7	-7	-1	38.4	39.5
-7	-8	-1	18.4	18.3
-7	-9	-1	38.4	-39.3
-7	-10	-1	12.6	-12.6
-7	-11	-1	23.4	23.5
-7	9	-2	9.7	-8.8
-7	8	-2	11.1	-10.1
-7	7	-2	25.0	24.4
-7	6	-2	19.4	19.5
-7	5	-2	26.6	-26.6
-7	4	-2	16.8	-17.7
-7	3	-2	26.4	25.1
-7	2	-2	20.6	23.3
-7	1	-2	35.2	-37.1
-7	0	-2	17.4	-16.3
-7	-4	-2	12.6	12.3
-7	-5	-2	10.5	10.5
-7	-6	-2	34.6	-34.4
-7	-7	-2	32.4	31.8
-7	-8	-2	17.1	16.8
-7	-9	-2	30.4	-29.8
-7	-10	-2	12.1	-10.9
-7	-11	-2	7.5	8.8
-7	9	-3	16.6	17.8
-7	8	-3	8.1	-9.3
-7	7	-3	11.1	-11.1
-7	6	-3	20.2	20.5
-7	5	-3	18.1	18.7
-7	4	-3	20.7	-19.9
-7	3	-3	13.3	12.5

H	K	L	FOBS	FCAL
-7	2	-3	24.1	24.9
-7	1	-3	14.9	-14.3
-7	0	-3	14.0	-12.0
-7	-3	-3	11.8	11.2
-7	-4	-3	20.6	19.9
-7	-5	-3	23.4	-22.7
-7	-6	-3	25.1	25.7
-7	-8	-3	16.9	17.4
-7	-9	-3	16.3	-17.5
-7	-10	-3	10.5	-6.8
-7	-11	-3	8.7	10.6
-7	-12	-3	8.4	8.1
-7	9	-4	8.5	-7.8
-7	8	-4	11.3	-11.4
-7	7	-4	9.5	9.6
-7	6	-4	15.1	15.4
-7	5	-4	14.2	-13.4
-7	4	-4	21.8	-23.8
-7	3	-4	13.8	15.0
-7	2	-4	16.4	15.9
-7	-3	-4	10.4	10.8
-7	-4	-4	12.2	12.8
-7	-5	-4	16.9	-17.2
-7	-6	-4	15.7	-17.0
-7	-7	-4	16.9	20.3
-7	-8	-4	14.5	17.1
-7	-9	-4	11.5	-13.2
-7	-10	-4	11.4	-13.3
-7	-11	-4	7.0	6.9
-7	6	-5	14.5	14.2
-7	5	-5	8.4	-8.1
-7	4	-5	14.0	-15.8
-7	3	-5	12.8	12.1
-7	2	-5	12.2	11.7
-7	1	-5	13.3	12.5
-7	-4	-5	12.3	13.3
-7	-5	-5	18.5	-16.7
-7	-6	-5	17.1	-17.6
-7	-7	-5	13.3	13.2
-7	-8	-5	16.9	17.4
-7	-2	-6	6.3	8.4
-7	-1	-6	6.9	-4.5
-7	-2	-6	8.8	-7.5
-7	-3	-6	7.9	6.7
-7	-4	-6	15.4	14.3
-8	12	-1	10.0	10.3
-8	11	-1	8.5	8.1
-8	10	-1	17.9	-17.3
-8	9	-1	13.3	-14.2
-8	8	-1	23.6	22.1
-8	7	-1	15.7	14.9
-8	5	-1	16.5	-16.0
-8	4	-1	8.6	-6.2
-8	1	-1	12.0	12.8
-8	0	-1	18.1	-18.8
-8	-1	-1	16.6	-16.2
-8	-2	-1	32.6	34.1
-8	-3	-1	18.0	15.5
-8	-4	-1	38.0	-38.0
-8	-5	-1	16.6	-15.5
-8	-6	-1	31.0	31.1
-8	-7	-1	7.4	5.4
-8	-8	-1	24.7	-24.8
-8	-10	-1	13.0	12.9
-8	11	-2	9.9	9.8
-8	10	-2	13.1	-11.6
-8	9	-2	9.3	-10.7
-8	8	-2	19.3	18.7
-8	7	-2	14.1	13.3
-8	6	-2	15.3	15.3
-8	5	-2	15.2	-14.2
-8	4	-2	6.8	7.1
-8	0	-2	11.5	-10.2
-8	-1	-2	19.8	-19.5
-8	-2	-2	32.3	31.3
-8	-3	-2	26.1	25.1
-8	-4	-2	35.7	-36.3
-8	-5	-2	23.9	-24.0
-8	-6	-2	23.5	25.1
-8	-7	-2	16.2	16.3
-8	-8	-2	11.8	-11.6
-8	-9	-3	7.6	-5.3
-8	9	-3	12.3	10.8
-8	7	-3	10.9	11.5
-8	6	-3	11.3	-10.2
-8	5	-3	12.0	-11.1
-8	3	-3	7.1	8.3
-8	2	-3	8.5	8.6
-8	1	-3	7.6	6.3
-8	0	-3	19.4	-18.3
-8	-1	-3	17.7	-15.7
-8	-2	-3	24.0	23.7
-8	-3	-3	24.2	24.8
-8	-4	-3	19.8	-20.9
-8	-5	-3	21.3	-23.0
-8	-6	-3	14.6	15.1
-8	-7	-3	13.7	15.7
-8	-8	-3	6.9	-6.7
-8	1	-4	11.2	9.9
-8	0	-4	14.5	14.4
-8	-1	-4	14.9	-15.7
-8	-2	-4	16.6	-16.6
-8	-3	-4	17.0	18.1
-8	-4	-4	16.8	17.9
-8	-5	-4	16.1	-15.7
-8	-6	-4	17.9	-18.2
-8	-7	-4	12.2	10.0
-8	1	-5	7.5	10.3
-8	0	-5	10.6	11.0
-8	-1	-5	11.3	-8.8
-8	-2	-5	17.7	-18.4

H	K	L	FOBS	FCAL
-8	-2	-5	10.4	9.4
-8	-3	-5	17.7	17.8
-8	-4	-5	10.2	-10.1
-8	-5	-5	13.8	-13.3
-8	-6	-5	8.3	7.5
-9	10	0	7.3	-6.3
-9	9	-1	10.8	8.2
-9	8	-1	7.9	5.8
-9	6	-1	6.2	-2.6
-9	5	-1	8.4	-9.1
-9	3	-1	16.1	17.6
-9	2	-1	17.5	16.9
-9	1	-1	29.2	-29.6
-9	0	-1	24.0	-23.7
-9	-1	-1	35.4	35.8
-9	-2	-1	13.7	12.1
-9	-3	-1	25.2	-25.4
-9	-4	-1	7.3	-6.8
-9	-5	-1	6.9	7.5
-9	-9	-1	11.1	-10.4
-9	-11	-1	17.5	17.0
-9	-12	-1	9.3	6.7
-9	9	-2	7.4	5.6
-9	5	-2	8.1	-7.3
-9	4	-2	10.0	-9.3
-9	3	-2	17.3	16.4
-9	2	-2	16.9	16.8
-9	1	-2	25.7	-23.2
-9	0	-2	20.8	-21.4
-9	-1	-2	26.6	26.5
-9	-2	-2	17.4	17.4
-9	-3	-2	13.7	-14.1
-9	-4	-2	9.1	-11.4
-9	-5	-2	6.4	7.4
-9	-9	-2	10.6	-10.3
-9	-10	-2	7.5	-7.0
-9	-11	-2	15.2	13.5
-9	5	-3	7.3	-7.1
-9	4	-3	11.8	-11.2
-9	3	-3	15.3	15.1
-9	2	-3	19.4	18.6
-9	1	-3	15.8	-15.8
-9	0	-3	15.4	-14.6
-9	-1	-3	12.0	11.9
-9	-2	-3	12.5	12.8
-9	-3	-3	9.8	-7.8
-9	-4	-3	9.6	-11.9
-9	-9	-3	11.3	-9.7
-9	5	-4	8.1	-7.4
-9	4	-4	10.2	-10.8
-9	3	-4	10.9	10.7
-9	2	-4	15.3	16.7
-9	1	-4	12.1	-12.2

H	K	L	FOBS	FCAL
-9	0	-4	16.2	-15.9
-9	-1	-4	9.0	6.9
-9	-2	-4	9.5	11.2
-10	8	-1	9.2	7.2
-10	7	-1	10.6	8.3
-10	6	-1	14.9	-14.0
-10	5	-1	15.8	-14.4
-10	3	-1	17.3	15.7
-10	2	-1	11.1	11.3
-10	1	-1	17.0	-16.9
-10	0	-1	9.7	-8.6
-10	-1	-1	17.0	16.0
-10	-2	-1	10.8	8.3
-10	-4	-1	10.7	-10.9
-10	-7	-1	10.3	8.4
-10	-8	-1	19.3	-18.7
-10	-9	-1	10.9	-8.7
-10	-10	-1	17.6	18.1
-10	7	-2	10.4	9.5
-10	6	-2	12.2	-10.8
-10	5	-2	14.8	-13.3
-10	4	-2	13.5	12.8
-10	3	-2	14.9	14.1
-10	1	-2	10.7	-12.1
-10	0	-2	7.3	8.3
-10	-1	-2	6.7	3.9
-10	-2	-2	8.1	-8.6
-10	-6	-2	12.9	14.2
-10	-7	-2	9.4	9.6
-10	-8	-2	16.0	-15.6
-10	7	-3	10.7	-10.5
-10	6	-3	12.3	10.6
-10	4	-3	13.9	14.3
-10	3	-3	14.9	14.1
-10	1	-3	8.7	-7.8
-10	-1	-3	10.6	-11.1
-10	-4	-3	7.7	-8.5
-10	-6	-3	13.5	12.3
-11	6	-1	12.1	-10.1
-11	5	-1	9.7	7.7
-11	4	-1	7.3	7.9
-11	-1	-1	11.3	11.5
-11	-2	-1	7.8	7.3
-11	-3	-1	17.4	-17.5
-11	-4	-1	13.5	-11.2
-11	-5	-1	16.6	15.5
-11	-6	-1	12.7	11.2
-11	-7	-1	10.0	-10.0
-11	-8	-1	7.0	-7.9
-11	-1	-2	9.7	9.4
-11	-2	-2	9.6	10.0
-11	-3	-2	14.9	-13.8
-11	-4	-2	12.1	-10.6
-11	-5	-2	13.6	13.6
-11	-6	-2	10.9	10.2
-12	1	-1	9.1	-6.9
-12	0	-1	14.9	14.4
-12	-1	-1	10.8	9.7
-12	-2	-1	14.8	-14.3
-12	-3	-1	11.2	-9.4

The bonding of the molybdenum to the seven membered ring, however, can not be equated to any structure thus far determined. This will be discussed later.

The molecular packing can be seen in Figure 8. It seems to be quite simple with no unusual features.

Because the structure of azulene dimolybdenum hexacarbonyl was determined principally to investigate the nature of the metal-azulene bonding, this will be considered first. As a result of the disorder in the azulene ring, two images were obtained. These can be seen in Figure 9, where they are oriented in such a way that probable equivalent distances are in equivalent positions. From this figure, it can be seen that the distances and angles in the two images are in excellent agreement except for those involving atom C(10'). Since there is no indication from the final difference Fourier for this atom being misplaced, apparently a few bad reflections have caused this atom to assume an improper position. With the exception of that atom, all other distances and angles agree within the sum of their standard deviations. However, when comparing these distances to those found in the X-ray determination of molecular azulene (54), Figure 10, the agreement is very poor. In both cases the C(4) - C(10) distances are large and in approximate agreement, but the variations in the C-C distances around the ring show no agreement. Because the ring is also disordered in molecular azulene, it was felt that perhaps more accurate distances and angles were those reported by A. W. Hanson (62) from the X-ray determination of azulene complexed with s-trinitrobenzene. In this complex, the azulene ring was disordered to the extent of only 7%.
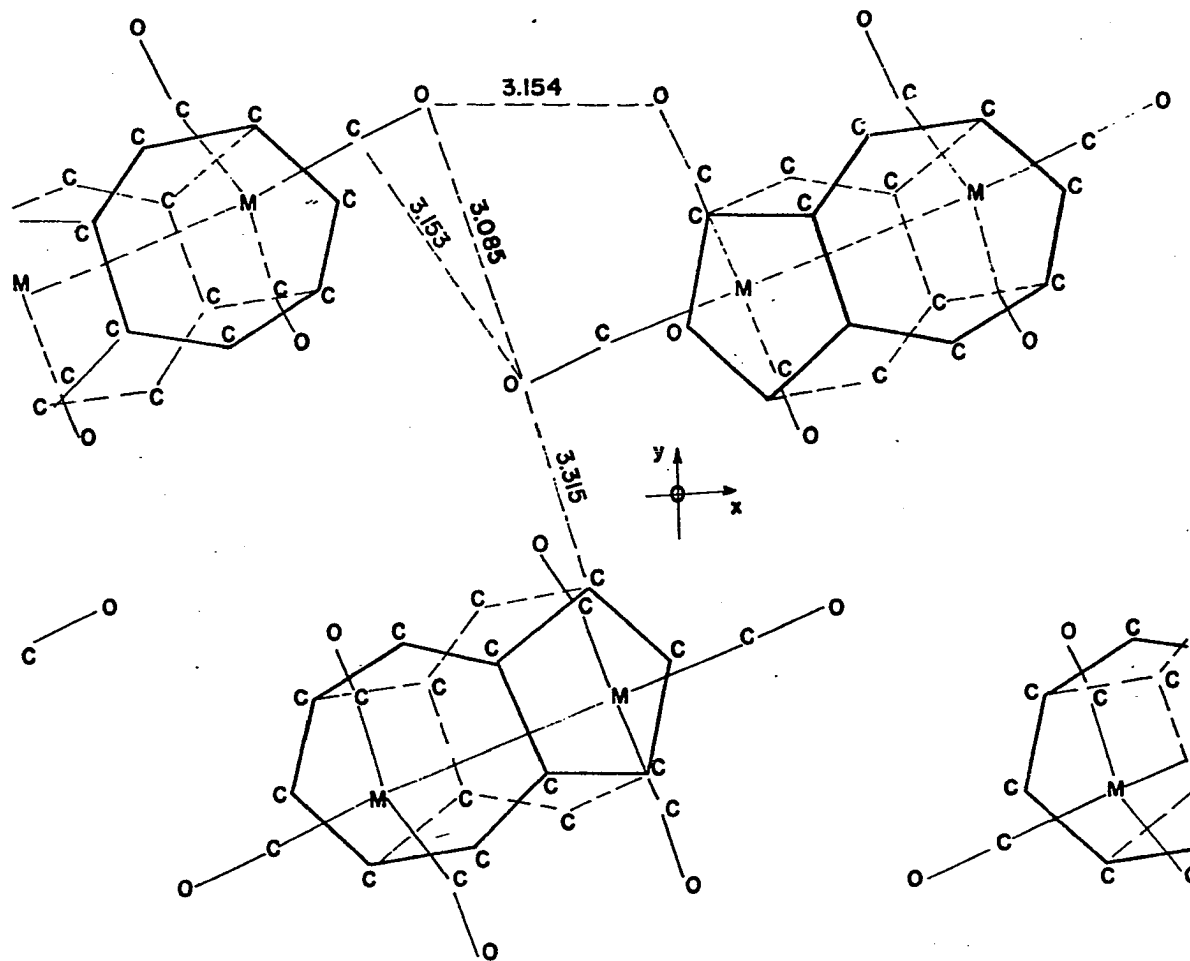
Figure 8. Molecular packing in $C_{10}H_8Mo_2(CO)_6$; a projection on the xy plane

Figure 9. Distances and angles in the two images of the disordered
            azulene ring
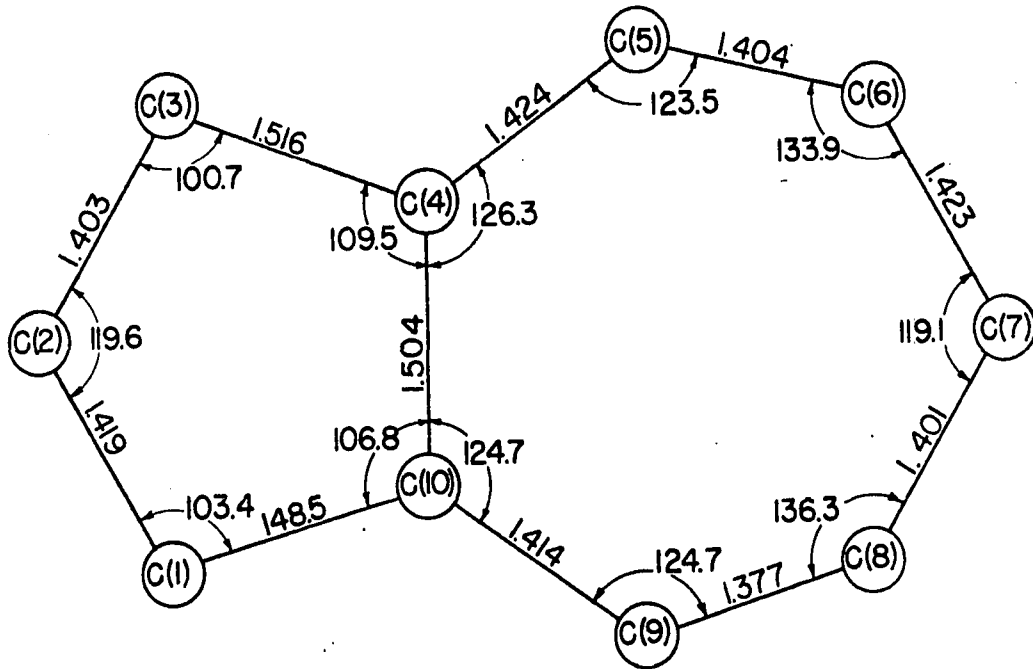
(a) Ring 1
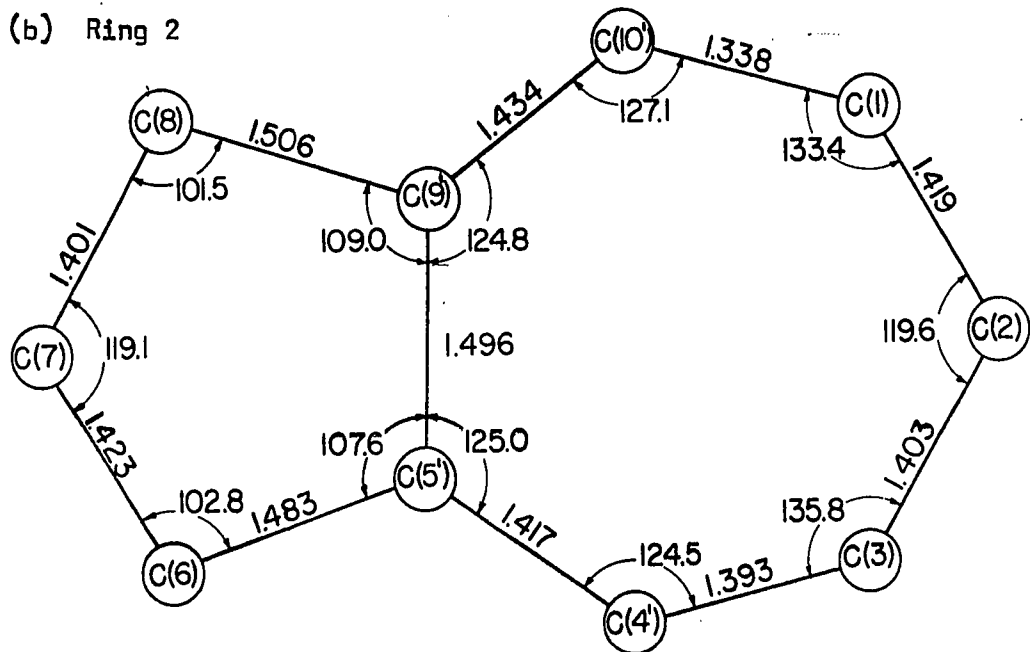
(b) Ring 2
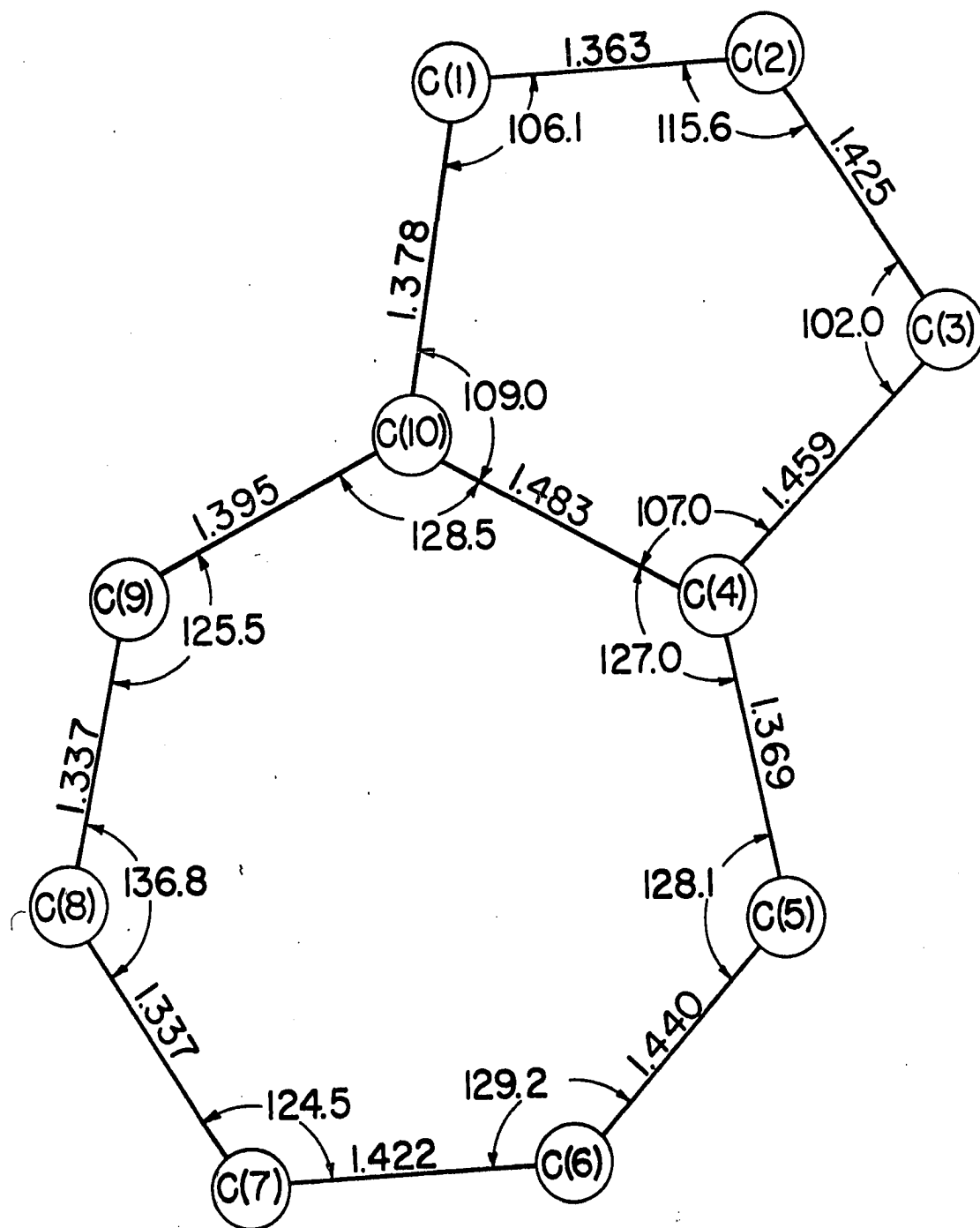
Figure 10. Distances and angles in molecular azulene

In his determination, the C(4) – C(10) distance was found to be 1.498Å while the other carbon–carbon distances were all within 0.008Å of the 1.395 average. From this determination, it became clear that perhaps the two images found in this determination were compromises of the actual disordered images. That is, in the azulene–molybdenum molecule, the C(1) – C(2) – C(3) and C(6) – C(7) – C(8) angles were found to be 119.6 and 119.1°, respectively, which represents an average of the 110.16 and 129.47° angles found by Hanson for the corresponding angles. The angles determined in molecular azulene are closer to those found by Hanson (115.6 and 124.5) but also exhibit the effect of a similar compromise resulting from the very close half-carbons in the distorted images. Thus, it must be concluded that the two azulene images in this structure, while in excellent agreement and while having rather small standard deviations associated with the distances and angles, represent only a good compromise to the actual ring distances and angles. In this connection, it has been pointed out by Ibers (63) that an incorrect model can give deceivingly small standard deviations and, thus, that standard deviations are meaningful only if calculated for the correct model. This fact prohibits the possibility of resolving the question of localized double bond character. However, while the detailed C-C bonding cannot be determined, the general nature of the metal–ring bonding can be discovered.

As can be seen in Table 8, the metal–five–membered ring bonds are all approximately equivalent and thus, this bonding can be considered as equivalent to molybdenum–cyclopentadienyl bonding. This molybdenum, thus, has a coordination number of seven if the ring is considered to occupy three

coordination sites as is customarily done. Coordination numbers greater

than six are not unusual for molybdenum although eight, as found in

$Mo(CN)_8^{4-}$ and MoF_8^{2-}, is much more common than seven. A description of the

7-coordination in the azulene compound is difficult due to the uncertainty

in exactly where the coordination to the five member ring occurs relative

to the molybdenum-carbonyl bonds. As a result of this uncertainty, the

coordination could be either a distorted trigonal prism with the seventh

coordination site normal to one of its faces (as TaF_7^{2-}), or a distorted

octahedron with the seventh site outside the center of one triangular face

$(NbOF_6^{3-})$. The bonding of molybdenum to the seven-membered ring, however,

is not as simple as the bonding of the other molybdenum. The molybdenum-

carbon bonds fall into three classes averaging 2.336, 2.499 and 2.940Å.

The bond order of the second relative to the first, using Pauling's formula

is $\frac{1}{2}$, while the third to the first is very small. Thus, in this case, the

molybdenum can be considered to be π-bonded to the end three carbons of the

ring similar to that which occurs in π-cycloheptatrienyl-π-cyclopentadienyl

molybdenum dicarbonyl (64). And yet, the bonding cannot be considered as

purely an allylic π-bond, because some π-bonding to all of the end five

carbons must be considered. By no means however, can the molybdenum be

considered bound to all seven carbons in the seven-membered ring. The

molybdenum atom involved in this bonding thus has a coordination number

between six and seven: six if the ring π-bond is purely allylic, and

seven if it is equally over five atoms. This rather complex situation will

prohibit any detailed discussion of the orbitals involved in the metal

bonding.

This rather unique bonding by the molybdenum to the seven-membered ring can be seen to arise as a result of the molybdenum-molybdenum bond distance being 3.262Å. Because the one molybdenum bonds equivalently to the five membered ring, the other molybdenum is forced to assume a π-bonding position closer to the end of the seven-membered ring than it would probably prefer. It can be seen from the dihedral angles in Table 8, and from Table 9, that the azulene ring has bent along the C(4) - C(10) bond enabling the molybdenum to π-bond to a greater extent over the five atom area. The azulene ring was found by Hansen to be very nearly planar.

The molybdenum-carbonyl bonding is in good agreement with molybdenum-carbonyl bonding observed in other compounds.(61, 65). It can be seen from Table 8 that two carbonyls opposed to the metal-metal bond have significantly shorter metal-carbon distances. This shortening it is felt, is real, especially since the same effect can be seen in the structure of π-cyclopentadienyl molybdenum tricarbonyl dimer (61), but unfortunately, the complexity of the azulene structure and its lack of symmetry prohibit any discussion of the cause.

The structure found for the molybdenum-complex gives much information which can be used to understand the structure of azulenedi-iron pentacarbonyl. The differences in this structure from the molybdenum molecule would arise primarily from the fact that an iron-iron bond is considerably shorter than a molybdenum-molybdenum bond, about 2.5Å to 3.25. This shortening would enable the azulene to remain more nearly planar and would result in an iron atom occupying a position relative to the seven membered ring as seen in Figure 4b. From the molybdenum structure, it would seem

Table 9. Least squares planes in $C_{10}H_8Mo_2(CO)_6$

Plane #	Generated from	Equation
1	rings 1 and 2	$-.162X + .039Y + .986Z + 2.021 = 0.0$
2	ring 1	$-.187X + .052Y + .981Z + 2.009 = 0.0$
3	ring 2	$-.125X + .017Y + .992Z + 2.146 = 0.0$
4	7-member ring 2	$-.143X - .041Y + .989Z + 2.297 = 0.0$
5	5-member ring 1	$-.132X + .108Y + .985Z + 1.685 = 0.0$
6	5-member ring 2	$-.258X - .039Y + .965Z - 2.225 = 0.0$

Distance from plane in Å

Name	(1)	(2)	(3)	(4)	(5)	(6)
C1	-0.0915	-0.0313	-0.0763	-0.0573	-0.2671	0.0426
C2	-0.1986	-0.1639	-0.1421	-0.0523	-0.4552	0.0076
C3	-0.1307	-0.1289	-0.0265	0.0364	-0.3471	-0.0568
C4	0.1798	0.1662	0.3032	0.2816	0.0699	0.0533
C4'	0.0083	0.0147	0.1-14	0.0584	-0.0785	-0.1095
C5	0.2582	0.2391	0.3863	0.2798	0.2543	-0.0443
C5'	-0.0063	-0.0073	0.0950	-0.0152	-0.0082	-0.2706
C6	-0.0962	-0.1157	0.0292	-0.1671	0.0134	-0.5703
C7	-0.2028	-0.1971	-0.1176	-0.3820	-0.0138	-0.7448
C8	-0.1412	-0.1026	-0.1041	-0.3425	0.0075	-0.5521
C9	0.2026	0.2583	0.2169	0.0534	0.2527	-0.0241
C9'	-0.0206	0.0144	0.0259	-0.1099	0.0012	-0.2448
C10	0.0334	0.0759	0.0713	0.0013	-0.0284	-0.0467
C10'	0.2056	0.2670	0.2150	0.1398	0.1449	0.1617
Mo1	1.9013	1.9350	1.9523	1.9494	1.7472	1.9236
Mo2	1.9074	1.9255	1.9729	1.7492	2.0305	1.4691
C11	3.2362	3.2944	3.2387	2.9870	3.3770	2.8406
O1	3.9615	4.0434	3.9266	3.6517	4.1213	3.5784
C12	2.5838	2.5966	2.6507	2.2949	2.8678	1.8787
O2	3.0194	3.0290	3.0873	2.6525	3.3995	2.1543
C13	3.2233	3.2095	3.3349	3.1244	3.3295	2.7287
O3	3.9476	3.9140	4.0878	3.8799	4.0507	3.4074
C14	3.1585	3.1579	3.2587	3.2510	3.0108	3.0840
O4	3.8228	3.8015	3.9533	3.9502	3.6700	3.7046
C15	2.5614	2.6041	2.6029	2.7175	2.2558	2.8285
O5	2.9706	3.0171	3.0086	3.1914	2.5771	3.3766
C16	3.2666	3.3383	3.2569	3.2044	3.1572	3.2846
O6	4.0351	4.1301	3.9884	3.9110	3.9467	4.0616

likely that an iron atom would π-bond to the five membered ring, bond to two carbonyls and to the other iron in an approximately octahedral manner. The other iron would then π-bond to an allylic three carbon portion of the ring or perhaps a butadiene four carbon portion. It would also bond to three carbonyls and the other iron, to also give an approximate octahedral arrangement. This description of the iron structure would explain the observed properties. That is, the model discussed would be expected to have two non-equivalent hydrogens: hydrogens attached to carbons π-bonded to an iron and these attached to carbons not involved in π-bonds. Also, the existence of isomers can be understood. If a methyl were attached to azulene at C(5), one isomer would be formed if an iron π-bonded to the C(5) side of the molecule and another if it bonded to the other side. In all of this discussion, it will be noticed that localized double bonds are not required and thus, the question of localization in this system remains unanswered.

THE STRUCTURE OF $(NPCl_2)_5$

Introduction

Single crystal structure determinations have been reported for two trimeric cyclic phosphonitrilic derivatives (66, 67) and for several tetrameric species (68-70). From these structural determinations, some success has been achieved in understanding the nature of the bonding in the cyclic phosphonitrilics (71-74). However, one difficulty in understanding the bonding as found in the lower members is the fact that geometric constraints play a large part in determining the observed configuration. As a result, the heat of formation data for the cyclic phosphonitrilics have not been successfully explained. Thus, we felt that study of a higher member of the series would be very profitable since in a higher member, the chosen configuration would be less a result of geometric constraints and more a result of favorable bonding conditions. For this reason, a study of decachloropentaphosphonitrile was undertaken.

Experimental

Crystals of the pentameric phosphonitrilic chloride were prepared (75) and kindly supplied to us by Dr. N. L. Paddock. The crystals were soft, waxy, translucent, irregular masses. Good Weissenberg and precession pictures were obtained from one of the crystals at room temperature in spite of its low, $41.3^{\circ}C$., melting point (75). Lattice constants and space group

were determined from the precession films. Because reflections could be seen on the films at high values of $\sin\theta/\lambda$ at room temperature, a large crystal was selected, mounted in a capillary and used for data collection. The three dimensional data were gathered using $Mo-K_\alpha$ radiation with a General Electric XRD-5 X-ray unit equipped with a single crystal orienter. The peak-heights of the 1963 reflections with $\sin\theta/\lambda$ less than 0.600 were checked, and the reflections which appeared significantly above the background level were scanned for 100 seconds at a scan rate of 2°/minute. For approximately one-hundred peaks along dense lattice rows, where some peak overlap was observed, a planimetered peak intensity was obtained from the recorder tracing. For the remainder of the peaks, a background value was found from a table of backgrounds compiled from many background scans. Lorentz, polarization and streak corrections were applied, but due to a low absorption coefficient, and the crystal's irregular shape, no absorption correction was made. Sharpened structure factors were calculated using the method of Jacobson, Wunderlich and Lipscomb (76), and a Patterson map generated.

Crystal data

$(NPCl_2)_5$, M = 579.43, m.p. = 41.3°, orthorhombic, a = 15.48 ± .03, b = 19.44 ± .03, c = 6.26 ± .02Å, volume = 1883.83Å^3, D_m = 2.02 g/cc, Z = 4, D_c = 2.04 g/cc, F(000) = 1120. Space group $P2_12_12_1$, $Mo-K_\alpha$ radiation, μ = 18.8cm.$^{-1}$.

Structure Determination

The structure determination of $(NPCl_2)_5$ proved to be quite difficult for two reasons. First, the sixty approximately equivalent chlorine and phosphorus atoms generated 3541 Patterson vectors. This in itself would be enough to make the structure determination difficult, but a second fea- ture compounded the problem. Since the nitrogen vectors could not be seen in the Patterson, the largest rigid body that could be searched for was the PCl_2 group. This group was so small that an impossible number of com- binations of Patterson peaks could be found consistent with it.

The sharpened Patterson map was finally deconvoluted to give the ini- tial model as follows: a map was generated using the minimum function from a triple superposition on three Harker peaks. This triple superposi- tion served to fix the electron density origin in Patterson space, and hence the symmetry elements. The resultant map also revealed three large, well-shaped peaks much higher than any others, even though the superposi- tions were carried out using vectors of multiplicity greater than three. The twenty-one Patterson vectors associated with these peaks were computed and were all found on the Patterson map. Because the three-fold super- position had not reduced the number of peaks sufficiently, a seven-fold superposition was carried out. The seven superposition vectors used were the original three Harker vectors, the vector associated with one of the large peaks seen on the first superposition map and the three vectors sym- metry related to it. The map resulting from these superpositions had many fewer peaks than the first map, but still had approximately forty peaks per

asymmetric unit of sufficient height to be heavy atoms (i.e. phosphorus and chlorine atoms). At this point, use was made of a symmetry map (77) (first-order consistency function) (78), generated from the Harker sections to reduce the number of possible atom positions. This pseudo-electron density map was obtained as follows: since each Harker section contains peaks which result from interactions between atoms in general positions x, y, z, and those related to them by some symmetry operation, it should be possible to say something about the electron density at x, y, z by looking at the U, V, W (U, V and W represent coordinates in Patterson space) corresponding to its Harker interactions. Specifically, consider the Harker section resulting from the interactions between positions x, y, z and $\frac{1}{2}-x$, $-y$, $z = \frac{1}{2}$ which are equivalent positions in the space group $P2_12_12_1$. The peaks in the Patterson with $W = \frac{1}{2}$ will either be peaks from Harker interactions (Harker peaks) or peaks from interactions where W coincidentally is equal to one-half. This means that for a peak to occur in electron density space along a line with fixed x and y coordinates, a peak must occur in Patterson space at $U = \frac{1}{2}-2x$, $V = -2y$ and $W = \frac{1}{2}$, although the converse cannot be said to be true absolutely. Thus, by considering this Harker section, a pseudo-electron density map can be generated by assigning to all points on lines parallel to the z-axis with coordinates x and y, the value occurring in the Patterson map at $U = \frac{1}{2}-2x$, $V = -2y$ and $W = \frac{1}{2}$. In a similar fashion, pseudo-electron density maps can be generated from the other Harker sections. If these maps are then superimposed origin-to-origin, using the minimum function, a symmetry map is obtained. This map by necessity, has peaks at all positions consistent with all the Harker sec-

tions and thus must have a peak at all atom positions. While this information might seem to be sufficient to solve the structure, there are several difficulties involved with the map that should be mentioned. First, non-Harker peaks can be positioned in such a way on a Harker section as to give rise to spurious peaks in the symmetry map. Second, while the map obtained has the space group symmetry, it will also contain a center of symmetry at the origin as a remnant of the Patterson center of symmetry, even in acentric space groups. This extra symmetry will give rise to a double image of the structure. Eight other images also result due to ambiguities in the origin. Other problems arise as a result of peaks falling on two Harker sections. These have a greater multiplicity than those on a single Harker layer and thus tend to cause unrealistically large peaks to occur at x, y, and z = 0, 1/4, 1/2, and 3/4. Another difficulty occurs as a result of the symmetry map being generated from every other Patterson point, (i.e. x = 1/40 is assigned the value at $U = \frac{1}{2}-2x = 18/40$ while the value at x = 2/40 is taken from U = 16/40, U = 17/40 being skipped). This results in a considerable loss in resolution in the symmetry map. A final difficulty results from the fact that a useful symmetry map can only be generated if enough symmetry elements are present in the space group to give reasonable resolution. However, in spite of these problems, the symmetry map can yield much information in space groups with four or more general positions, especially when used in conjunction with other procedures. In this structure, the symmetry map was used after the sevenfold-superposition map was obtained. Considering the two together, the forty possible atomic positions were reduced to nine likely positions. No attempt was made to make chemical sense out of these positions, but they

were immediately used to generate an electron density map. The new peaks which occurred in this map, were checked against the symmetry map and the sevenfold-superposition map, and if found consistent with both, were used with the original positions to generate another electron density map. By proceeding in this cautious manner, from four successive electron density maps, all fifteen heavy atoms were found without an error, and two of the original nine atoms were found to have been misplaced. One cycle of full matrix least squares was run on the positional parameters of the heavy atoms and an electron density map generated from the new parameters. From this map, the nitrogen atoms were located and thus, the phosphorus and chlorine atoms distinguished. Using Hartree-Fock-Slater atomic scattering factors (79), five cycles of isotropic refinement lowered the reliability factor, $R = \Sigma ||F_o| - |F_c|| / \Sigma |F_o|$, to 0.15, but indicated very little further decrease. The temperature factors of the chlorine atoms were unusually high at this point, two being as high as eleven, but considering the low melting point, they were not considered unreasonable. A difference Fourier map indicated much anisotropy in all atoms, but particularly in the chlorine atoms with the largest isotropic temperature factors. Four cycles of anisotropic least squares refinement succeeded in reducing the reliability factor to a final value of 0.0717. Before the last cycle of least squares was run, the weighting scheme was checked, found to be inadequate and modified such that a plot of $\Delta^2 \omega$ (where $\Delta^2 = (F_o - F_o)^2$ and $\omega = $ (scale factor)^2/sigma^2) versus F_o for groups of one-hundred reflections yielded a horizontal line.

Table 10. Final parameters and their standard errors from least squares refinement of $(NPCl_2)_5$

Atom	X	Y	Z	Beta 11	Beta 22	Beta 33	Beta 12	Beta 13	Beta 23
P1	0.08245 (0.00025)	0.01793 (0.00020)	0.66797 (0.00077)	0.00318 (0.00015)	0.00256 (0.00012)	0.03617 (0.00143)	0.00008 (0.00012)	0.00132 (0.00048)	-0.00217 (0.00039)
P2	0.14009 (0.00031)	0.16339 (0.00023)	0.66596 (0.00093)	0.00536 (0.00022)	0.00264 (0.00013)	0.04529 (0.00180)	-0.00013 (0.00014)	0.00430 (0.00060)	0.00030 (0.00046)
P3	0.00417 (0.00027)	0.24112 (0.00022)	0.85156 (0.00086)	0.00465 (0.00019)	0.00267 (0.00013)	0.04345 (0.00169)	-0.00044 (0.00013)	0.00376 (0.00059)	-0.00040 (0.00045)
P4	-0.11967 (0.00026)	0.13675 (0.00020)	1.00801 (0.00076)	0.00422 (0.00018)	0.00210 (0.00011)	0.03141 (0.00137)	-0.00011 (0.00012)	0.00255 (0.00049)	-0.00079 (0.00036)
P5	-0.08817 (0.00023)	-0.00250 (0.00019)	0.84797 (0.00075)	0.00317 (0.00015)	0.00231 (0.00011)	0.03297 (0.00130)	-0.00038 (0.00011)	0.00155 (0.00045)	-0.00029 (0.00038)
N2	0.09502 (0.00111)	0.22766 (0.00072)	0.75519 (0.00380)	0.00843 (0.00096)	0.00309 (0.00046)	0.10923 (0.01178)	-0.00012 (0.00056)	0.01496 (0.00305)	-0.00546 (0.00197)
N1	0.09597 (0.00116)	0.09471 (0.00063)	0.68544 (0.00332)	0.01035 (0.00107)	0.00230 (0.00039)	0.07134 (0.00828)	-0.00126 (0.00055)	0.00315 (0.00305)	-0.00246 (0.00160)
N3	-0.04460 (0.00100)	0.17769 (0.00077)	0.93161 (0.00392)	0.00689 (0.00082)	0.00387 (0.00054)	0.09738 (0.01138)	-0.00102 (0.00056)	0.00541 (0.00271)	0.00674 (0.00210)
N4	-0.11549 (0.00117)	0.05935 (0.00078)	0.97876 (0.00341)	0.01045 (0.00117)	0.00391 (0.00055)	0.07430 (0.00867)	0.00123 (0.00068)	0.00719 (0.00312)	-0.00349 (0.00197)

Table 10 (continued)

Atom	X	Y	Z	Beta 11	Beta 22	Beta 33	Beta 12	Beta 13	Beta 23
N5	0.00654	-0.01390	0.78622	0.00501	0.00482	0.04321	0.00013	0.00127	0.00207
	(0.00086)	(0.00077)	(0.00253)	(0.00064)	(0.00054)	(0.00561)	(0.00051)	(0.00168)	(0.00159)
1C1	0.18530	-0.03198	0.76228	0.00502	0.00549	0.06793	0.00138	-0.00216	0.00188
	(0.00030)	(0.00030)	(0.00108)	(0.00022)	(0.00020)	(0.00260)	(0.00017)	(0.00065)	(0.00065)
2C1	0.25691	0.15987	0.78947	0.00759	0.00628	0.09151	-0.00013	-0.00352	-0.00297
	(0.00037)	(0.00033)	(0.00137)	(0.00032)	(0.00025)	(0.00381)	(0.00023)	(0.00097)	(0.00091)
3C1	0.02161	0.30804	1.07951	0.01047	0.00735	0.05771	0.00048	-0.00429	-0.00902
	(0.00043)	(0.00037)	(0.00114)	(0.00040)	(0.00028)	(0.00256)	(0.00029)	(0.00087)	(0.00074)
4C1	-0.13842	0.15210	1.31093	0.01823	0.00878	0.03363	0.00018	0.00673	-0.00049
	(0.00058)	(0.00042)	(0.00101)	(0.00070)	(0.00033)	(0.00191)	(0.00043)	(0.00100)	(0.00073)
5C1	-0.12069	-0.08362	1.01498	0.00861	0.00454	0.07504	-0.00025	0.00593	0.00865
	(0.00036)	(0.00028)	(0.00116)	(0.00032)	(0.00019)	(0.00297)	(0.00020)	(0.00095)	(0.00065)
6C1	0.07558	-0.00683	0.36174	0.00838	0.00789	0.03689	-0.00039	-0.00102	-0.00491
	(0.00037)	(0.00034)	(0.00089)	(0.00033)	(0.00028)	(0.00166)	(0.00026)	(0.00067)	(0.00065)
7C1	0.16581	0.17992	0.36276	0.01495	0.00877	0.06461	0.00306	0.01115	0.01298
	(0.00054)	(0.00041)	(0.00124)	(0.00058)	(0.00035)	(0.00301)	(0.00039)	(0.00123)	(0.00092)
8C1	-0.06543	0.29474	0.64632	0.01138	0.00610	0.05511	-0.00096	-0.00762	0.00537
	(0.00043)	(0.00033)	(0.00116)	(0.00041)	(0.00023)	(0.00247)	(0.00026)	(0.00097)	(0.00069)
9C1	-0.22860	0.17062	0.88263	0.00488	0.00585	0.08768	0.00051	-0.00496	0.00001
	(0.00031)	(0.00031)	(0.00129)	(0.00022)	(0.00022)	(0.00331)	(0.00018)	(0.00081)	(0.00079)
10C1	-0.16091	-0.01031	0.59687	0.00958	0.00822	0.06375	-0.00059	-0.01429	-0.00136
	(0.00041)	(0.00038)	(0.00110)	(0.00037)	(0.00031)	(0.00271)	(0.00029)	(0.00087)	(0.00082)

Table 11. Distances (with distances corrected for thermal libration) and angles in $(NPCl_2)_5$

Atoms	Distance	Distance (cor.)	Error	Atoms	Angle	Angle (cor.)	Error
P1-N1	1.511 Å	1.516 Å	0.011 Å	P1-N1-P2	158.98°	158.96°	1.20°
N1-N2	1.505	1.509	0.012	P2-N2-P3	133.61	133.62	0.93
P2-N2	1.536	1.541	0.014	P3-N3-P4	157.20	157.26	1.07
N2-P3	1.553	1.561	0.015	P4-N4-P5	149.80	149.80	1.32
P3-N3	1.530	1.534	0.013	P5-N5-P1	143.47	143.57	0.95
N3-P4	1.488	1.492	0.013	N5-P1-N1	118.28	118.09	0.85
P4-N4	1.517	1.523	0.014	N1-P2-N2	119.08	119.11	0.79
N4-P5	1.515	1.521	0.014	N2-P3-N3	116.01	116.10	0.79
P5-N5	1.532	1.540	0.012	N3-P4-N4	117.28	117.22	0.91
N5-P1	1.521	1.527	0.013	N4-P5-N5	121.22	121.21	0.86
P1-1Cl	1.956	1.965	0.006	1Cl-P1-6Cl	102.44	102.51	0.30
P2-2Cl	1.968	1.972	0.008	2Cl-P2-7Cl	101.47	101.60	0.40
P3-3Cl	1.950	1.957	0.008	3Cl-P3-8Cl	101.51	101.71	0.36
P4-4Cl	1.941	1.947	0.009	4Cl-P4-9Cl	102.09	102.18	0.38
P5-5Cl	1.958	1.963	0.006	5Cl-P5-10Cl	102.73	102.78	0.33
P1-6Cl	1.979	1.987	0.009				
P2-7Cl	1.966	1.972	0.010				
P3-8Cl	1.974	1.984	0.008	Cl-P-N	108.72	average	
P4-9Cl	1.973	1.980	0.007				
P5-10Cl	1.940	1.948	0.008				
1Cl-6Cl	3.068	3.083	0.010				
2Cl-7Cl	3.046	3.056	0.013				
3Cl-8Cl	3.039	3.056	0.011				
4Cl-9Cl	3.044	3.055	0.012				
5Cl-10Cl	3.044	3.056	0.011				
1Cl-2Cl	3.894	3.908	0.009				
6Cl-7Cl	3.890	3.900	0.011				
8Cl-9Cl	3.794	3.801	0.009				

Table 12. Amplitudes and direction cosines of the principle thermal axes R

Atom	R	RMS amp.($\mathring{R}$)	Cos (X)	Cos (Y)	Atom	R	RMS amp.($\mathring{R}$)	Cos (X)	Cos (Y)
P1	1	0.2806	.1341	-.4924	1Cl	1	0.3728	-.0500	.2952
	2	.2118	.4704	.8302		2	.3343	-.4143	-.8754
	3	.1893	.8722	-.3858		3	.2239	-.9088	.3828
P2	1	.3194	-.4958	-.0121	2Cl	1	.4352	.1646	.2480
	2	.2338	-.7357	.5372		2	.3416	.2238	-.9520
	3	.2210	-.4615	-.8434		3	.2966	.9606	.1793
P3	1	.3093	-.4390	.1154	3Cl	1	.4364	.2895	.7320
	2	.2329	-.4979	.7943		2	.3521	.9342	-.3564
	3	.2096	-.7479	-.5965		3	.2607	.2084	.5806
P4	1	.2670	.5321	-.1590	4Cl	1	.4776	-.9792	-.0347
	2	.2085	.8312	.2853		2	.4100	-.0275	.9989
	3	.1976	.1614	-.9452		3	.2447	-.2009	.0324
P5	1	.2597	.2518	-.0117	5Cl	1	.4318	-.2813	-.4447
	2	.2180	.4676	.8770		2	.3225	-.9000	.4296
	3	.1821	.8473	-.4804		3	.2235	-.3328	-.7859
N1	1	.3948	-.5461	.2041	6Cl	1	.4021	-.0670	.9452
	2	.3421	-.8149	.0956		2	.3203	-.9840	-.0096
	3	.1960	-.1944	-.9743		3	.2485	-.1650	-.3264
N2	1	.5075	.4239	-.1553	7Cl	1	.5300	-.5814	-.6161
	2	.2733	.7987	.5287		2	.3642	-.7977	.5600
	3	.2146	.4371	-.8345		3	.2516	-.1598	-.5539
N3	1	.4581	-.1661	-.2711	8Cl	1	.4241	-.6770	.4591
	2	.3083	-.8211	.5704		2	.3340	-.6476	-.7429
	3	.2148	-.5461	-.7753		3	.2700	-.3496	.4872
N4	1	.4176	.5780	-.0670	9Cl	1	.4231	-.2005	-.0223
	2	.3437	.7086	.5354		2	.3361	-.1219	-.9914
	3	.2382	.4047	-.8419		3	.2309	-.9721	.1290
N5	1	.3208	-.1286	-.7720	10Cl	1	.4379	.6808	.0005
	2	.2769	-.2129	.6345		2	.3985	.0834	-.9935
	3	.2435	-.9686	-.0370		3	.2229	.7277	.1134

Results

A list of the 1319 observed and calculated structure factors used in the structure refinement is given in Figure 11. In Table 10 are listed the final positional and thermal parameters with standard deviations. The more important interatomic distances and angles with standard deviations can be found in Table 11.

Because of the very considerable anisotropy observed for many of the atoms (see Table 12), an analysis of the thermal motion was considered to be worthwhile. A rigid body thermal analysis was carried out, treating the entire molecule as a rigid body (80). The unweighted centroid of the molecule was used as the origin and was found to give the best fit between the individual anisotropic thermal parameters and those calculated from the rigid body thermal parameters. In Table 13 are given the rigid body vibrational and librational amplitudes along the principal axes and their direction cosines relative to the unit cell axes. In the last column of

Table 13. Translational and librational thermal amplitudes and direction cosines

	RMS amp.	Cos (X)	Cos (Y)	Cos (Z)	
Tx	0.2846$\overset{\text{o}}{\text{A}}$	-0.1081	0.9535	0.2814	85.87
Ty	0.2760	-0.9612	-0.1725	0.2152	104.33
Tz	0.2434	-0.2537	0.2472	-0.9352	15.03
ω_x	5.4359$^{\text{o}}$	0.3634	-0.9243	-0.1168	79.13
ω_y	3.9419	0.9316	0.3599	0.0507	115.78
ω_z	2.1306	0.0039	0.1266	-0.9919	28.75

Figure 11. Comparison of observed and calculated structure factors
            for $(NPCl_2)_5$

Figure 11 (Continued)

Figure 11 (Continued)

H	K	L	FOBS	FCAL	ACAL	BCAL
10	5	2	23.9	23.5	-11.5	-20.5
10	6	2	22.5	21.6	-1.2	21.5
10	7	2	11.5	11.8	3.6	-11.2
10	8	2	23.3	22.4	-18.7	-12.4
10	9	2	25.0	24.1	16.9	-17.1
10	10	2	38.7	39.6	-18.1	35.2
10	12	2	10.3	12.9	-2.7	12.7
10	13	2	25.2	25.8	-20.7	-15.3
10	16	2	11.7	10.6	-4.3	9.7
10	17	2	12.5	13.1	-1.0	-13.0
10	0	3	42.1	38.0	0.0	-38.0
10	1	3	36.3	34.4	25.5	-23.1
10	2	3	32.4	32.7	3.6	-32.5
10	3	3	24.7	24.4	10.0	22.2
10	4	3	16.2	14.4	6.9	-12.6
10	5	3	17.8	21.0	21.0	-0.8
10	6	3	15.7	16.0	14.3	-7.2
10	7	3	10.1	6.9	5.1	-4.7
10	8	3	31.5	33.1	2.9	-33.0
10	10	3	12.2	10.5	4.3	-9.6
10	11	3	14.5	14.8	1.7	14.7
10	13	3	0.4	6.6	2.9	-6.0
10	14	3	13.1	17.2	5.0	-16.4
10	1	4	9.3	9.8	9.6	1.7
10	3	4	9.4	11.6	-9.3	-6.8
10	4	4	14.2	14.5	-10.5	-10.0
10	5	4	9.8	12.7	-12.6	1.7
10	6	4	8.1	11.9	4.2	-11.2
10	7	4	8.6	11.5	-11.5	-0.2
10	12	4	8.2	8.9	-8.2	-3.4
10	13	4	16.2	16.4	-14.4	8.0
10	0	5	10.8	9.7	0.0	-9.7
10	1	5	11.4	11.0	-10.1	4.3
10	3	5	8.1	7.2	-6.7	2.7
10	4	5	10.6	8.3	1.8	8.1
10	5	5	14.1	9.9	-7.5	-6.4
10	7	5	9.4	10.5	-10.3	2.2
10	10	5	9.2	8.6	-7.7	3.7
10	11	5	11.9	7.9	-4.2	-6.7
10	4	6	11.3	11.5	10.7	-4.2
11	2	0	31.9	33.1	0.0	-33.1
11	3	0	43.8	44.3	0.0	44.3
11	4	0	26.1	22.0	0.0	22.0
11	5	0	10.7	4.8	0.0	-4.8
11	7	0	9.3	7.9	0.0	-7.9
11	8	0	46.9	47.5	0.0	-47.5
11	9	0	12.5	13.4	0.0	13.4
11	10	0	17.2	17.3	0.0	17.3
11	0	1	51.4	51.1	0.0	-51.1
11	1	1	15.0	12.1	-11.0	-5.1
11	2	1	43.9	47.3	8.3	-46.6
11	3	1	24.2	23.1	17.7	-14.9
11	4	1	60.4	63.9	-11.6	-62.8
11	5	1	8.8	3.6	3.6	1.3
11	6	1	19.1	18.1	-18.0	1.8
11	7	1	21.5	23.0	5.2	-22.4
11	8	1	45.4	46.2	13.8	-44.1
11	9	1	18.5	18.3	9.6	-15.6
11	10	1	10.4	10.4	5.3	-8.9
11	12	1	10.1	10.3	-9.2	-4.7
11	13	1	15.3	18.2	11.1	-14.5
11	14	1	14.6	14.5	-13.9	-3.9
11	15	1	11.3	11.6	-1.2	-11.6
11	0	2	9.8	13.5	13.5	-0.0
11	1	2	11.1	11.4	7.6	-8.5
11	3	2	23.1	21.9	-21.4	5.1
11	4	2	15.1	12.5	-1.4	12.4
11	5	2	19.7	20.6	2.8	20.5
11	6	2	20.2	19.1	-14.0	13.0
11	7	2	25.4	26.0	-25.8	3.3
11	8	2	13.0	13.2	10.9	7.5
11	10	2	12.3	10.9	-9.5	-5.6
11	11	2	24.8	22.8	-20.5	10.1
11	12	2	8.5	7.2	4.1	5.9
11	15	2	8.2	12.4	-9.5	-8.1
11	0	3	30.6	32.2	0.0	32.2
11	1	3	15.2	11.1	-7.1	8.6
11	2	3	16.9	15.3	15.3	-0.8
11	3	3	16.1	16.4	15.4	-5.8
11	4	3	12.3	10.7	-10.6	-1.7
11	5	3	10.0	10.9	0.9	-10.9
11	6	3	13.4	15.2	3.2	14.9
11	8	3	11.1	14.5	11.5	-8.8
11	9	3	8.3	6.8	-0.3	6.7
11	13	3	13.9	16.2	-16.2	0.5
11	2	4	10.2	8.4	-8.1	2.2
11	3	4	12.0	10.9	6.7	8.6
11	4	4	14.3	12.6	-10.7	-6.6
11	5	4	15.2	13.1	5.4	11.9
11	6	4	9.4	8.2	-7.3	-3.7
11	7	4	9.0	7.7	3.7	-6.7
11	10	4	11.6	15.3	-5.5	-14.3
11	11	4	15.2	15.6	14.7	5.4
11	0	5	10.7	11.8	0.0	11.8
11	2	5	10.9	10.7	4.2	9.8
11	3	5	10.5	7.0	-5.2	4.7
11	4	5	18.2	16.4	-0.9	16.4
11	8	5	16.9	16.3	3.2	16.0
11	9	5	8.3	8.5	-3.6	7.8
11	10	5	10.7	8.3	4.9	6.7
12	0	0	55.3	55.9	55.9	0.0
12	1	0	23.1	24.2	-24.2	-0.0
12	2	0	37.5	37.6	37.6	0.0
12	3	0	27.9	25.8	25.8	-0.0
12	4	0	80.5	82.6	82.6	0.0
12	5	0	13.2	8.2	8.2	-0.0
12	6	0	29.8	30.5	30.5	0.0
12	8	0	37.5	38.6	38.6	0.0
12	9	0	24.4	27.4	27.4	-0.0
12	10	0	18.8	20.3	20.3	0.0
12	11	0	8.1	4.8	4.8	-0.0
17	17	0	23.1	23.8	23.8	0.0
12	0	1	10.0	11.3	0.0	11.3
12	1	1	20.6	19.5	19.5	-0.1
12	2	1	18.6	16.9	2.2	-16.7
12	3	1	10.8	10.5	5.2	-9.1
12	5	1	18.9	15.9	7.0	14.2
12	6	1	12.2	13.8	0.5	13.8
12	7	1	14.7	13.0	-3.2	-12.6
12	8	1	12.9	10.1	-0.3	-10.1
12	9	1	11.8	13.1	-2.8	-12.8
12	10	1	19.5	16.6	16.0	-5.4
12	11	1	16.1	17.2	-6.4	-15.9
12	12	1	10.6	9.6	0.1	9.6
12	13	1	11.4	10.9	-6.2	9.0
12	14	1	15.8	16.2	12.5	-10.3
12	17	1	9.4	9.2	-3.1	-8.7
12	0	2	52.7	53.7	-53.7	0.0
12	1	2	13.1	8.7	-2.3	-8.4
12	2	2	28.3	27.8	-10.3	25.9
12	3	2	9.9	6.8	-1.7	6.6
12	4	2	31.0	31.2	-3.7	-30.9
12	5	2	13.3	13.9	-8.0	-11.3
12	6	2	13.2	13.9	-10.0	9.6
12	7	2	12.5	14.7	-13.5	-5.9
12	8	2	16.5	18.2	-15.4	9.6
12	13	2	15.7	17.7	-10.0	-14.6
12	0	3	25.6	24.0	0.0	-24.0
12	1	3	13.8	15.9	3.2	-15.6
12	3	3	14.3	15.4	-11.5	10.2
12	5	3	15.1	15.1	2.0	14.9
12	6	3	12.2	12.3	-0.2	-12.3
12	7	3	13.2	13.6	2.2	13.4
12	9	3	10.6	11.5	-1.1	-11.4
12	10	3	10.8	6.2	8.8	8.8
12	11	3	17.2	18.2	5.5	17.3
12	13	3	13.7	12.7	3.7	12.2
12	0	4	32.6	32.9	-32.9	0.0
12	1	4	10.9	10.2	3.7	
12	2	4	17.4	15.8	-15.7	-1.0
12	4	4	18.6	15.9	-15.5	3.2
12	5	4	12.2	8.4	4.6	7.1
12	6	4	10.5	9.5	-9.0	3.3
12	8	4	21.3	21.2	-21.2	1.6
12	10	4	9.5	9.1	-5.9	6.8
12	12	4	8.2	7.3	-5.5	4.8
12	4	5	8.3	5.6	5.6	-0.2
13	2	0	8.3	8.0	0.0	8.0
13	5	0	15.7	13.8	0.0	-13.8
13	6	0	22.4	23.0	0.0	23.0
13	7	0	8.7	9.9	0.0	-9.9
13	11	0	18.9	18.2	0.0	-18.2
13	12	0	14.2	11.8	0.0	11.8
13	13	0	8.8	8.8	0.0	-8.8
13	14	0	23.5	21.5	0.0	21.5
13	15	0	8.1	9.6	0.0	-9.6
13	16	0	9.4	0.0	0.0	-9.4
13	0	1	31.0	30.6	0.0	-30.6
13	1	1	26.6	23.3	-22.9	4.2
13	4	1	21.2	21.1	11.5	-17.7
13	5	1	9.9	9.5	8.7	3.9
13	7	1	15.6	13.6	-12.4	-5.5
13	8	1	11.5	14.8	-4.2	-14.2
13	11	1	9.8	8.6	7.1	4.9
13	12	1	18.8	18.5	8.6	-16.4
13	16	1	7.9	7.4	2.7	-6.9
13	1	2	15.2	11.6	11.3	-2.8
13	2	2	15.3	20.6	-16.6	-12.2
13	3	2	13.6	14.0	-14.0	-0.5
13	4	2	15.6	16.4	-16.3	-0.9
13	5	2	8.7	8.0	-5.6	-5.7
13	7	2	13.0	13.0	-12.3	4.3
13	8	2	20.8	20.6	-8.2	-18.9
13	10	2	24.5	24.9	-18.0	-17.2
13	11	2	16.9	14.7	-14.5	2.6
13	14	2	8.5	8.9	-8.8	-1.4
13	15	2	15.5	14.6	-12.7	7.2
13	0	3	23.8	20.9	0.0	-20.9
13	2	3	9.9	8.4	5.9	-5.9
13	3	3	13.4	13.4	13.4	0.3
13	4	3	10.3	13.5	-12.5	-5.1
13	5	3	10.1	11.8	8.3	8.4
13	10	3	12.6	13.4	-13.2	2.3
13	1	4	18.0	16.4	3.3	16.0
13	3	4	14.3	12.1	9.4	-7.4
13	4	4	9.9	6.6	4.7	4.7
13	5	4	13.1	11.2	8.3	7.5
13	7	4	12.8	13.0	9.6	8.8
13	8	4	10.9	10.2	9.4	-3.9
13	10	4	8.6	8.0	7.4	-3.1
13	1	5	8.3	5.4	-5.4	0.1
13	3	5	11.2	8.6	8.6	-0.2
13	4	5	13.1	10.3	4.6	9.3
14	0	0	22.7	17.2	17.2	0.0
14	1	0	8.0	7.6	-7.6	-0.0
14	4	0	24.8	24.3	24.3	-0.0
14	5	0	15.7	15.4	-15.4	-0.0
14	8	0	9.4	13.5	13.5	0.0
14	9	0	26.3	25.1	-25.1	-0.0
14	11	0	20.7	21.1	-21.1	-0.0
14	12	0	20.3	18.0	18.0	0.0
14	15	0	10.0	8.1	-8.1	-0.0
14	1	1	17.7	15.8	-14.9	-5.3
14	2	1	11.2	13.1	8.2	-10.3
14	4	1	17.2	17.4	2.6	-17.2
14	5	1	18.8	18.4	-12.0	13.9
14	6	1	18.3	18.0	10.4	-14.7
14	7	1	17.9	18.4	-15.3	-10.2
14	8	1	12.5	13.0	13.0	-0.6
14	10	1	11.3	13.2	6.8	-11.4
14	11	1	10.2	9.8	-9.6	-2.1
14	12	1	9.6	8.4	1.9	-8.1
14	0	2	9.0	11.8	-11.8	0.0
14	2	2	13.3	11.3	10.9	-3.1
14	4	2	9.0	9.3	6.1	-7.0
14	5	2	17.1	16.0	16.0	0.6
14	7	2	9.2	8.2	5.3	6.2
14	8	2	11.4	12.0	-4.1	-11.2
14	9	2	9.3	10.5	-3.8	-9.8
14	12	2	9.9	9.9	-6.0	-8.0
14	13	2	13.7	12.3	12.2	-2.0
14	0	3	33.0	32.2	0.0	32.2
14	1	3	10.4	8.2	-8.0	-2.1
14	2	3	19.2	18.1	0.8	18.0
14	6	3	19.7	19.5	-4.3	19.0
14	7	3	13.7	14.1	-7.0	12.2
14	8	3	15.4	15.5	-0.1	15.5
14	10	3	10.5	8.4	1.9	8.2
14	0	4	19.6	18.3	-18.3	0.0
14	5	4	11.6	12.4	12.2	2.5
15	5	0	10.1	11.5	0.0	-11.5
15	12	0	11.2	9.5	0.0	-9.5
15	0	1	10.0	7.1	0.0	-7.1
15	2	1	12.4	13.9	-1.6	13.8
15	5	1	19.4	19.3	-7.0	18.0
15	6	1	10.7	10.6	9.1	5.4
15	7	1	15.9	13.4	-7.5	11.1
15	9	1	15.9	17.0	6.2	15.9
15	10	1	13.0	11.7	-7.7	8.7
15	11	1	11.0	12.2	-7.2	9.9
15	12	1	10.6	9.6	9.4	-1.5
15	13	1	13.9	10.4	-1.6	10.3
15	0	2	23.5	25.2	-25.2	-0.0
15	1	2	10.1	9.5	-4.4	8.2
15	2	2	14.1	14.1	-13.9	-2.5
15	3	2	9.5	9.3	-5.5	-7.5
15	5	2	15.5	15.5	12.3	-9.4
15	6	2	17.9	20.9	-20.9	-0.4
15	7	2	16.7	15.8	-15.6	2.4
15	10	2	11.4	10.6	-8.4	6.6
15	11	2	8.2	8.6	-1.5	-8.4
15	1	3	10.5	8.7	8.7	0.5
15	2	3	15.3	14.6	-13.4	5.6
15	5	3	12.3	9.3	2.7	8.8
15	7	3	10.7	10.6	10.0	-3.4
15	8	3	13.3	13.0	-13.0	0.4
15	0	4	15.2	14.3	14.3	0.0
15	2	4	8.9	9.8	9.8	1.2
15	3	4	9.9	7.5	1.6	-7.3
15	4	4	12.3	11.1	10.4	-3.8
16	0	0		8.9	8.9	0.0
16	1	0	23.2	23.3	-23.3	0.0
16	2	0	11.1	12.3	-12.3	0.0
16	4	0	9.9	9.4	-9.4	0.0
16	5	0	8.7	7.5	7.5	-0.0
16	6	0	18.0	15.8	-15.8	-0.0
16	7	0	13.6	16.6	-16.6	-0.0
16	9	0	12.7	14.2	-14.2	-0.0
16	10	0	20.6	18.8	-18.8	-0.0
16	1	1	9.7	9.8	8.8	4.2
16	2	1	14.9	17.1	-4.7	-16.4
16	3	1	11.5	10.3	-10.3	-0.3
16	4	1	12.4	14.7	-5.3	-13.7
16	5	1	11.9	11.3	11.2	-1.6
16	6	1	11.3	10.8	-8.4	-6.8
16	7	1	9.9	9.2	6.8	-6.2
16	8	1	9.7	9.7	-7.8	-5.7
16	9	1	14.9	13.7	-4.6	12.9
16	10	1	9.9	8.1	-5.0	-6.3
16	4	2	11.8	10.3	-9.8	-3.0
16	8	2	12.0	8.4	5.0	-6.8
16	0	3	17.6	20.7	0.0	20.7
16	2	3	14.8	15.7	1.9	15.6
16	4	3	11.3	9.5	5.2	8.0
16	5	3	12.9	11.3	1.2	-11.3
16	6	3	15.5	15.9	4.8	15.2
17	1	0	22.0	19.9	0.0	19.9
17	3	0	11.3	5.4	0.0	5.4
17	4	0	12.0	10.6	0.0	-10.6
17	5	0	22.6	18.9	0.0	18.9
17	7	0	12.2	10.3	0.0	10.3
17	0	1	12.6	7.5	0.0	7.5
17	1	1	13.3	12.0	0.0	7.1
17	2	1	16.0	13.6	-0.2	13.6
17	3	1	12.0	12.9	-12.7	-1.9
17	6	1	16.4	16.2	-1.6	16.1
17	1	2	14.8	14.3	10.3	-10.0
17	2	2	14.5	14.2	-7.0	12.4
18	0	0	14.0	10.5	-10.5	0.0
18	2	0	24.9	21.8	-21.8	0.0
18	4	0	14.7	13.2	-13.2	0.0
18	1	1	13.6	10.4	6.4	8.1
18	3	1	10.5	10.0	10.0	0.2

Figure 11 (Continued)

this table, the angles between the anisotropic ellipsoid axes and the
plane of the P-N ring are also listed. In Table 11, the distances and an-
gles corrected for rigid-body thermal motion (81, 82) can be seen.

Several least squares planes were calculated from the final position-
al parameters. The equations of these planes and the distances of the
atoms from them can be seen in Table 14.

Table 14. Least squares planes in $(NPCl_2)_5$

Plane #	Generated from	Equation
1	all P & N atoms	$0.4758x - 0.1272y + 0.8703z + 1.2224 = 0.0$
2	all P atoms	$0.4580x - 0.1427y + 0.8774z + 1.3340 = 0.0$
3	all N atoms	$0.4977x - 0.1338y + 0.8598z + 1.1115 = 0.0$

Distance from plane in $\overset{o}{R}$

Name	(1)	(2)	(3)
P1	-0.0221	0.0468	-0.0785
P2	0.0321	0.0412	0.0333
P3	-0.1509	-0.1195	-0.1877
P4	0.0465	0.1502	-0.0699
P5	-0.1485	-0.1187	-0.3801
N1	-0.0171	0.0257	-0.0501
N2	0.0270	0.0332	0.0239
N3	0.0824	0.1498	0.0072
N4	0.1094	0.2339	-0.0239
N5	0.1411	0.2457	0.0428
1Cl	1.3723	1.4321	1.3316
2Cl	1.5737	1.5573	1.6056
3Cl	1.0532	1.0697	1.0248
4Cl	1.5195	1.6372	1.3809
5Cl	0.6216	0.7922	0.4468
6Cl	-1.6786	-1.6140	-1.7238
7Cl	-1.4699	-1.4862	-1.4357
8Cl	-1.9134	-1.8881	-1.9464
9Cl	-1.5221	-1.4043	-1.6585
10Cl	-2.1320	-1.9910	-2.2739

The highest peak on a final difference Fourier map corresponded to approximately 0.7 electrons/$\overset{o}{A}$. The large peaks were all located close to atom positions, particularly nitrogen atoms.

Description of the Structure

The structure consists of discrete molecules of $(NPCl_2)_5$ which exist as very nearly planar ten-membered rings (see Table 14). The ring consists of alternating phosphorus and nitrogen atoms with two chlorine atoms bonded to each phosphorus. The molecule has no symmetry (higher than 1), but a mirror perpendicular to the ring, through atoms P(5) and N(2) is approached (see Figure 12). The molecule is distorted considerably from D_{5h} symmetry, primarily because N(1) and N(3) are puckered in toward the ring center. The chosen configuration enables all intra-molecular chlorine-chlorine distances to be larger than $3.9\overset{o}{A}$, considerably larger than the van der Waals contact distance.

The phosphorus-chlorine distances, the Cl-P-Cl and N-P-N angles are quite consistent in the molecule and are in good agreement with the data reported for other cyclic phosphonitriles. Significant differences, however, are found in the P-N distances and particularly in the P-N-P angles. The P-N distances vary from 1.49 to $1.55\overset{o}{A}$, but do not imply alternating double bonds, whereas the P-N-P angles range from 133.4 to 159.0°.

The four molecules in a unit cell are related to each other by two-fold screw axes and are packed such that the chlorine atoms in different molecules are staggered (see Figure 13). The shortest intermolecular
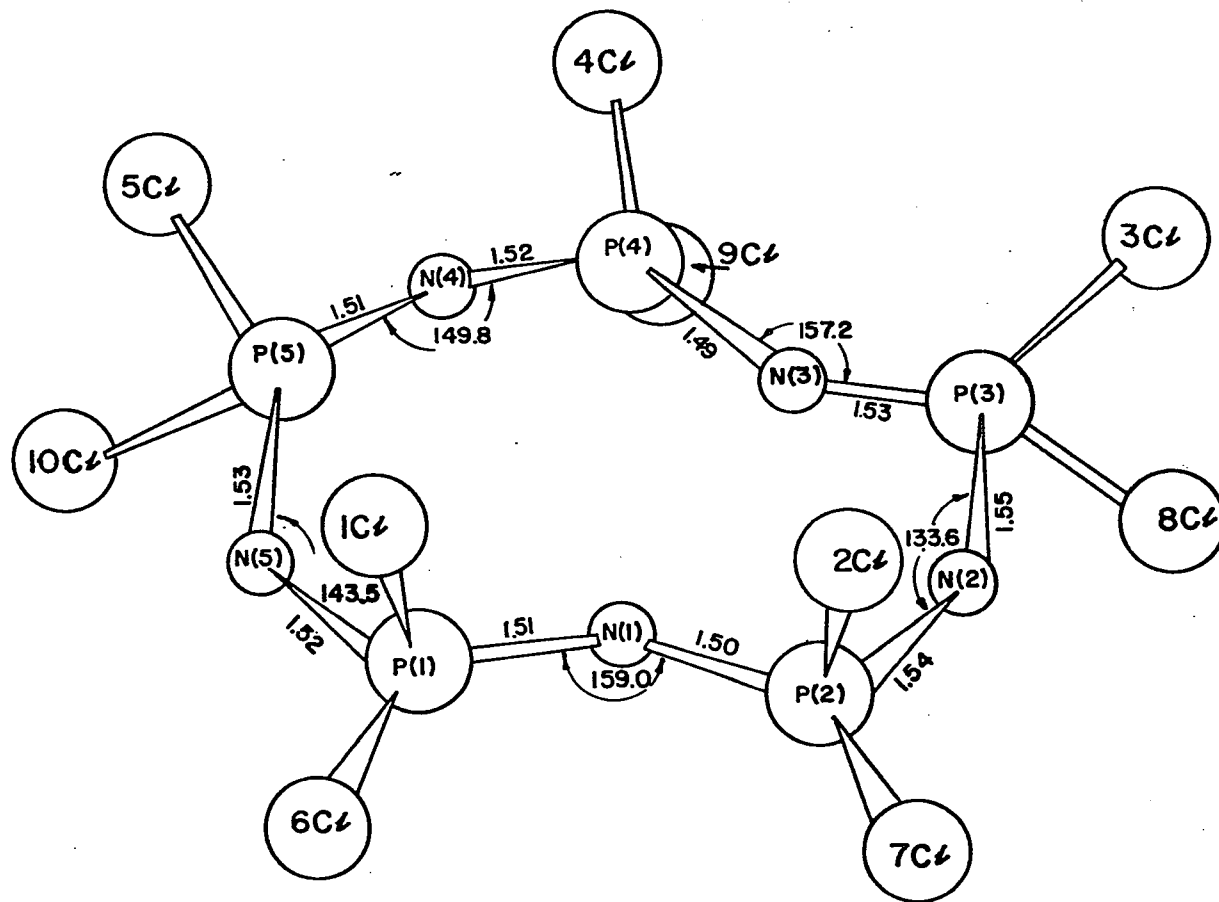
Figure 12. The molecular configuration of $(NPCl_2)_5$

Figure 13. Packing in $(NPCl_2)_5$; a projection on the xy plane (the dashed lines indicate the shortest intermolecular distances)
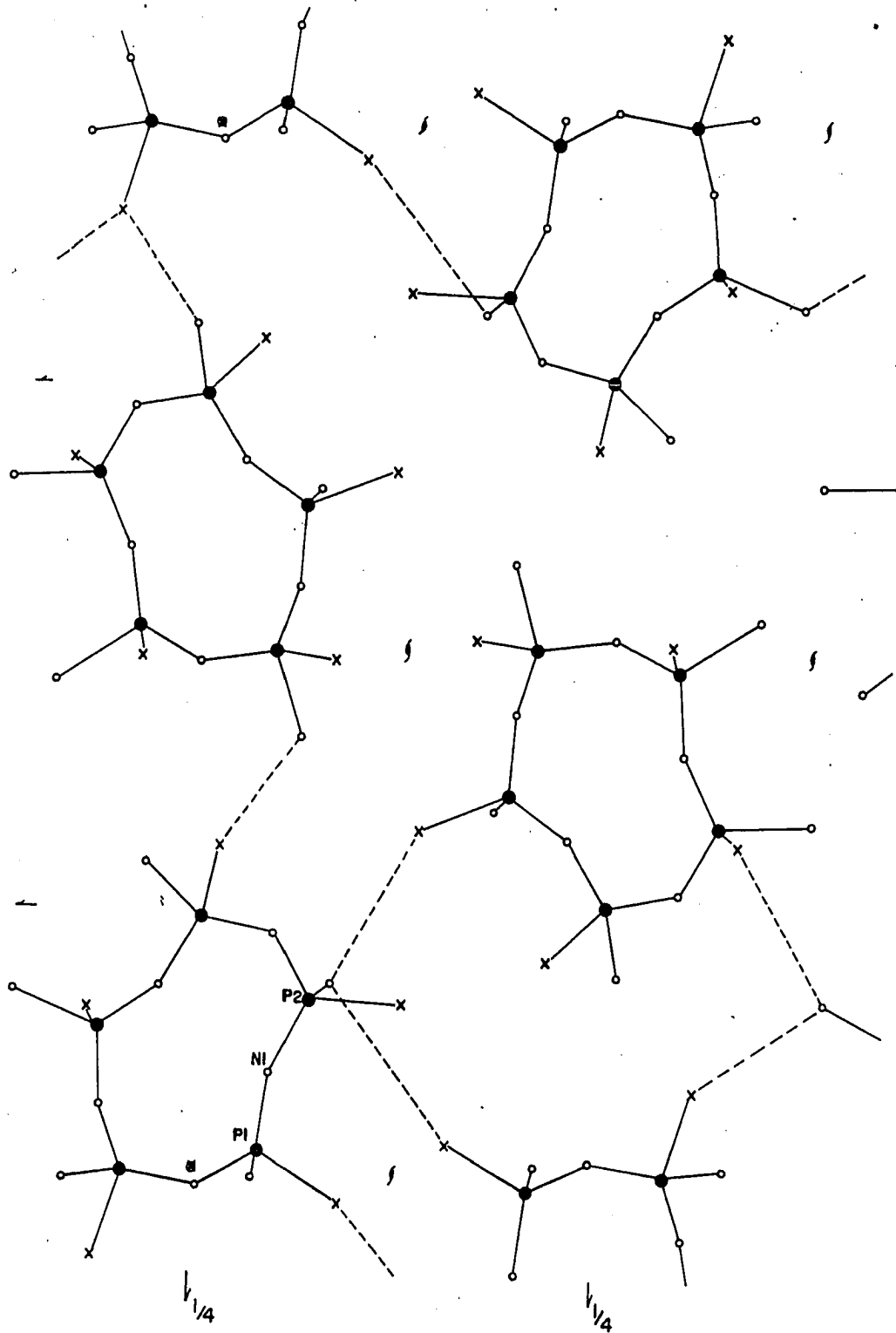
contacts are of the chlorine-chlorine type, but all are larger than the 3.60Å van der Waals chlorine-chlorine distance. The shortest intermolecular contacts are listed in Table 15.

Table 15. Intermolecular distances.

Atom 1	Atom 2	Symmetry transformation on atom 2[a]	Distance	Error
7Cl	2Cl	T_z = unit cell trans-	3.876Å	0.014Å
7Cl	3Cl	T_z lation in z	3.785	0.010
8Cl	3Cl	T_z	3.804	0.014
8Cl	4Cl	T_z	3.657	0.011
9Cl	4Cl	T_z	3.858	0.014
10Cl	4Cl	T_z	3.646	0.011
2Cl	9Cl	$2_1^z(x) + 2T_z$	3.889	0.010
3Cl	9Cl	$2_1(x) + 2T_z^z$	3.897	0.010
3Cl	5Cl	$2_1(y)$	3.638	0.010
1Cl	6Cl	$2_1(z)$	3.829	0.010
1Cl	7Cl	$2_1(z)$	3.739	0.009
1Cl	8Cl	$2_1(y) + T_y + T_z$	3.888	
7Cl	9Cl	$2_1(x) + T_y^z$	3.671	
8Cl	5Cl	$2_1(y) + T_z^z$	3.862	
9Cl	5Cl	$2_1(z) - T_x^z - T_z$	3.688	
9Cl	10Cl	$2_1(z) - T_x^x$	3.800	
10Cl	5Cl	$2_1(z) - T_x^x$	3.876	

Discussion

In Figure 14 can be seen projections of a molecule of decachloropenta-phosphonitrile and its rigid-body ellipsoids. The large thermal motion in atoms 4Cl and 7Cl, attached to P4 and P2 respectively, can be understood from this figure. These atoms are in contact with chlorine atoms in molecules above and below respectively (see Figure 15). The amplitude of libration about the ω_x axis is quite large and this motion forces these two
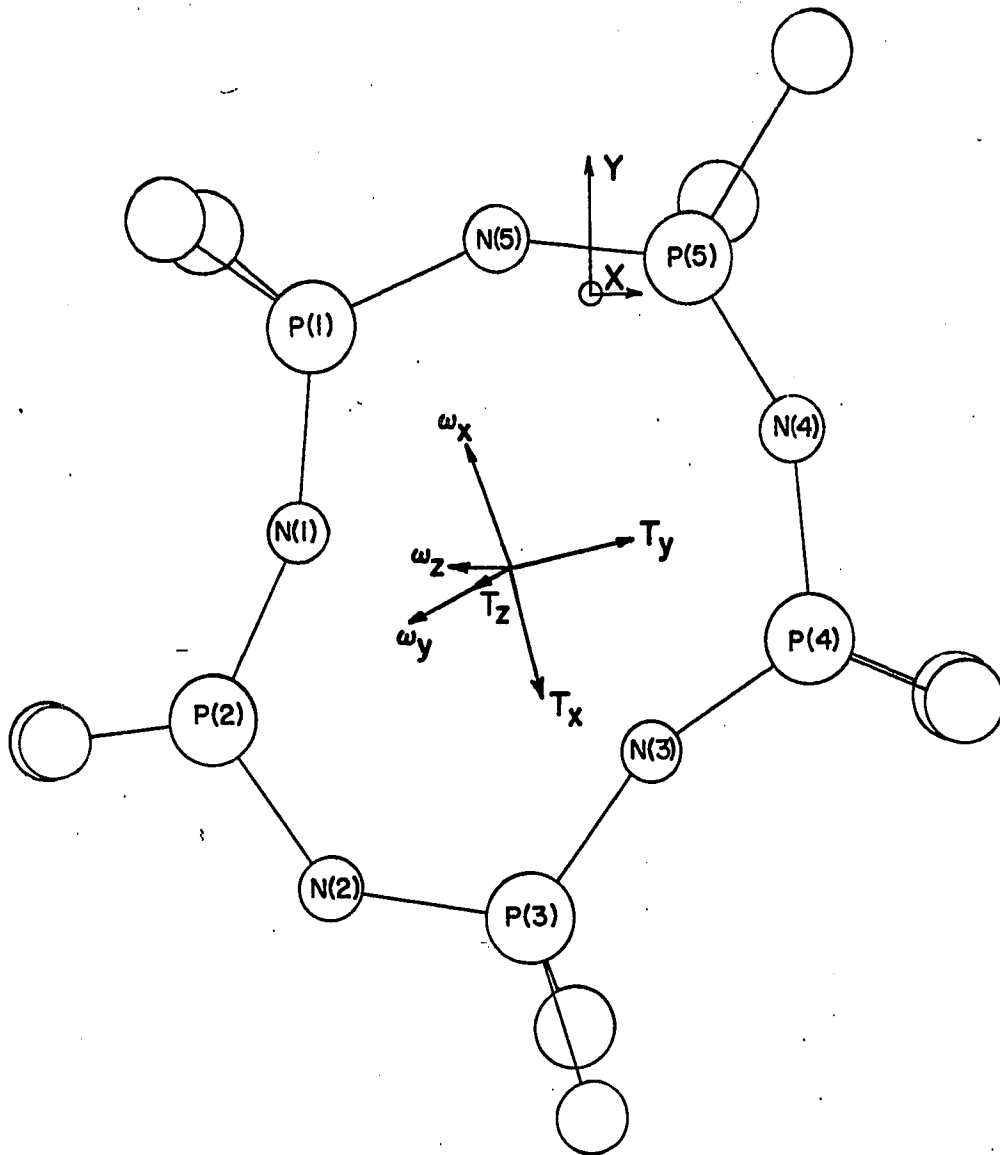
Figure 14. The translational and librational vectors projected on the P-N least squares plane
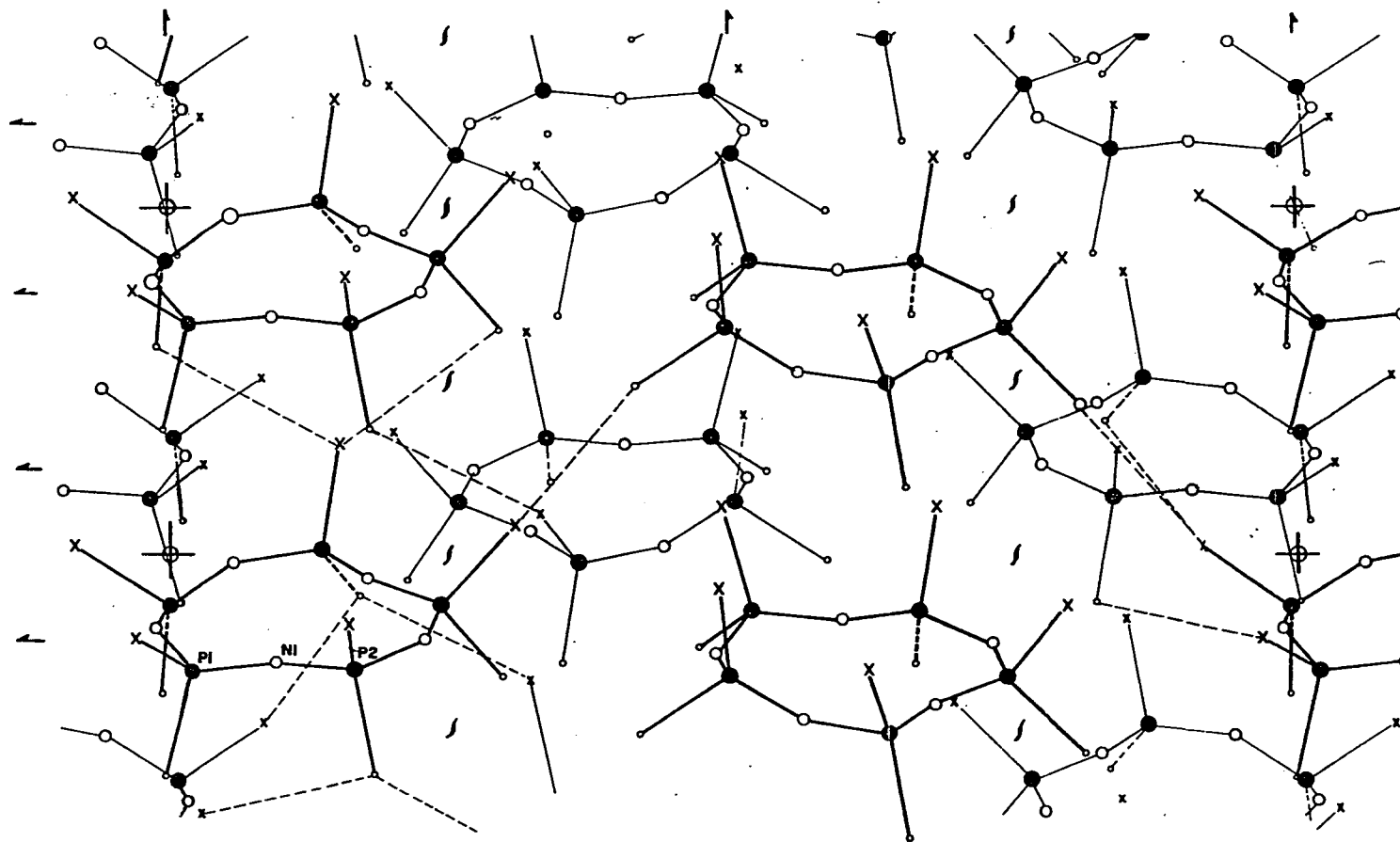
Figure 15. Molecular packing in $(NPCl_2)_5$; projection on the xz plane

chlorines to move away from the atoms with which van der Waals contacts exist. The effect of this is much anisotropy in the thermal motion of these atoms. The effect is most pronounced for 4Cl which can be seen to have a smaller vibrational amplitude along the Z-axis than any other chlorine atom because of its van der Waals contact with two atoms above it. Its very large isotropic temperature factor and anisotropy then is a result of being forced to move in the xy plane as the molecule librates about the ω_x axis.

Consideration of the van der Waals contacts also leads to an understanding of the magnitudes of the librational motion. Nearly every van der Waals contact has a large component in the xy plane; thus, the ω_z librational amplitude is quite small. On the other hand, there are only a. few van der Waals contacts restraining librational motion about the ω_x axis.

Listed in Table 16, is a summary of X-ray structural data of the cyclic phosphonitrilics. From this table, the shortening of the P-N distances and the increase in the P-N-P angles in the pentamer relative to the other cyclic chlorides is obvious. A closer look at these two discrepancies reveals, however, that the two effects are not unrelated. That is, a plot of the average of two adjacent P-N distances versus the included P-N-P (see Figure 16), reveals a definite correlation between the effects. A very smooth curve can be drawn through the eight points of the phosphonitrilic chlorides. On this same plot, it can be seen that the points corresponding to the phosphonitrilic fluorides fall below those of the chlorides. This can be understood by considering the effect of fluorine
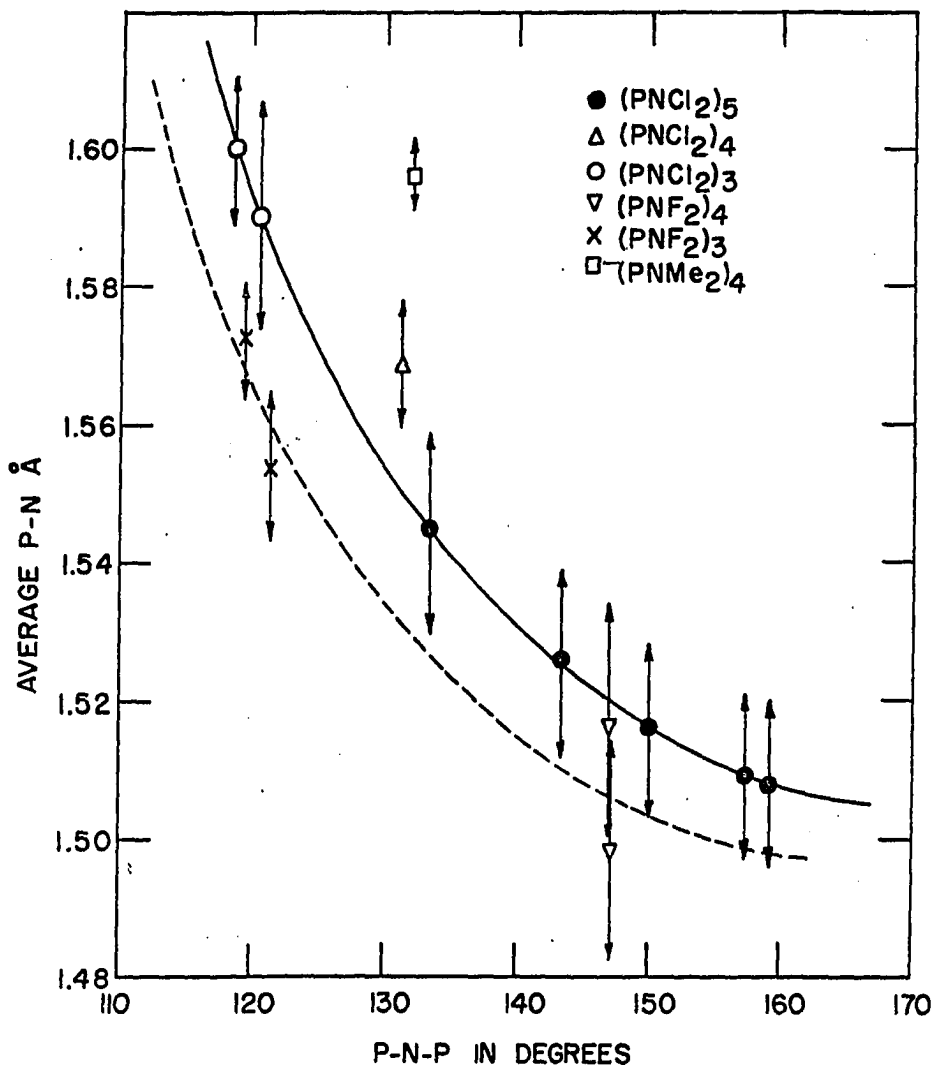
Figure 16. The correlation between P-N-P angle and P-N distance

Table 16. Results of cyclic phosphonitrilic X-ray structure determinations

Compound	Average distances in Å		Average angle			Configuration
	P-N	P-X	X-P-X	N-P-N	P-N-P	
$(F_2PN)_3$	1.560	1.521	99.1^o	119.4^o	120.3^o	planar
$(F_2PN)_4$	1.51	1.51	99.9	122.7	147.	planar
$((CH_3)_2PN)_4$	1.596	1.805	104.1	119.8	131.9	puckered
$((CH_3)_2N)_8P_4N_4$	1.59	1.79	102.	121.	129.	puckered
$(Cl_2PN)_3$	1.59_5	1.97_5	102.	120.	119.	planar
$(Cl_2PN)_4$	1.570	1.989	102.8	121.2	131.3	puckered
$(Cl_2PN)_5$	1.521	1.961	102.2	118.4	148.6	nearly planar

in similar compounds. For example, the axial P-Cl distance decreases from 2.19 to 2.05Å in going from PCl_5 (83) to PF_3Cl_2 (84). This decrease and the smaller effect observed in the phosphonitrilics can be understood to be a result of contraction of the orbitals on the phosphorus due to the electron-withdrawing power of fluorine. It would be expected that electron- withdrawing would particularly effect the sigma bond and this perhaps explains the much larger effect in the phosphorus halogen system where multiple bonds do not obscure the effect. The effect of substituting fluorine for chlorine atoms thus appears to shorten the P-N distance, but only a few hundredths of an Angstrom. The above discussion of course, presupposes that no intra-molecular van der Waals forces or intermolecular effects have a significant influence in these compounds, but such an assumption seems to be justified. It can also be seen that the point from $(NPMe_2)_4$ falls above the line, which can be explained to be a result of

electrons being donated to the electronegative phosphorus thus swelling its orbitals.

To understand the relationship between the P-N distance and the P-N-P angle, the bonding between the phosphorus and nitrogen atoms must be considered. This bonding can be regarded as resulting from three types of bonds: sigma, π(dπ-pπ bonding perpendicular to the P-N plane), and π' (dπ-pπ bonding in the plane of the ring).

From Table 16, the very good agreement between the Cl-P-Cl and N-P-N angles and the P-Cl distances would seem to imply that the sigma bonds are forming in a very similar manner in the cyclic phosphonitrilic chlorides. The sigma bonds in all of these compounds can be considered to result from approximate sp^3 hybrids on the phosphorus atoms bonding to p-orbitals of the chlorine atoms and to some kind of sp-hybrid on the nitrogen atoms.

Because of the considerable shortening of the P-N distances from the 1.78$\overset{o}{A}$ observed single bond P-N distance (85), considerable multiple bonding must be occurring. This multiple bonding however, can only occur through the d-orbitals on the phosphorus atom since the s- and p-orbitals have already been used to form the sigma bonds. The π type of pπ-d bonding was first recognized as being important (86, 87). The nature of this bonding has been much discussed (71-74). The first treatment (86) used the coordinate system in Figure 17a and considered the bonding to arise from overlap of the phosphorus d_{xz} and d_{yz} orbitals with p_z orbitals on the nitrogen atoms. This treatment has been developed in some detail (72), but a second approach (71) can be given which in many respects, is easier to visualize. This approach, as seen in Figure 17b, differs in that two hybrid d-orbitals are formed on the phosphorus atoms as follows:

(a)

(b)

(c)

(d).
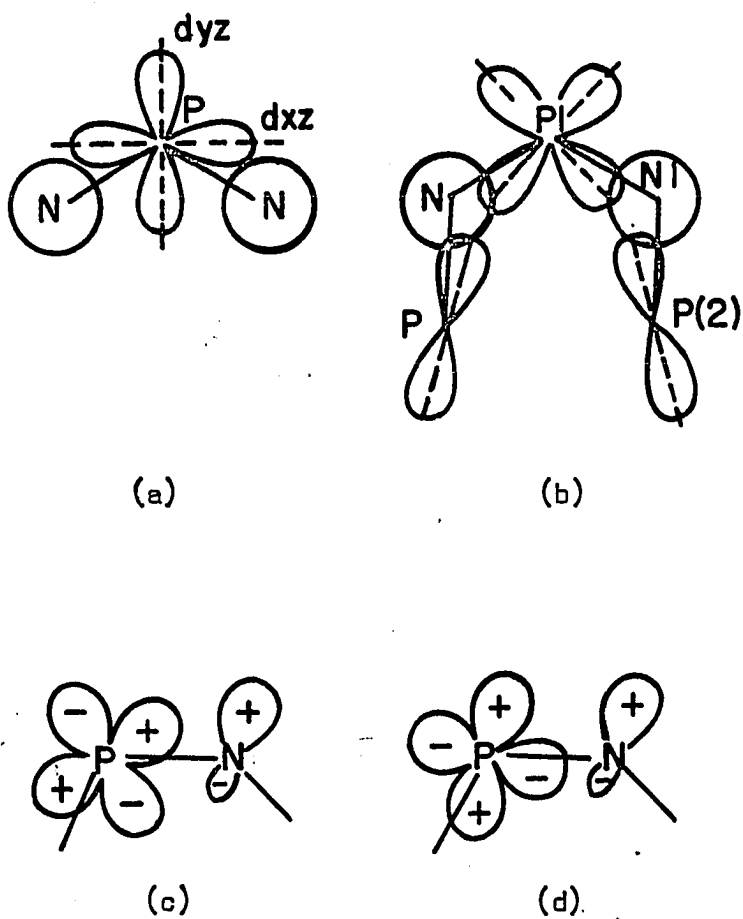
Figure 17. The π-bonding in $(NPCl_2)_5$

$$d_\pi^a = 1/\sqrt{2}(d_{xz} + d_{yz})$$
$$d_\pi^b = 1/\sqrt{2}(d_{xz} - d_{yz}).$$

The hybridization has the effect of rotating the two d-orbitals 45° with respect to the coordinate system defined in the first treatment. As a result of this rotation, the d-orbitals are very nearly directed at the nitrogen p_z orbitals. From the above, it can be seen that the second approach requires the d_{xz} and d_{yz} to contribute equally to the dπ-p bonding whereas in the first, any mixing coefficient could be used. It should be noted that this last approach effectively limits delocalization to a three atom area, whereas the first treatment has the appearance of delocalizing the electrons over the entire molecule. Another feature which should be noted is the fact that this second treatment, as a result of the only partial delocalization, allows a certain degree of flexibility at the phosphorus atoms whereas in the first treatment, no flexibility was apparent. Recently the two approaches have been shown to give nearly equivalent results (73), the second treatment accounting for 85-95% of the total delocalization energy. The remaining 5-15% is the contribution resulting from delocalization over greater portions of the molecule. This small latter contribution can be thought of as arising from the overlap occurring between the three-center islands of delocalization as a result of the angle at the phosphorus atom being 120° opposed to 90°. This latter result justifies the use of equivalent contributions from the two d-orbitals in dπ-pπ bonding.

Thus far, the discussion of the bonding has not in any way explained

the observed correlation between P-N distance and P-N-P angle. That is, the sigma and π-bonding are virtually independent of the P-N-P angle. In considering π'-bonding however, a dependence becomes evident. The π'-bonding has been discussed by others (72) as perhaps being involved in the bonding in the cyclic phosphonitrilics; however, the extent of the effect has been rather uncertain (74). The structure of $(NPCl_2)_5$ clearly shows the importance of this type of bonding. In Figure 17c and 17d, can be seen the two types of π'-bonding which are possible. This bonding results in the delocalization of the electrons from some kind of sp hybrid on the nitrogen over the entire molecule. Consideration of overlap integrals indicates the $d_{x^2-y^2}$-sp bonding to be stronger (72). This type of bonding and delocalization can also be seen to be strongly dependent on the P-N-P angle. That is, as the P-N-P angle increases, the P-N bond will be strengthened as a result of two factors. First, with an increase in the angle, the large positive lobes will approach closer, giving greater overlap, and second, as the angle increases, the s-character of the hybrid decreases, changing the hybrid to a more nearly pure p-orbital which also has the effect of increasing the d-sp overlap and consequently strengthening the P-N bond.

From the above considerations of the bonding in the cyclic phosphonitrilics, the bonding in $(NPCl_2)_5$ can be understood to involve sigma, π, and π' bonding. The effect of π' bonding can be seen to be quite significant in this structure and apparently is the cause of the reduction of the P-N bond distances from 1.60Å in the phosphonitrilics. Its effect is also shown by Figure 16, where the correlation of P-N distances with P-N-P

angles can only be explained by invoking π' bonding.

It should be mentioned at this point that while the π' bonding is maximized in a planar molecule, it cannot be said to be strong enough to force a planar configuration. In Table 17 is reproduced a table of over-

Table 17. Overlap integrals[a] of the nitrogen p- and lone-pair orbitals with phosphorus d-orbitals[b]

Overlap	Tub (S_4)	Chair (C_{2h})	Structure[c] Saddle (D_{2d})	Crown (C_{4v})	Planar molecule (D_{4h})
$p\pi\text{-}d_{xz}$	0.109	0.080	0.113	0.068	0.139
$p\pi\text{-}d_{yz}$	0.063	0.046	0.065	0.039	0.080
$p\pi\text{-}d_{x^2\text{-}y^2}$	0.069	0.097	0.081	0.122	0
$p\pi d_{xz}$	0.040	0.056	0.047	0.070	0
$sp^d\text{-}d_{xz}$	0.058	0.082	0.068	0.102	0
$sp\text{-}d_{yz}$	0.033	0.047	0.039	0.059	0
$sp\text{-}d_{x^2\text{-}y^2}$	0.147	0.123	0.150	0.112	0.166
$sp\text{-}d_{xy}$	0.042	0.056	0.040	0.062	0.012

[a]Magnitudes only. In the tub and the chair structure, the values are averages over all the overlaps of the named types. For example, the individual values for $p\pi\text{-}d_{xz}$ overlap in the tub are 0.080 and 0.137.

[b]The d-orbital exponents are the same throughout, equal to 0.47. The nitrogen orbital exponents are those given by Slater's rules.

[c]Values quoted are for ring bonds of 1.64Å, P = $120°$, N = $135°$. The values for 1.60Å and N = $132°$ would not be significantly different. In the planar structure the angles are P = $120°$, N = $150°$.

[d]The lone-pair orbital is an sp hybrid with mixing coefficient chosen to fit the nitrogen bond angle.

lap values calculated by Craig and Paddock (72). From this table, it is apparent that while some sp-$d_{x^2-y^2}$, π'-overlap is lost, some $p\pi$-$d_{x^2-y^2}$ overlap is gained in going from a planar to a tub configuration. Thus, more subtle factors such as molecular packing, intramolecular contacts and d-orbital energy levels, it is felt, must be responsible for the final configuration assumed.

The above discussion of bonding, while not able to unambiguously explain the chosen molecular conformations of the cyclic phosphonitrilics, is able to offer an explanation of the observed heats of formation (74), for phosphonitrilic chlorides. These data, calculated from heats of polymerization, as seen in Table 18, indicate a definite increase in stability of the $PNCl_2$ unit as the ring size increases. The largest increase in

Table 18. Properties of phosphonitrilic chlorides as a function of ring size.

n in $(PNCl_2)_n$	3	4	5	6	7
$\bar{E}$ $(P-N)_n$ - $\bar{E}$ $(P-N)_3$ (kcal.)	0	0.39	0.54	0.60	0.62
Chemical shift (p.p.m.) relative to 85% H_3PO_4	-20	+7	+17	+16	+18
$_n$(O-H) in phenol (cm.$^{-1}$)	135	125	115	105	95

stability occurs in going from the trimer to the tetramer. This can easily be understood in light of the observed importance of π'-bonding. The trimer is constrained to a configuration with a 120° P-N-P angle. An angle this small prohibits any significant overlap between the phosphorus

$d_{x^2-y^2}$ and nitrogen sp^2 hybrid resulting in very weak π'-bonding. In moving to the tetrameric chloride considerably more configurational freedom is gained and the $d_{x^2-y^2}$ is now able to overlap to a much greater extent than was possible in the trimer. The pentamer, of course, allows even greater freedom to achieve maximum overlap for all the phosphorus d-orbitals. Increasing the ring size above the pentamer however, allows only slightly greater conformational freedom, and thus, by this time, the molecule has been able to take a configuration which virtually maximized overlap while minimizing intramolecular repulsions and packing forces. The increase in heats of formation, per $PNCl_2$ unit, can thus be attributed to the increased π'-bonding. The lower members of the phosphonitrilic series are constrained to a configuration which prohibits effective phosphorus-nitrogen multiple bonding.

In light of this discussion, the structure of the hexameric phosphonitrilic chloride would not necessarily be expected to take a planar configuration. However, whatever configuration is assumed, large P-N-P angles would certainly be expected, which would allow considerable π'-bonding.

Potential Uses of the Symmetry Map

Several new methods were used in attempts to deconvolute the Patterson and obtain the correct model of the $(NPCl_2)_5$ structure. All of these made use of the symmetry map in some way. Although none of the attempts were wholly successful, the difficulties inherent in the methods and their

promising aspects will be discussed here. In the discussion use will be made of results obtained after the structure was solved and the methods were checked in known situations.

The first, and perhaps most obvious, use of the symmetry map is in superposition attempts with the Patterson map. If a peak in the symmetry map can be identified as an atom position, then a superposition of the Patterson origin at this point should give the model of the structure. This is the case because the Patterson contains N images, one for each of the N atoms positioned at the origin. If, then, the Patterson origin is superimposed on an atom position in the symmetry map, the other N-1 atoms corresponding to the Patterson image of the structure with that atom at the origin should coincide with their symmetry map peaks and an image of the structure should be the result. One of the difficulties that arises in attempting this is in determining that a peak in the symmetry map corresponds to a real atom position. As was mentioned earlier, peaks can be generated in the symmetry map through accidental coincidence of non-Harker peaks. If one of these is chosen and the Patterson origin superimposed on it, obviously, the result will be nonsense. A second difficulty can arise even if a real atom position is chosen in the symmetry map. Because initially, the exact center of a real atomic position is not known, and because the peaks in the symmetry map are very narrow and often shift from their true center, a superposition on a peak can easily be one row or column misplaced. Superposition with this uncertainty can produce a map missing many peaks at atom positions as a result of the narrowness of some peaks. Additionally, many peaks will be generated from accidental coinci-

dence of peaks of the "N" Patterson images with the several symmetry map images. The extra peaks will be quite numerous and very definitely obscure the image. Of course, it is true that with no additional assumptions, multiple superpositions on a peak and its symmetry related peaks in the symmetry map could be made to eliminate these peaks. However, attempts such as this are even more apt to destroy peaks corresponding to atom positions because an error in the first superposition will occur in the additional superpositions, and its effect will be multiplied. These facts were obvious from superposition results using the final refined atom positions. Even a superposition right at an atom center on the symmetry map destroyed some peaks corresponding to atom positions. The lack in resolution and displaced peak positions in the symmetry map are possible explanations although it is perhaps possible that the peak positions in the Patterson map are also shifted as a result of the sharpening process, (particularly around the origin), further complicating the superposition attempt. The result of four superpositions on four symmetry related atom positions did have peaks at most atom positions. These peaks however, in most cases, corresponded to only one or two numbers and would be easily mistaken for the many spurious narrow peaks occurring at random places in the resultant map.

It is obvious that the problems in the above Patterson-symmetry map superpositions, are primarily a result of a lack of peak breadth in the symmetry map. This being the case, the easiest solution would appear to be to use every point of the Patterson to generate a symmetry map eight times as large as the Patterson, and to then superimpose this larger map with another Patterson of equivalent size. While this is an obvious solu-

tion, the mechanics of such a superposition would be prohibitive. In the case of $(NPCl_2)_5$, the output from such an effort would exceed 4000 pages. This output could probably be condensed to some extent by improved output format, and perhaps made more reasonable. Perhaps a simpler solution would be to make use in some way, of all Patterson points by averaging each with its adjacent points. Through some such process, peak breadth in the symmetry map could be improved. The improved resolution could also be implemented by generating the symmetry map from an unsharpened Patterson or at least a Patterson that is not fully sharpened. This last suggestion is probably the easiest to carry out and has, perhaps, the most promise. Better results would be expected from this approach because the unsharpened Patterson would have peaks of increased size with the result that when every other point is considered to generate the symmetry map, the map will still have peaks of a size comparable to the sharpened Patterson peak size.

Assuming that the methods of generating the symmetry map can be improved to give good peak size, the Patterson symmetry map superpositions cannot be carried out unless a peak in the symmetry map can be identified as an atom position. An approach was explored that would give this information. The method called vector verification has been explored by others (88), and was found to give promising results (89). The method is based on the fact that the value of the summation of all points in a map produced by superimposing a Patterson on a symmetry map at an atom position would be larger than a superposition at an unoccupied position. This can easily be understood from the preceding discussion where it was

pointed out that such a superposition on an atom position would result in peaks coinciding in the two maps. Superimposing on a random point, on the other hand, would produce only accidental peak coincidences which supposedly would be fewer in number than those resulting from superposition on an atom position. If the superpositions could be carried out for every point in the symmetry map, and the resulting sum put in a new map at that position, those areas with the largest values would be probable atom positions. This has been attempted by Gorres and Jacobson (88); however, with the IBM 7074, it was not possible to run such a program in a reasonable time. Instead, summations could only be generated for superpositions at a few individually chosen points which were considered as likely atom positions. Some values of these summations can be seen in Table 19. Most of these points are taken from Figure 18, which is part of layer 3/20 of the symmetry map. From these values, it can be seen that for some large, well shaped peaks, as A, a very small summation at the level of the background values is obtained. This implies that this peak does not represent an atom position. The summations at B and C on the other hand, are large, and thus, strongly suggest that these peaks correspond to atom positions. These results were verified by calculating the atom positions in the symmetry map from the final model. Positions B and C were found to correspond to P_1 and P_5 respectively, while position A was not found to coincide with any atom in any image. It can also be seen, however, that a small sum was computed at point D which corresponds to a phosphorus atom. This discrepancy was felt to arise from the fact that even though peaks were coinciding, the relative background level was lower, thus producing a

Table 19. Values of symmetry map-Patterson superposition summations

Atom	X(80ths)	Y(80ths)	Z(20ths)	Sum	Sum 50	Position[a]
P1	6.6	1.4	3	4974700	61122	B
P2	11.2	13.1	3	4380015	51151	E
P3	79.7	19.3	3	3512599	60644	D
P4	70.5	10.9	0	4284348		
P5	7.1	79.9	3	4748241	70584	C
4Cl	68.9	12.2	6	4060629		
7Cl	53.3	25.6	3	4659551		
10Cl	67.1	79.2	12	4513140		
N2	7.6	18.1	15	4035090		
	7.0	20.0	3	3258270	37454	A
	17.0	18.0	3	3717535	37843	F
	.3	9.0	14	3287327	36572	G
	6.8	12.7	3		35144	
	11.2	14.1	3		49715	
	11.2	13.1	3		51151	E
	11.2	12.1	3		42747	
	13.2	13.1	3		45151	

[a]Position as indicated in Figure 18.
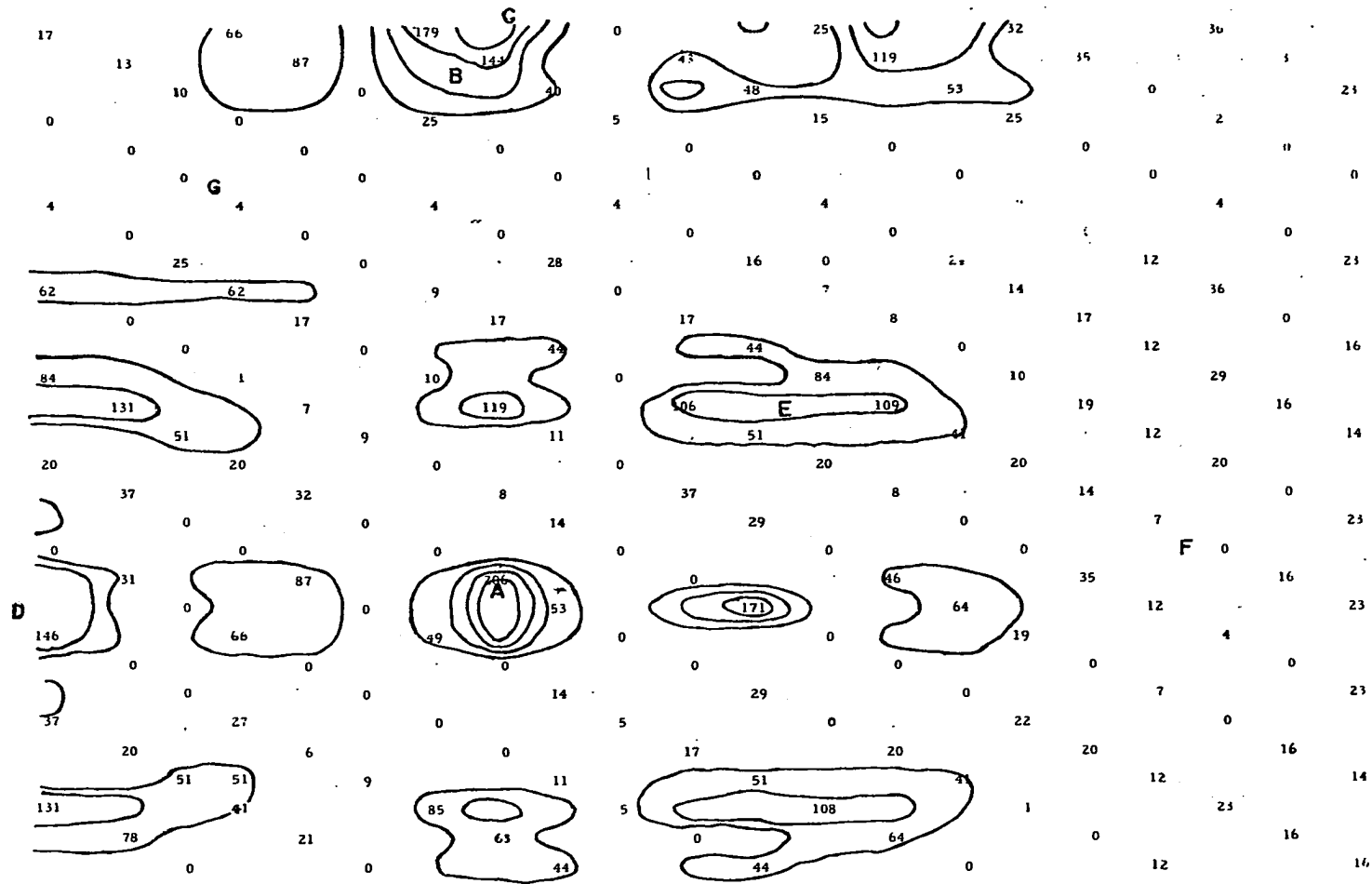
Figure 18. A portion of the symmetry map generated from the $(NPCl_2)_5$ Patterson

smaller sum. It can be noticed that the difference between peak values and background values is not very great and thus, some errors would not be unexpected. In an attempt to avoid this difficulty, and to achieve better distinction between peak values and background values, summations were made only of those points in the resultant superposition map which exceeded a prescribed, preset value. In the $(NPCl_2)_5$ structure, a heavy atom-heavy atom peak was estimated to have a magnitude of 55 and thus a cut-off value of 50 was chosen in this case. Summations for several points using this cut-off value are listed in Table 19, column 6. The difference between the peak values and the background values can be seen to be relatively larger compared to the total summations. Particularly, the value of the summation of the superposition at point D is considerably above the background, thus implying an atom position. From this discussion, it would seem that Patterson-symmetry map superposition summations, particularly using cut-off values, offer a promising method of locating atom positions. Even greater agreement would be expected using a symmetry map containing peaks with greater peak width (as can be seen from the summations at the bottom of Table 19, being displaced from the peak center by one row or column reduces the value of the summation much closer to the background level). If this method can be developed such that it, without error, indicated atom positions, it can be used with the Patterson-symmetry map superpositions discussed earlier to find a trial model for a structure. Coupling these two techniques offers a straightforward method which could be applied to any crystal structure for which a meaningful pseudo-electron density map of some kind can be generated (the symmetry map represents only one kind of pseudo-electron density map that can be used in the methods discussed).

A DIRECT METHOD ATTEMPT TO SOLVE

THE STRUCTURE OF $C_{68}H_{48}O_8Cl_4$

Introduction

The X-ray structure determination of chlorophenoxybenztropone dimer was attempted by two people using various Patterson methods.(90). Very little success was achieved by either.

Recently, several structures have been published which were solved by the use of direct methods (91-94). Particularly, Karle and Karle seem to have developed their method, called symbolic addition, to the point where it can be almost routinely applied. Their method, as most others, starts with Sayre's equation (95) which assumes all the atoms in the structure to be equivalent and fully resolved from each other. The equivalency assumption was of some concern in considering direct method work on the dimer structure because of the relatively large chlorine atoms. However, the publication of the structure of $C_{23}H_{22}N_2OS_2$ (96) solved by the symbolic addition method, indicated that the method would also work on $C_{68}H_{48}O_8Cl_4$ which is similar in heavy atom-light atom composition. With these considerations in mind, the symbolic addition method was attempted as a fresh approach toward the solution of the chlorophenoxybenztropone structure. The attempt, while not successful, will be discussed here to show the practical application of this method to a problem. The literature, though containing many structures solved by the symbolic addition method, is completely void of any discussion of how the method is applied. The

following then, represents a discussion of how the method can be applied as deduced from many literature articles reporting its results.

The Use of Symbolic Addition

Observed structure factors and unit cell information were taken from the thesis of John Jacobs (90). From the observed structure factors, unitary and normalized structure factors were generated. The unitary factors were calculated from the formula (97):

$$U(hkl) = \sqrt{I(hkl)} \; (\mathcal{E}_2 / \bar{I}^2)^{\frac{1}{2}},$$

where $\bar{I}$ is the average intensity of reflections in a specified range of $\sin \theta$ and $\mathcal{E}_m$ is defined as:

$$\mathcal{E}_m = \sum_j n_j^{\;m}$$

where n_j represents the fraction of the total number of electrons in the unit cell associated with the jth atom. This formula was used because of the uncertainty in $F(000)$. If, however, $F(000)$ can be obtained from, for example, a Wilson plot (98), the unitary structure factors should be calculated from (97):

$$U_{(hkl)} = \frac{F(hkl)}{\hat{f} \; F(000)}$$

where $\hat{f}$ is a function of theta and corrects for the decrease in the atomic scattering curves with $\sin \theta / \lambda$. These unitary structure factors are structure factors calculated assuming the atoms are points with constant scattering power rather than three dimensional volumes with scattering power

decreasing with $\sin\theta/\lambda$.

From the unitary structure factors, normalized structure factors were calculated from the formula:

$$E(hkl) = U(hkl)/\mathcal{E}_2^{\frac{1}{2}}.$$

These structure factors also represent scattering from point atoms, but are scaled in such a way that the distribution of magnitudes is a constant for centric space groups, independent of the number of point atoms and their size. The calculated centric distribution of magnitudes and the observed distribution for the dimer were:

E	Calc.	Obs.
> 3	0.3	0.5
> 2	5.0	4.5
> 1	32.0	32.0.

The average magnitudes of the normalized structure factors are also useful in determining whether the data are consistent with a centric distribution. The magnitudes found as compared to calculated centric and acentric values are:

	Acentric	Centric	Obs.
average $\|E_2\|$	0.89	0.80	0.81
average $\|E^2-1\|$	0.74	0.97	0.92

These data unquestionably suggest that the chlorophenoxybenztropone dimer structure is centric and hence, in space group $P\bar{1}$. In addition, Don Dahm, using a Howells, Phillips and Rogers (99) plot of the observed data, found a nearly perfect fit to a centric distribution.

With this evidence for a centric space group, it is meaningful to proceed to determine the signs of the observed structure factors. In the

symbolic addition method, this is done by means of Sayre's equation (cal-
led sigma two, by Karle and Karle):

$$S(hkl) = S(h'k'l') S (h+h' \ k+k' \ l+l'),$$

where S stands for the sign. This relation is reliable only if the unitary
structure factors for all three reflections are large in magnitude. More
generally, the relation can be written:

$$S(hkl) = S(\sum_{h'} U(h'k'l')U(h+h' \ k+k' \ l+l')),$$

where h' is summed over all data. Probability expressions have been de-
rived for the above two expressions (100). They are:

$$\text{Prob.} = \tfrac{1}{2}+\tfrac{1}{2}\tanh(\frac{\mathcal{E}_3}{\mathcal{E}_2^3}|U(hkl)U(h'k'l')U(h+h' \ k+k' \ l+l')|)$$

$$\text{Prob.} = \tfrac{1}{2}+\tfrac{1}{2}\tanh(\frac{\mathcal{E}_3}{\mathcal{E}_2^3 + (m-1)\mathcal{E}_2\mathcal{E}_4 - m\mathcal{E}_3^2}|U(hkl) \sum_{h'} U(h'k'l')U(h+h' \ k+k' \ l+l')|),$$

respectively, where m is the number of terms in the last summation. Using
these equations, the probability for Sayre's relation can be calculated for
specific examples and found often to exceed 90%. Sayre's equation can then
be assumed to hold absolutely in these cases, enabling some signs to be de-
termined. For example, if both 023 and 046 have large unitary structure
factors, Sayre's relation will say that the sign of 046 is positive with a
high probability:

$$\pm(023) = \pm (023)S(046).$$

In the usual case, as with the dimer, this type of relation will not deter-
mine enough signs to allow Sayre's equation to be applied to more general

reflections. Thus, by some means, some additional signs must be deduced to allow determination of enough signs to generate an electron density map with reasonable resolution. Oftentimes, Harker-Kasper inequalities (101) can unambiguously give the signs of some reflections. However, when a structure has the large number of light atoms, which tend to have large temperature factors, the unitary structure factors will be small in magnitude, and Harker-Kasper inequalities will not produce any absolute information on signs. This situation was the case with the dimer data. Having explored this possibility, the method of Karle and Karle was used. All the Sayre's triplets were generated, which involved normalized structure factors greater than 2.00 and their probabilities calculated. Most of the probabilities were greater than 90%, and thus, were assumed to hold absolutely. In order to determine signs, the following signs were assumed:

Reflection	N.S.F.	Sign
3 $\underline{0}$ $\underline{0}$	2.32	+
4 $\overline{7}$ $\underline{1}$	3.64	+
0 6 $\underline{3}$	3.71	+
0 4 4	3.34	a
$\underline{2}$ 3 3	2.91	b
$\overline{3}$ $\overline{4}$ $\underline{3}$	2.00	c
4 3 2	2.28	d.

These signs were assumed because they had large normalized structure factors and because they occurred in many triplet relations and thus would serve to determine additional signs. The first three reflections were assumed positive to fix the origin. These, however, must be linearly independent (102). This means that first, none can have all even Miller indices, and second, that the difference between the Miller indices of any two of the set cannot give all even values. As an example, the set

(203, 220, 641) is not linearly independent for two reasons. First, the 220 reflection has all even Miller indices and, second, the difference between the first and third reflections (2-6=-4, 0-4=-4, 3-1=2) gives all even values.

From these assumed signs, and the relations involving reflections with normalized structure factors greater than two, the signs of 45 other reflections were determined in terms of the above algebraic symbols. These reflections, with their signs, are listed on the left side of Table 20.

At this point, the triplets involving reflections with normalized structure factors greater than 1.5, were generated. The 45 known reflections occurred in many new relations and thus, determined many new signs. The 42 new reflections determined from the initial signs are listed on the right side of Table 20. In this table, it can be seen that many signs were determined from more than one triplet. The consistency of the signs produced from different triplets proved to be remarkable. As can be seen in the table, the sign of the 082 reflection was found to be "abcd" from eight different, independent triplets. Several cases of apparent discrepancies were also found, some of which are given in the table. Some of these discrepancies occurred often and had high probabilities associated with both signs. Discrepancies such as this could be interpreted, not as errors, but as equivalency of two algebraic expressions. Thus, from the 0 12 $\bar{6}$ reflection, bcd would seem to be positive. In addition, it is known that all signs cannot be positive because this would produce a peak at the origin. From these relations, the signs corresponding to the algebraic

Table 20. Algebraic signs determined using symbolic addition

H	K	L	Sign	H	K	L	Sign	Prob. (%)	No.of rel.
0	0	0	ab	0	2	4	d	97	2
0	0	3	ad	0	2	-4	abd	91	3
0	4	1	abd	0	6	-1	ab	97	3
0	4.	2	bcd				acd	96	1
0	4	-2	b	0	6	-6	ad	99	2
0	4	-3	c	0	8	-2	abcd	100	8
0	4	-4	a	0	8	-4	+	89	2
0	-4	-5	abc				cd	82	3
0	4	-7	d	0	12	-6	+	100	1
0	6	-3	+				bcd	93	2
0	8	0	cd	-1	-1	3	abcd	84	2
0	8	-5	bc	1	3	5	abc	91	2
0	8	-6	ab	1	4	2	d	90	4
0	10	1	acd	-1	4	-7	bcd	97	2
0	10	-1	bcd	1	-8	-4	+	95	4
0	-12	4	acd	-1	-8	4	bd	93	2
-1	1	-3	ad	2	0	1	cd	97	3
1	4	0	abd	2	0	-8	bd	96	3
2	0	0	bc	-2	1	-1	cd	99	4
2	0	-2	ac	-2	1	-3	abcd	95	5
2	3	3	b	-2	1	-7	ab	93	1
2	3	5	a	2	-2	-6	acd	88	4
2	-4	-2	d	-2	3	-6	b	99	3
-2	-4	6	c	2	-4	-1	acd	94	3
-2	-4	7	bcd	2	-4	-4	abd	97	3
2	-6	-5	bd	2	-4	5	acd	93	2
-2	-7	1	ab	2	-7	-1	bc	94	3
2	-10	-1	abd	2	-7	4	cd	99	4
-2	-11	3	a	2	8	-4	bd	85	3
3	0	0	+	2	9	2	a	93	2
3	0	-2	ab	-2	-11	3	a	90	1
3	0	3	ad	2	-11	2	b	96	2
3	-4	-1	abd	-2	11	-4	a	88	2
-3	4	-2	b	3	0	2	ab	88	1
-3	-4	3	c	3	0	4	cd	91	1
-3	8	-3	ac	-3	-2	2	bc	93	1
4	3	0	acd	-3	4	-2	b	92	2
4	-3	-2	d	-3	-8	5	bc	93	3
4	-3	-5	a	3	-10	1	bcd	92	1
4	-7	-1	+	-3	-10	3	acd	91	1
-4	-7	1	ac	4	-3	-2	d	92	1
-4	7	-2	ad	4	-3	-3	b	93	2
-4	-7	4	cd	4	3	3	c	99	4
6	0	-1	bc	-4	-3	6	b	95	2
-6	0	2	ab	5	0	1	cd	84	2

symbol can sometimes be determined. In this case, a unique correlation between the signs and algebraic symbols could not be determined, but the possibilities were reduced to three. All other combinations of sign assignments resulted in many more contradictions and some high probability (greater than 90%) contradictions. The most probable sign assignments were found to be, in order from most consistent to least:

	#1	#2	#3
a	+	+	+
b	+	-	-
c	-	+	-
d	-	-	+.

Considering only these assignments, additional signs were determined. By specifying plus or minus for the algebraic signs, many apparent discrepancies vanished and as a result, many more reflections could be given signs with high probability. In this way, over 150 reflections were assigned a plus or minus sign consistent with the three probable sign combinations above. The signed reflections for which the signs were known with greater than 80% probability, were then used to generate an E-map (103) (an electron density map using normalized structure factors). E-maps, since they are generated using structure factors calculated from point atoms, will produce better resolution than would be obtained from a regular electron density map calculation. The E-maps generated, did have quite sharp peaks and also, had no peaks at the centers of symmetry. They were thus consistent with the space group in which the origin electron density must be zero with all atoms in general positions and thus, all three maps had to be considered further. These maps were then compared with a sharpened Patterson generated from all the observed data in order to see in which one a

set of four peaks corresponding to chlorine atoms could be found. In all three maps, the largest peak in the E-map was perfectly consistent with a large Patterson peak at $U=2x$, $V=2y$, and $W=2z$. Likewise, in each of the three maps, several other large peaks also were found consistent with their Patterson vectors of $U=2x$, $V=2y$, and $W=2z$. However, when checking vectors between unrelated peaks, it was not possible in any of the maps to find a set of three peaks wholly consistent with Patterson peaks. Quite a few sets could be found where vectors 1 and 3, and 2 and 3 were consistent, but where vectors 1 and 2 were not. The agreement observed seemed in each case to be more than a result of chance, but still was not wholly consistent. A discussion with Dr. T. A. Beineke at this point revealed that often, E-maps can give very distorted peak heights. To check into this, electron density maps were generated for the three sign assignments using the observed struc- ture factors. These maps did have relative peak heights different from their corresponding E-maps. The large peaks, however, considered in the E-maps, were still the largest peaks in the electron density map and their positions remained unchanged. In each of the cases a peak also came up at the origin, but these were considered to be a probable result of the limited data used in the calculation.

The results of the direct method work were not successful in obtaining a model of the structure, but the consistency observed in the results leaves the feeling that something about the assignment is correct. This work and attempt did have the result of teaching the simplicity and potential usefulness of direct methods. The discussion here presents a straightforward application of direct sign determination to centric problems. The steps can be summarized as follows:

(1) Calculate unitary and normalized structure factors.

(2) Check distribution and average values of normalized structure factors for consistency with a centric atomic distribution.

(3) Attempt to determine signs using Harker-Kasper inequalities.

(4) Generate Sayre's triplets with probabilities greater than 90% (generally those involving normalized structure factors greater than two).

(5) Assign three origin fixing, linearly independent reflections and as few algebraic signs to others as are needed to determine a large number of signs.

(6) Assume all triplets in (4) to be valid and determine the signs of as many reflections as possible with the signs of (5).

(7) Generate all triplets with unitary structure factors greater than 1.5.

(8) Determine signs of additional reflections using the signs of (6) and the triplets of (7).

(9) From the signs of (8), try to find most consistent sign assignment for algebraic signs (5).

(10) Considering these sign assignments, determine as many signs of reflections with normalized structure factors greater than 1.00 as plus or minus.

(11) Generate E-maps.

(12) Eliminate any E-maps with a peak at the center of symmetry.

(13) Find model.

RESEARCH PROPOSITIONS

(1) It is felt that further investigation of the effect of ligands on the

shielding constants of metals and the resultant effect on metal-metal

bond distances would be very valuable. The Hg_2^{+2} salts and compounds

with Fe-Fe bonds are two possible systems from which such information

could be deduced.

(2) The use of accurate orbital exponents, particularly with an under-

standing of how they are effected by ligands (proposition 1), applied

to metal oxides has great potential for determining the nature of

cation-cation interactions. With a thorough understanding of these

exponents as deduced from interactions in known systems, it is con-

ceivable that the exact nature of magnetic ordering could be predict-

ed for a compound with known structure.

(3) As a result of the disorder in azulenedi-molybdenum hexacarbonyl,

very little could be deduced about the nature of the bonding in the

azulene. It is proposed that the structure of one of the isomers of

guaiazulenedi-iron pentacarbonyl be solved. The side groups on the

azulene would prevent ring disorder and the lighter iron atoms would

enable the carbon-carbon distances to be determined more accurately.

As a result, the nature of the bonding in π-bonded azulene might be

clearly discovered.

(4) The structure of a linear phosphonitrilic, it is felt, would yield

further understanding of the nature of the π-bonding occurring be-

tween phosphorus and nitrogen. Only one very crude X-ray determina-

tion of a semi-crystalline linear phosphonitrilic polymer has been reported to date. With a structure determination of a linear phosphonitrilic, an improved understanding of the nature of $d\pi-p\pi$ bonding might be achieved.

(5) It is proposed that a detailed molecular orbital calculation of $(NPCl_2)_5$, or perhaps the simpler trimer or tetramer, be carried out. From such a calculation, it would be hoped that the electron distribution in the d-orbitals, the molecular orbital energy levels and the reason for the assumed configuration might be discovered.

(6) It is felt that further work with the symmetry map applying some of the ideas suggested in the body of this thesis could develop symmetry map methods to the point where they could complement Patterson methods in the solution of light atom crystal structures.

(7) The preparation of crystalline stannous salts $M^{+n}(Sn(CH_3CO_2)_3)$ has recently been reported. Attempts were made several years ago in X-ray chemistry group I to prepare and grow single crystals of $Sn(CH_3CO_2)_2$. The preparation was successful, but only exceedingly thin fibers could be obtained. The stanous salts represent a potentially interesting system to study with the possibilities of either a tin-tin bond or a bridging acetate to achieve tetrahedral coordination around the tin atoms.

(8) Reflection spectra of solid antimony (III)-antimony (V) salts and $MCuCl_3$ salts, particularly at different temperatures, coupled with their known structures might further elucidate the nature of charge transfer in these compounds and in the latter case yield information

on the position of the molecular orbital energy levels.

(9) For purely educational reasons, it is proposed that a self-consistent charge and configuration, molecular orbital calculation based on the semiempirical Wolfsberg-Helmholz be carried through for some simple MX_6 system.

LITERATURE CITED

1. Klug, H. P. and G. W. Sears, Jr., J. Am. Chem. Soc., 68, 1133 (1946).

2. Hoard, J. L. and L. Goldstein, J. Chem. Phys., 3, 199 (1935).

3. Wells, A. F., J. Chem. Soc., 1662 (1947).

4. Vossos, P. H., L. D. Jennings and R. E. Rundle, J. Chem. Phys., 32, 1590 (1960).

5. Vossos, P. H., D. R. Fitzwater and R. E. Rundle, Acta Cryst., 16, 1037 (1963).

6. Willet, R. D., C. Dwiggins, Jr., R. F. Kruth and R. E. Rundle, J. Chem. Phys., 38, 2429 (1963).

7. Willet, R. D., J. Chem. Phys., 44, 39 (1966).

8. Williams, D. E., "LCR-2, A Fortran Lattice Constant Refinement Program," U.S. Atomic Energy Commission Report IS-1052 (Iowa State University of Science and Technology, Ames. Institute for Atomic Research). 1964.

9. Wehe, D. J., W. R. Busing and H. A. Levy, "Fortran Program for Single Crystal Orienter Absorption Corrections," U.S. Atomic Energy Commission Report ORNL-TM-299 (Oak Ridge National Laboratory, Oak Ridge, Tennessee). 1962.

10. Levy, H. A., Acta Cryst., 9, 679 (1956).

11. Mullikan, R. S., C. A. Rieke, R. Orloff and H. Orloff, J. Chem. Phys., 17, 1248 (1949).

12. Kauzman, W., Quantum Chemistry, Academic Press, Inc., New York, N.Y., (1957).

13. Clementi, E. and D. L. Raimondi, J. Chem. Phys., 38, 2686 (1963).

14. Slater, J. C., Phys. Rev., 36, 57 (1930).

15. Powell, H. M. and R. V. C. Ewens, J. Chem. Soc., 286 (1939).

16. Figgis, B. N. and C. M. Harris, J. Chem. Soc., 855 (1959).

17. Tishehenko, G. N., Tr. Inst. Krist. Akad. Nauk SSSR, 11, 93 (1955).

18. Asmussen, R. W. and H. Soling, Z. anorg. allgem. Chem., 283, 3 (1956).

19. Dahl, L. F., T. Chiang, P. W. Seabaugh and E. M. Larsen, _Inorg. Chem._, 3, 1236 (1964).

20. Lewis, J., D. J. Machin, I. E. Newnham and R. S. Nyholm, _J. Chem. Soc._, 2036 (1962).

21. Figgis, B. N. and R. L. Martin, _J. Chem. Soc._, 3837 (1956).

22. Martin, R. L. and H. Waterman, _J. Chem. Soc._, 2545 (1957).

23. Ross, I. G., _Trans. Faraday Soc._, 55, 1057 (1959).

24. Ross, I. G. and J. Yates, _Trans. Faraday Soc._, 55, 1064 (1959).

25. Tonnet, M. L., S. Yamada and I. G. Ross, _Trans. Faraday Soc._, 60, 840 (1964).

26. Forester, L. S. and C. J. Ballhausen, _Acta Chem. Scand._, 16, 1385 (1962).

27. Boudreaux, E. A., _Inorg. Chem._, 3, 506 (1964).

28. Kokoszka, G. F., H. C. Allen and G. Gordon, _J. Chem. Phys._, 42, 3693 (1965).

29. Reimann, C. W., G. F. Kokoszka and G. Gordon, _Inorg. Chem._, 4, 1082 (1965).

30. Hansen, A. E. and C. J. Ballhausen, _Trans. Faraday Soc._, 61, 631 (1965).

31. Anderson, P. W., _Phys. Rev._, 79, 350 (1950).

32. Anderson, P. W., _Phys. Rev._, 115, 2 (1959).

33. Goodenough, J. B., _J. Phys. Chem. Solids_, 6, 287 (1958).

34. Goodenough, J. B., _J. phys. radium_, 20, 155 (1959).

35. Goodenough, J. B., _Phys. Rev._, 117, 1442 (1960).

36. Kanamori, J., _J. Phys. Chem. Solids_, 10, 87 (1959).

37. Goodenough, J. B., _J. Appl. Phys._, 31, 359S (1960).

38. Jellinek, F., _Nature_, 187, 871 (1960).

39. Jellinek, F., _J. Organometallic Chem._, 1, 43 (1963).

40. Cotton, F. A., W. A. Dollase and J. S. Wood, _J. Am. Chem. Soc._, _85_, 1543 (1963).

41. Ibers, J. A., _J. Chem. Phys._, _40_, 3129 (1964).

42. Weiss, E. and E. O. Fischer, _Z. anorg. allgem. Chem._, _286_, 142 (1956).

43. Dyatkina, M. E. and E. M. Shustorovich, _Russ. J. Inorg. Chem._, _4_, 179 (1959).

44. Cotton, F. A., "Chemical Applications of Group Theory," Interscience Publishers, New York, N.Y., 1963.

45. den Boer, D. H. W., P. C. den Boer and H. C. Longuet-Higgins, _Mol. Phys._, _5_, 387 (1962).

46. Berry, R. S., _J. Chem. Phys._, _35_, 29 (1961).

47. Bailey, M. F. and L. F. Dahl, _Inorg. Chem._, _4_, 1298 (1965).

48. Bailey, M. F. and L. F. Dahl, _Inorg. Chem._, _4_, 1306 (1965).

49. Bailey, M. F. and L. F. Dahl, _Inorg. Chem._, _4_, 1314 (1965).

50. Mc Tarlane, W. and S. O. Grim, _J. of Organometallic Chem._, _2_, 147 (1966).

51. Burton, R., L. Pratt and G. Wilkinson, _J. Chem. Soc._, 4290 (1960).

52. Wheland, G. W., _Resonance in Organic Chemistry_, John Wiley and Sons, Inc., New York, N.Y., (1955).

53. Ferguson, L. N., "The Modern Structural Theory of Organic Chemistry", Prentice-Hall, Inc., Englewood Cliffs, N.J., (1963).

54. Robertson, J. M., H. M. M. Shearer, G. A. Sim and D. G. Watson, _Acta Cryst._, 15, 1 (1962).

55. Williams, D. E. and R. E. Rundle, _J. Am. Chem. Soc._, _86_, 1660 (1964).

56. Furnas, T. C., Jr., Single crystal orienter instructions manual. General Electric Company, Milwaukee, Wisconsin. 1957.

57. Alexander, L. E. and G. S. Smith, _Acta Cryst._, _15_, 983 (1962).

58. Lawton, S. L. and R. A. Jacobson, "The Reduced Cell and Its Crystallographic Applications," U.S. Atomic Energy Commission Report IS-1141 (Iowa State University of Science and Technology, Ames. Institute for Atomic Research). 1965.

59. <u>Trans. of the Am. Cryst. Ass.</u>, <u>1</u>, 30 (1965).

60. Busing, W. R. and H. A. Levy, U.S. Atomic Energy Commission Report ORNL 59-12-3 (Oak Ridge National Laboratory, Oak Ridge, Tennessee). 1959.

61. Wilson, F. C. and D. P. Shoemaker, <u>J. Chem. Phys.</u>, <u>27</u>, 809 (1957).

62. Hanson, A. W., <u>Acta Cryst.</u>, <u>19</u>, 19 (1965).

63. Ibers, J. A. and W. C. Hamilton, <u>J. Chem. Phys.</u>, <u>44</u>, 1748 (1966).

64. King, R. B. and M. B. Bisnette, <u>Tetrahedron Letters</u>, <u>18</u>, 1137 (1963).

65. Dunitz, J. D. and P. Pauling, <u>Helv. Chim. Acta</u>, <u>43</u>, 2188 (1960).

66. Wilson, A. and D. F. Carroll, <u>J. Chem. Soc.</u>, 2548 (1960).

67. Dougill, M. W., <u>J. Chem. Soc.</u>, 3211 (1963).

68. Mc Geachin, H. McD. and F. R. Tromans, <u>J. Chem. Soc.</u>, 4777 (1961).

69. Dougill, M. W., <u>J. Chem. Soc.</u>, 5471 (1961).

70. Hazekamp, R., T. Migchelsen and A. Vos, <u>Acta Cryst.</u>, <u>15</u>, 539 (1962).

71. Dewar, M. J. S., E. A. C. Lucken and M. A. Whitehead, <u>J. Chem. Soc.</u>, 2423 (1960).

72. Craig, D. P. and N. L. Paddock, <u>J. Chem. Soc.</u>, 4118 (1962).

73. Craig, D. P., <u>J. Chem. Soc.</u>, 4682 (1965).

74. Jacques, J. K., M. F. Mole and N. L. Paddock, <u>J. Chem. Soc.</u>, 2112 (1965).

75. Lund, L. G., N. L. Paddock, J. E. Proctor and H. T. Searle, <u>J. Chem. Soc.</u>, 2542 (1960).

76. Jacobson, R. A., J. A. Wunderlich and W. N. Lipscomb, <u>Acta Cryst.</u>, <u>14</u>, 598 (1961).

77. Mighell, A. D. and R. A. Jacobson, <u>Acta Cryst.</u>, <u>16</u>, 443 (1963).

78. Hamilton, W. C., <u>Acta Cryst.</u>, <u>18</u>, 866 (1965).

79. Hanson, H. P., F. Herman, J. D. Lea and S. Skillman, <u>Acta Cryst.</u>, <u>17</u>, 1040 (1963).

80. Cruickshank, D. W. J., <u>Acta Cryst.</u>, <u>9</u>, 754 (1956).

81. Cruickshank, D. W. J., _Acta Cryst._, 9, 757 (1956).

82. Cruickshank, D. W. J., _Acta Cryst._, 14, 896 (1961).

83. Rouault, M., _Ann. Phys._, 14, 78 (1940).

84. Brockway, L. O. and J. Y. Beach, _J. Am. Chem. Soc._, 60, 1836 (1938).

85. Hobbs, E., D. E. C. Corbridge and B. Raistrick, _Acta Cryst._, 6, 621 (1953).

86. Craig, D. P. and N. L. Paddock, _Nature_, 181, 1052 (1958).

87. Craig, D. P., _J. Chem. Soc._, 997 (1959).

88. Gorres, B. T. and R. A. Jacobson, _Acta Cryst._, 17, 1599 (1964).

89. Mighell, A. D. and R. A. Jacobson, _Acta Cryst._, 17, 1554 (1964).

90. Jacobs, J. J., "The Crystal Structure Analysis of p-chlorophenoxy-benztropone," unpublished Ph.D. thesis. Library, Iowa State University of Science and Technology, Ames, Iowa. 1964.

91. Mootz, D., _Acta Cryst._, 19, 726 (1965).

92. Dragonette, K. S. and I. L. Karle, _Acta Cryst._, 19, 978 (1965).

93. Klug, H. P., _Acta Cryst._, 19, 983 (1965).

94. Karle, I. L. and K. Britts, _Acta Cryst._, 20, 118 (1966).

95. Sayre, D. M., _Acta Cryst._, 5, 60 (1952).

96. Karle, I. L. and J. Karle, _Acta Cryst._, 19, 92 (1965).

97. Lipson, H. and W. Cochran, "The Determination of Crystal Structures," The Crystalline State, Vol. 3, G. Bell and Sons, Ltd., London, England, 1957.

98. Wilson, A. J. C., _Nature_, 150, 152 (1942).

99. Howells, E. R., D. C. Phillips and D. Rogers, _Acta Cryst._, 3, 210 (1950).

100. Cochran, W. and M. M. Woolfson, _Acta Cryst._, 8, 1 (1955).

101. Harker, D. and J. S. Kasper, _Acta Cryst._, 1, 70 (1948).

102. Hauptman, H. and J. Karle, "Solution of the Phase Problem. 1. The Centrosymmetric Crystal". ACA Monograph Number 3. Edwards Brothers, Inc., Ann Arbor, Michigan, 1953.

103. Karle, I. L., H. Hauptman, J. Karle and A. B. Wing, _Acta Crystal_, _11_, 257 (1958).

ACKNOWLEDGMENT